INVESTIGATION OF SHUNT ACTIVE POWER FILTER FOR POWER QUALITY IMPROVMENT

A THESIS SUBMITTED TO THE

GRADUATE SCHOOL OF APPLIED SCIENCES

OF

NEAR EAST UNIVERSITY

by

Mohammed KMAIL

In Partial Fulfillment of the Requirements for the Degree of Master of Science

in

Electrical and Electronic Engineering

NICOSIA 2012

DECLARATION

I hereby declare that all information in this document has been obtained and presented in accordance with academic rules and ethical conduct. I also declare that, as required by these rules and conduct, I have fully cited and referenced all material and results that are not original to this work.

Name: Mohammed KMAIL

Signature:

Date:

ABSTRACT

In the recent decades, the world has seen an expansion in the use of non-linear loads. These loads draw harmonic non-sinusoidal currents and voltages in the connection point with the utility and distribute them through it. The propagation of these currents and voltages into the grid affect the power systems in addition to the other clients' equipments. As a result, the power quality has become an important issue for both consumers and distributers of electrical power. Active power filters have been proposed as efficient tools for power quality improvement and reactive power compensation. In this work, harmonic problem is introduced and discussed. The different traditional and modern harmonic solutions topologies are presented. Shunt active power filter as the most famous and used active filter type is introduced. The use of SAPF for harmonic current and reactive power compensation is studied. Different control methods of APF in addition to different harmonic extraction methods are presented and discussed. Self Tuning Filter for the improvement of the SAPF's efficiency in the case of distorted and unbalance voltage system is presented and discussed. Different studied SAPF control strategies are implemented in MATLAB\Similink and results are tabulated and discussed.

Keyword

Active Power Filter, Instantaneous Power Theory, Self Tuning Filter, Harmonics, Non Linear Load.

ACKNOWLEDGEMENTS

I would like to begin by thanking the Almighty God who has been my help and the source of my strength throughout the duration of my studies.

I'm also grateful to my supervisor Assoc. Prof. Dr. Özgür Cemal ÖZERDEM for his total support and encouragement during the two years of my study in the university. I would like also to great all the Professors, Doctors, all the staff and students of NEU. A special thank to my friend and research partner, Samet Biricik for his support and advices. Without forgetting my best friends Mohammed Bahaa, Mohammed Elamin, Ahmed, Youssef, Kanaan, to my cousin Amjad, and to all my friends.

Dedicated with love to my parents, my brothers and sisters who have been always with me . . .

LIST OF TABLES

LIST OF FIGURES

List of Used Symbols

PQ:	Active and reactive instantaneous power.
L_f :	Active power filter’s inductance (coupling inductance).
R_f :	Active power filter’s resistance (coupling resistance).
S :	Apparent power.
C_{dc} :	Capacitance of direct current capacitor.
V_{dc}^{*} :	Capacitor’s reference voltage.
k_{pdc}, k_{idc} :	Constants of direct voltage proportional integral controller.
k_{pi}, k_{ii} :	Constants of filter current proportional integral controller.
f_c :	Cut of frequency of low pass filter.
ζ :	Damping factor.
d-q:	Direct and indirect current theory.
V_{dc} :	Direct current capacitor voltage.
R_d :	Direct current resistance.
L_d :	Direct current side inductance.
D :	Distorted power.
I_{leff} :	Effective value of alternative load current.
i_{fabc} :	Filter currents.
$i_{f\alpha\beta}$:	Filter currents in stationary reference frame.
i_{fdq} :	Filter currents in synchronous reference frame.
f :	Fundamental frequency of grid.
x_1 :	Fundamental of signal x.
i_{sabc} :	Grid currents.
$i_{s\alpha\beta}$:	Grid currents in the stationary reference.
i_{sdq} :	Grid currents in the synchronous reference.
L_s :	Grid inductance.
i_{sabc}^{*} :	Grid reference currents.

R_s :	Grid resistance.
v_{sabc} :	Grid voltage system.
$v_{s\alpha\beta}$:	Grid voltage in stationary frame.
v_{sdq} :	Grid voltage in synchronous reference.
x_h :	Harmonic component of order h.
$\tilde{i}_{l\alpha}$, $\tilde{i}_{l\beta}$:	Harmonic currents in stationary frame.
p :	Instantaneous active power.
q :	Instantaneous reactive power.
i_{labc} :	Load currents.
$i_{l\alpha\beta}$:	Load currents in stationary reference frame.
i_{ldq} :	Load currents in synchronous reference frame.
L_l :	Load side inductance.
R_l :	Load side resistance.
$\bar{U}_d$:	Mean value of rectified voltage.
i_{dc}^* :	Output current of voltage controller.
$v_i, i = 1, 2, ..., 6$:	Output voltages of voltage source inverter.
P_{dc}^* :	Power at the output of voltage controller.
I_d :	Rectified current.
U_d :	Rectified voltage.
i_{fabc}^* :	Reference filter's currents.
$i_{f\alpha\beta}^*$:	Reference filter currents in stationary reference frame.
i_{fdq}^* :	Reference filter currents in synchronous reference frame
$I_{s\max}^*$:	Reference peak value of grid current.
$\vec{v}^*$:	Reference vector of output voltage of voltage source inverter.
$S_i, i = 1, 2, ..., 6$:	Sectors of output voltage of voltage source inverter.
S_{abc} :	States of voltage source inverter.
$S_{\alpha\beta}$:	States of voltage source inverter in stationary frame.

S_{dq} : States of voltage source inverter in synchronous refrence frame.

T_s : Switching period.

t : Time

List of Used Abbreviations

P:	Active power.
AC:	Alternative current.
ANN:	Artificial neural networks.
APF:	Active power filter.
S:	Apparent power.
F_c :	Crest factor.
DC:	Direct current.
F_d :	Distorsion factor.
F:	Farad.
f:	Frequency.
GTO:	Gate turn off thyristor.
H:	Hinri.
HAPF:	Hybrid active power filter.
Hz:	Hertz.
IGBT:	Insolated gate bipolar transistor.
IP :	Integral proportional controller.
LPF :	Low pass filter.
MOSFET:	Metal Oxid Silicon Field Effect Transistor.
PF:	Power factor.
PI :	Proprtional integral controller.
PLL:	Phase locked loop.
PWM:	Pulse width modulation.
Q:	Reactive power.
RLC:	Resistor, inductor, and capacitor.
RMS:	Root mean square value.
SAPF:	Shunt active power filter.
SVPWM:	Space vecteur pulse width modulation.
SPWM:	Sinusoidal Pulse width modulation.
SRF:	Synchronous reference frame.
STF:	Self tuning filter.
THD:	Total harmonic distorsion.
UPQC:	Unified power quality conditionner.

VAr:	Reactive Volt Ampere.
VSC:	Voltage source converter.
VSI:	Voltage source inverter.

CHAPTER 1

INTRODUCTION

The increasing use in the industry of non linear loads based on the power electronic elements introduced serious perturbation problems in the electric power distribution grids. Also, regular increase in the harmonic emissions and current unbalance in addition to high consumption of reactive power can be noticed. The flow of harmonic currents in the electric grids can cause also voltage harmonics and disturbance. These harmonic currents can interact adversely with a wide range of power system equipments, control systems, protection circuits, and other harmonic sensible loads. The energy distributers as like as consumers were then concerned by imposing some regulations protecting against the expansion of harmonic problem. Many regulations concerning the harmonic emissions have been proposed by the international electrical committees like IEC-61000 and by the recommendations IEEE Std. 519-92 [1, 2].

The consumption of reactive power in industrial and domestic loads presents also an important issue in the discussion of power quality problems. The reactive power consumed by non resistive loads causes higher RMS current values in addition to extra heating of power transmission and distribution systems. The use of batteries of capacitors or synchronous machines for local reactive power production has been proposed for a long time. The accelerated development of power electronics and semiconductor production has encouraged the use of STATIC VAR compensators for the reactive power compensation. However, these solutions looks inefficient and can cause extra problems in power systems in the case of high current and voltage harmonic emissions. The fact that these systems are especially designed to compensate the fundamental based reactive power, in addition to high possibilities of interaction between these compensation elements and system harmonics make it unstable solutions in modern technologies.

In order to face the problem of harmonics, many solutions have been proposed. These solutions included modifications on the load itself for less harmonic emissions like the case of special structure single phase and three phase rectifier, and PWM rectifiers. Or the connection on the polluted power grids of other traditional or modern compensation systems.

Most of traditional harmonic reduction solutions includes the use of harmonic trapping passive filters based on RLC elements calculated in accordance with the harmonic ranges to be trapped. In addition, these passive filters can be designed to compensate reactive power simultaneously with the desired harmonics. Nevertheless, these solutions are of poor efficiency due to different factors [3].

- Insufficient fitness for large bands of harmonic frequencies, which implies the use of many filters.
- Possibility of series and parallel resonance with the grid which lead to dangerous amplification of neighboring frequency harmonics.
- Highly dependent on the grid and load parameters and main frequency.
- Bulky equipments [4, 5].
- Very low flexibility for load variations which implies new filter design for each load variation.

During the last three decades, researchers were encouraged by the development of power electronics industry, the revolution in digital signal processing production and the increasing demand for efficient solutions of power quality problems including harmonics problem. They were encouraged to develop modern, flexible, and more efficient solutions for power quality problems. These modern solutions have been given the name of active compensators or active power filters. The objective of these active power filter abbreviated mostly APF is to compensate harmonic currents and voltages in addition to selective reactive power compensation. The use of APFs for harmonic and reactive power compensation and DC power generation was proposed in [4]. The main advantages of the APFs are their flexibility to fit load parameters' variations and harmonic frequencies in addition to high compensation performance.

Many types of APF have been proposed and used in harmonic compensation. Series APF is used for voltage harmonics compensation. Shunt APF was proposed for current harmonics and reactive power compensation. The Unified Power Quality Filter or Conditioner combines the two types Shunt and Series APF in one device responsible for the simultaneous compensation of voltage, current harmonics and reactive power. Different combinations of APFs with passive filters have been also used and proposed in the literary in the so-called Hybrid APFs (HAPFs). The combination between the traditional and the modern in one HAPF has the aim of amelioration of different types of APF compensation performance, also the minimization of cost and complexity of compensation systems. It is considered to combine the advantages of old passive filter and the new APFs and reject the drawbacks related to each of them when used individually.

Although there are different types of APF, the Shunt APF is still the most famous and used type APF. The main function of Shunt Active Power Filter is to cancel harmonic currents occurring in power grids. The principle of SAPF is to generate harmonic currents equal in magnitude and opposite in phase to those harmonics that circulate in the grid. The non-linear loads absorb non-sinusoidal currents from the grid. Whereas, the SAPF current is generated in a manner that grid current keeps the sinusoidal form. SAPF is controlled to be seen with the non-linear load by the grid either as linear resistive load; in case of reactive power compensation, capacitive or inductive load in the case when the APF is not responsible for reactive power compensation.

There are two main structures for the control of Shunt Active Power Filter; these are the direct control and the indirect control of APF. In the direct control the main idea is to generate filter current references using the appropriate methods. The generated reference currents are then to be compared with the measured APF currents. The error is then used to produce control signals of the filter. The indirect control interests in controlling the grid currents instead of filter currents. It compares the measured grid currents with their generated references. The error is then sent to the control circuit which determines the control signal of the APF.

LITERATURE REVIEW

The literary of APF is very rich and covers many aspects including power topologies, control theories, and harmonic extraction and reference generation methods of APF. The instantaneous active and reactive power PQ theory and the synchronous reference frame SRF or d-q theory based on Park transform had attracted the attention of researchers due to their simple principle and high efficiency. The direct control strategy of APF has been the mostly used in literary. In [6] the author presented the use of PQ theory for harmonic extraction. The direct control based on PI current and voltage controllers, also a fix and auto adaptive band hystereses in addition to fuzzy logic DC voltage controller were studied. [4] has presented in his PHD thesis a study of SAPF and series APF. He discussed the use of PQ theory and SRF theory for current and voltage harmonics extraction. The control of APF using PI controllers in addition to the use of RST controllers was covered. A new modified RST controller was proposed in this work. PQ theory, modified PQ theory, SRF theory were presented by [7]. Current and voltage control based on linear PI controllers, sliding mode controllers, linearization, and backstepping control methods were also presented in his work. Fuzzy logic DC voltage control with sliding mode current control based on sine multiplication extraction theory was presented by [8]. Instantaneous active and reactive power theory with hysteresis SVPWM control was studied in [9]. The function of APF with DC power generation was proposed in [10]. In [11], fuzzy logic and hysteresis control based on SRF theory was presented and discussed.

In [12], the use of PQ, SRF and sine multiplication theories was discussed in addition to the PI and hysteresis controllers. Sine multiplication theory based SAPF with IP current controller was proposed by [13]. The use of fuzzy logic controller with sine multiplication theorem in single phase APF has been presented in [14]. In [15], an adaptive fuzzy low pass filter for harmonic extraction has been proposed to ameliorate the performance of APF. three phase APF based on SRF theory with SVPWM control was proposed in [16]. PQ theory, active and reactive currents theory performance was studied under unbalanced voltage system in [17]. Study of PQ, SRF, constant active and reactive power theory, constant (unity) power factor algorithm, sine multiplication theory have been proposed in [18]. Sliding mode based DC voltage controller for grid current's peak detection was proposed by [19]. The use of self tuning filter in unbalanced distorted grid voltage conditions (STF) has been proposed by [20, 21, 22, and 23]. PQ, SRF, and modified PQ theory were studied in [23]. The use of two legs with midpoint capacitor, three legs and four legs VSI with PQ theory in balanced and unbalanced voltage system has been studied in [20].

Artificial intelligence has been recently introduced in the harmonic extraction and the control of active power filter. In [24] a comparison between the performance of UPQC based on PI controller and ANN based controller was presented. The use of ANN for harmonic content extraction was proposed and discussed by [25]. The use of adaptive neural network in the control of series APF was proposed in [26].

Separately, the indirect control of APF has been discussed and proposed in different works. In [27, 28, and 29] indirect control based on PI controller has been proposed. sliding mode control of DC voltage with indirect PI current controllers were used in [30]. Finally, Indirect fuzzy logic control has been proposed in [8].

THESIS OVERVIEW

This thesis contains four chapters arranged as follow:

First chapter presents a general introduction on power quality and active power filters. It includes also a literature review and thesis overview.

The second chapter discusses different power quality problems and focuses on the study of harmonics, harmonic sources, and their effects on grids and equipments. It discusses also the different traditional and modern solutions of harmonic problems.

In the third chapter, the study is pointed toward the shunt active power filter and its uses. The study of two level three phase APF topology is presented in this chapter. Many harmonic extraction methods are introduced in this chapter including the active and reactive instantaneous power theory and the synchronous reference theory. Other extraction methods were also studied in this chapter in addition to the study of control of SAPF based on simple PI controllers.

The results of all studied control strategies were tabulated and discussed in the fourth chapter where three cases were considered. The first case was when the grid is stable and balanced, for the second case the grid voltages were unbalanced and distorted. The third case considered the use of SAPF for harmonics and reactive power compensation in the case of distorted and unbalanced voltages. The results of three cases were tabulated and discussed in this chapter.

CHAPTER 2

POWER SYSTEMS AND POLLUTION

Electric systems and grids are complex dynamic systems. These systems suffer usually from unexpected or sudden changes of the currents and voltages. These changes are due mainly to the different types of linear and non-linear loads to which they are connected. In addition, to different types of accidents which can intervener into the grid [31]. With the increasing use of power semiconductors in the most of industrial and domestic procedures, the electric grids are polluted with different harmonic currents and voltages. These harmonics affect the normal function of the most of the grid connected devices; in addition to considerable economic losses. Many classic and modern solutions have been proposed in the literary for the harmonic problems. In this chapter, the harmonic problem as one of the most common power quality problems will be presented. The different modern and traditional solutions will then be discussed.

2.1 Power Systems Distortion and Problems

In power systems, different voltage and current problems can be faced. The main voltage problems can be summarized in short duration variations, voltage interruption, frequency variation, voltage dips, and harmonics. Harmonics represent the main problem of currents of power systems.

2.1.1 Voltage Variation for Short Duration

The short duration voltage variation is the result of the problems in the function of some systems or the start of many electric loads at the same time. The defaults can increase or decrease the amplitude of the voltage or even cancel it during a short period of time [31]. The increase of voltage is a variation between 10-90% of the nominal voltage. It can hold from half of a period to 1 minute according to the IEEE 1159-1995. According to the same reference, the increase in voltage is defined when the amplitude of the voltage is about 110-180% of its nominal value.

2.1.2 Voltage Interruption

The cutoff of the voltage happens when the load voltage decreases until less than 10% of its nominal value for a short period of time less than 1 minute. The voltage interruption can be the effect of defaults in the electrical system, defaults in the connected equipments, or bad control systems. The main characteristic of the voltage interruption is the period over which it happens.

2.1.3 Frequency Variations

In the normal conditions the frequency of the distribution grid must be within the interval 50 ± 1 Hz. The variations of the frequency of the grid can appears to the clients who are using auxiliary electric source (solar system, thermal station…etc). These variations are rare and happen in the case of exceptional conditions like the defaults in the turbines.

2.1.4 Unbalance in Three Phase Systems

The three phase system is unbalanced when the currents and voltages are not identical in amplitude; or when the phase angle between each two phases is not 120°. In the ideal conditions, the three phase system is balanced with identical loads. In reality, the loads are not identical, in addition to the problems of the distribution grids which can interfere.

2.1.5 Voltage Dips (Sags)

The voltage dips are periodic perturbations. They appear as a natural effect of the switching of the transistors. They are due also to the start of big loads like motors. Lifts, lights, heaters…etc. this phenomena causes bad functioning of the protection equipments.

2.1.6 Harmonics

Power systems are designed to operate at frequencies of 50 or 60 Hz. However, certain types of loads produces currents and voltages with frequencies that are integer multiples of the 50 or 60 Hz fundamental frequency. These frequencies components are a form of electrical pollution known as harmonic distortion. There are two types of harmonics that can be encountered in a power system [32].

- ✓ Synchronous harmonics.
- ✓ Asynchronous harmonics.

Synchronous harmonics are sinusoids with frequencies which are multiples of the fundamental frequency. The multiplication factor is often referred to as the harmonic number. The synchronous harmonics can be subdivided into two categories.

- ✓ Sub-harmonics: when the harmonic frequency is less than the fundamental frequency.
- ✓ Super harmonics: when the harmonic frequency is more than the fundamental frequency.

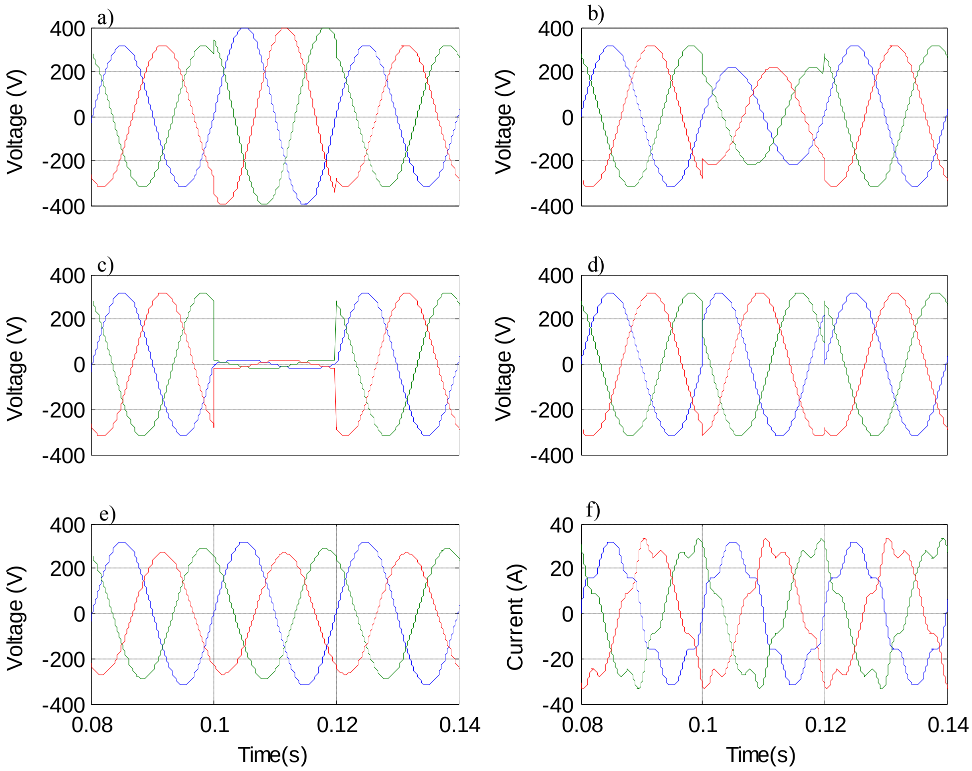

Figure 2.1: Most encountered power system problems. a) Voltage swells. b) Voltage sags. c) Voltage interruption. d) Frequency variation. e) Voltage unbalance. f) Harmonics.

Harmonics are familiar to the musicians as the overtones from an instrument. They are the integer multiples of the instrument's fundamental or natural frequency that are produced by a series of standing waves of higher and higher order.

Exactly the same thing happens in power circuits when non-linear loads create harmonic currents that are integer multiples of the supply fundamental frequency. The rapid growth of solid-state power electronics has greatly increased the number and size of these loads. The concept of harmonics was introduced in the beginning of the 19^{th} century by Joseph Fourier. Fourier has demonstrated that all periodic non-sinusoidal signals can be represented by infinitive sum or series of sinusoids with discontinuous frequencies as given by Eqn. 2.1.

$$i(t) = I_0 + \sum_{h=1}^{\alpha} I_h \cos(h\omega t + \varphi_h) \tag{2.1}$$

The component I_0 in the Fourier series is the direct component. The first term of the sum with the index h=1 is the fundamental of the signal. The rest of the series components are called the harmonics of the range h. Figure 2.2 Shows the form of a wave containing the third harmonic (h=3). In the three phase electric grid, the principle harmonic components are the harmonics of ranges (6*h±1) [33].

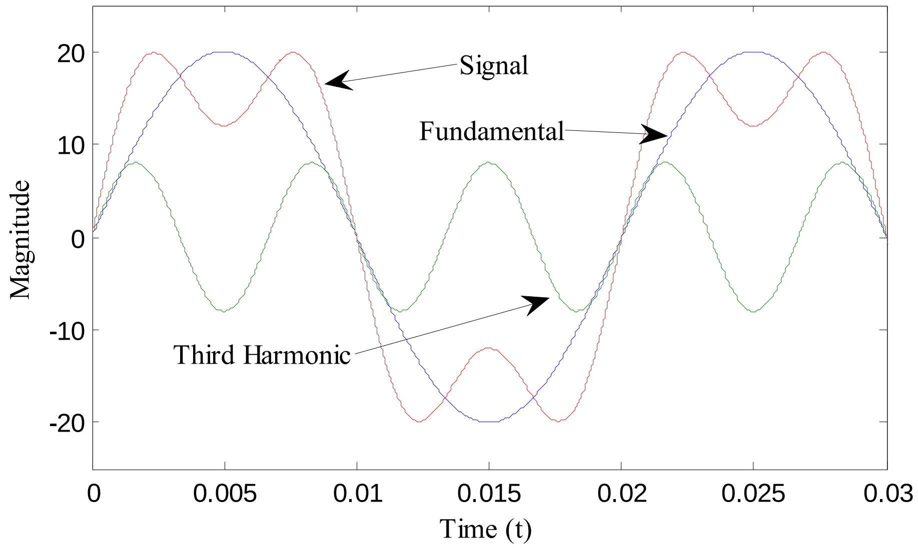

Figure 2.2: Harmonic content of a signal and its fundamental.

Transformer exciting current, arc furnaces, rectifiers, and many other loads will produce harmonics in the utility lines. Most utilities limit the allowable harmonic current levels to the values shown in IEEE 519.

2.1.6.1 Total Harmonic Distortion (THD)

The total harmonic distortion of a signal is a measurement of the harmonic distortion present in current or voltage. It is defined as the ratio of the sum of the powers of all harmonic components to the power of the fundamental frequency. Harmonic distortion is caused by the introduction of waveforms at frequencies in multiplies of the fundamental.

$$THD(\%) = \frac{\sqrt{\sum_{i=2}^{\alpha} x_i^2}}{|x_1|} \qquad (2.2)$$

The THD is a very useful quantity for many applications. It is the most commonly used harmonic index. However, it has the limitation that, it is not a good indicator of voltage stress within a capacitor because that is related to the peak value of voltage waveform [11].

2.1.6.2 Distortion Factor

The distortion factor F_d is defined as the ratio between the fundamental and the signal in RMS values. It is given by:

$$F_d = \frac{I_{L1}}{I_{rms}} \qquad (2.3)$$

It is then equal to unity when the current is purely sinusoidal and decreases when the distortion appears.

2.1.6.3 Crest Factor

The crest factor of a signal F_c is defined by Eqn. (2.4):

$$F_c = \frac{crest\,value}{effective\,value} \qquad (2.4)$$

For sinusoidal waves, the crest factor is 1.41. It can achieve the value of 5 in the case of highly distorted waves.

2.1.6.4 Effects of Harmonics

Harmonic currents will flow into the utility feeder and may create a number of problems in so doing. They may be trapped by power factor correction capacitors and overload them or cause resonant over-voltages. They can distort the feeder voltage enough to cause problems in computers, telephone lines, motors, and power supplies, and may even cause transformer failures from eddy current losses. The harmonic currents may be trapped by installing series LC filters resonant at the offending frequencies. These filters should be designed to offer low impedance at the resonant frequency compared to the source impedance at that frequency. But, again, there is a hidden “gotcha.” If a filter is installed that has a series resonance at the 7th harmonic, it will also have a parallel resonance with the utility at a lower frequency when the source inductance is added to the filter inductance. If this parallel resonance should lie on or near the 5th harmonic, there is the possibility of the resonant over-currents described earlier. The installation of series resonant traps will always introduce parallel resonances at frequencies below the trap frequencies. Good practice dictates that multiple resonant traps be installed first at the lowest harmonic frequency of concern and then in sequence at the higher-frequency harmonics. If switched, they should be switched on in sequence starting with the lowest frequency trap and switched out in sequence starting from the highest frequency trap [34].

The voltage or current distortion limit is determined by the sensitivity of loads (also of power sources), which are influenced by the distorted quantities. The least sensitive is heating equipment of any kind. The most sensitive kind of equipments is those electronic devices which have been designed assuming an ideal (almost) sinusoidal fundamental frequency voltage or current waveforms. Electric motors are the most popular loads which are situated between these two categories.

2.1.6.5 Power Factor

Power factor is defined as the ratio of real power to volt-amperes and is the cosine of the phase angle between the voltage and the current in an AC circuit. These are neatly defined quantities with sinusoidal voltages and currents. Power factor can be improved by adding capacitors on the power line to draw a leading current and supply lagging VArs to the system. Power factor correction capacitors can be switched in and out as necessary to maintain VAr and voltage control [34].

For a sinusoidal signal, the power factor is given by the ratio between the active and the apparent power. Electrical equipments' parameters are normally given under nominal voltage and current. A low power factor can indicate bad use of these equipments. The apparent power can be defined by:

$$S = V_{rms} . I_{rms} = V_{rms} . \sqrt{\frac{1}{T}\int_0^T i_L^2 dt} \tag{2.5}$$

The active power P can be given by the relation:

$$P = V_{rms} . I_{L1} . \cos(\alpha 1) \tag{2.6}$$

The reactive power Q is defined by:

$$Q = V_{rms} . I_{L1} . \sin(\alpha 1) \tag{2.7}$$

The power factor in this case can be given by Eqn. 2.8.

$$\mathrm{P.F} = \frac{P}{S} = \frac{P}{\sqrt{P^2 + Q^2}} \tag{2.8}$$

In the case where there is harmonics, a supplementary power called the distorted power D appears. This power can be given by the relation 2.9.

$$D = V_{rms} . \sqrt{\sum_{n=2}^{\alpha} I_{Ln}^2} \tag{2.9}$$

The apparent power can then be expressed as:

$$S = \sqrt{P^2 + Q^2 + D^2} \tag{2.10}$$

The power factor is then given by:

$$PF = \frac{P}{\sqrt{P^2 + Q^2 + D^2}} \tag{2.11}$$

From eqn. 2.11, we can notice that the power factor decreases because of the existence of harmonics in addition to the reactive power consumption [35]. The Fresnel diagram of the power is given in Figure 2.3.

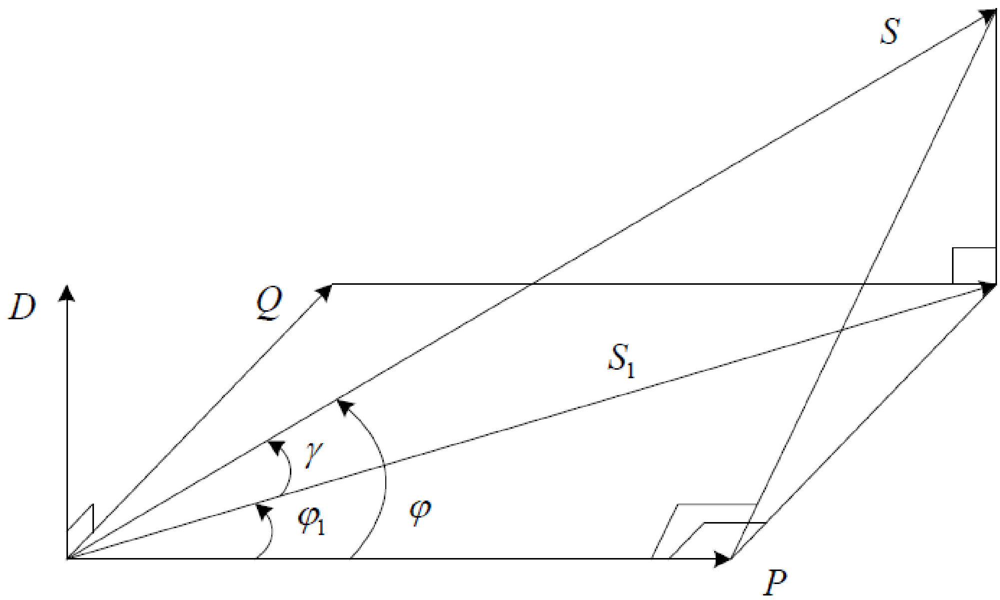

Figure 2.3: Fresnel representation of the power [36].

φ: The phase between active power P and apparent power S.

$φ_1$: The phase between active power P and apparent power S_1.

γ: The phase between apparent power in a linear system and that in a non-linear system.

2.2 Harmonic Currents Sources

The main cause of harmonics is the injection of harmonic currents by the non-linear loads. The bridges of diodes are the most non-linear loads present in the power applications because they don't need a control and they have long life duration with low cost [33]. There are also many other harmonic producing loads such as [11, 37]:

- ✓ Industrial equipments (welding machines, arc furnaces, induction furnaces, rectifiers).
- ✓ Offices equipments (computers, photocopiers,…etc).
- ✓ Domestic devices (TVs, micro-wave furnaces, neon lightening,…etc).
- ✓ Power inverters.
- ✓ Power transformers when working in the saturation zone also are considered as non-linear loads that produce harmonics.

The feeding of non-linear loads generates harmonic currents which spread into the electrical grid. The spread of current harmonics into the feeding impedances (transformers and grid) creates harmonic voltages in these feeders. Remembering that the conductor impedance increases with the frequencies of the currents which pass through it, different impedance will appear for each range of current harmonics. The harmonic current of range h will create through the impedance harmonic voltage. All the loads connected to the same point will be fed with the same perturbed voltage [37]. The equivalent circuit per phase of a non-linear load connected to the grid is given by Figure 2.4.

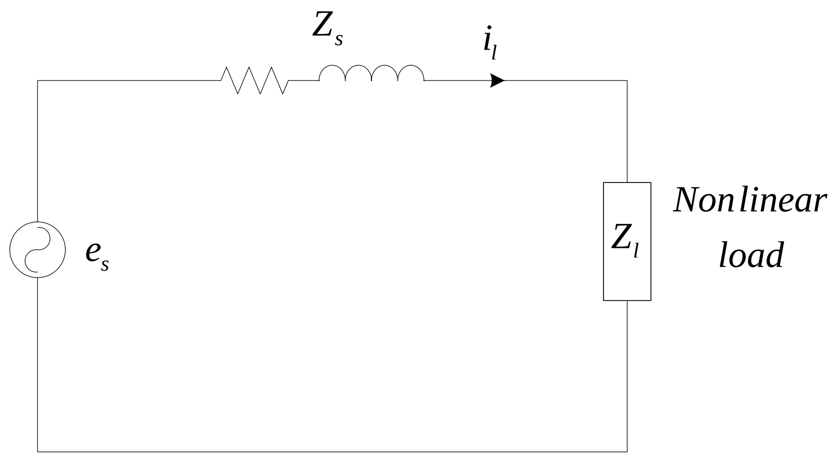

Figure 2.4: Equivalent circuit per phase of a non-linear load connected to the grid [35].

The spread of harmonic currents from different loads can be represented as in Figure 2.5.

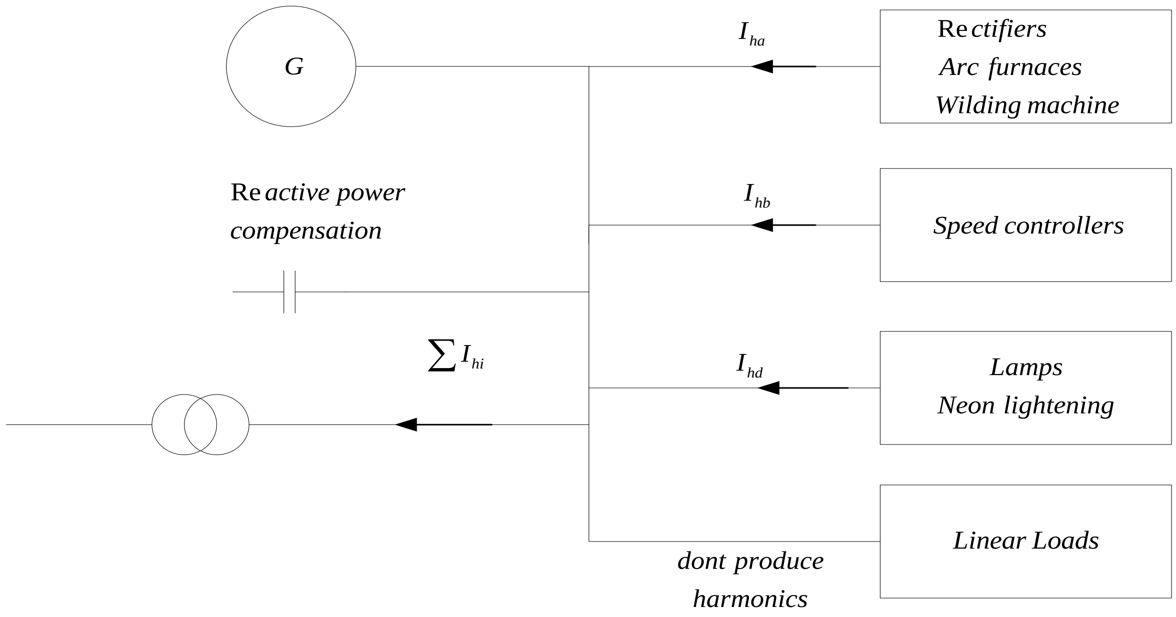

Figure 2.5: Spread of harmonic currents into the grid [37].

2.3 Economic effects of harmonics

- ✓ Premature aging of materials which forces its replacement, in addition to an initial over sizing of these materials.
- ✓ The overloading of the grid which implies to increase the nominal power and to oversize the installations, causing more and more losses.
- ✓ The current distortions cause sudden triggers and the stop of production equipments.

These material costs, energetic and production losses affect the competitiveness and the productivity of factories and companies.

2.4 Solutions for the Harmonics

The filtering of the grid currents and voltage is a priory problem for the distributer as like as the client. Because the limits on harmonic emission are not equally applied in the low of the different countries, the producers of the different electrical devices try to construct devices that satisfy for the conditions and limits of the international standards. The electric companies, from its side, use different filtering equipments and encourage the researches toward finding new efficient solutions for the power quality problems. The clients install also sometimes reactive power and harmonic compensation batteries to ameliorate the power factor and reduce the energy consumption bill.

Many traditional and modern solutions for harmonics mitigation and power quality improvement were proposed in literary. Some of these solutions investigate in the load to minimize the harmonic emission while the others propose the use of external filtering equipments that prevent the spread of harmonics into the grid [7].

2.4.1 In-Line Reactors

In-line reactor or choke is a simple solution to control harmonic distortion generated by adjustable speed drives. The solution is come up with inserting a relatively small reactor, or choke, at the input of the drive. The inductance prevents the capacitor to be charged in a short time and forces the drive to draw current over a longer time and reduces the magnitude of the current with much less harmonic content while still delivering the same energy [38].

2.4.2 Transformers with Passive Coupling

Some types of triangle zigzag coupling of transformers allow the elimination of the harmonics of order 3 and its multiples. The cost of these coupling types is the augmentation of the source impedance, and then the augmentation of voltage harmonic distortion [33, 38].

2.4.3 Passive Filters [33]

Passive filter, which is relatively inexpensive in comparison with the other harmonic reduction methods, is the most used method. Inductance, capacitor and the load as a resistance are tuned in a way to control the harmonics. However, they suffer from interfering with the power systems. Actually, passive filters are designed to shunt harmonics from the lines or block their flow through some parts of the systems by tuning the elements to create a resonance at the selected frequency. These filters are tuned and fixed according to the impedance of the point at which they will be connected and hence cannot be adjusted instantaneously in accordance to the load. As a result their cutoff frequency changes unexpectedly after any change in the load impedance resulting in producing a resonance with other elements installed in the system.

2.4.3.1 Resonant Filter

The resonant passive filter shown in Figure 2.6 is constructed by an inductor connected in series with a capacitor calculated in accordance with the harmonic range that to be eliminated. This filter has low impedance to the concerned harmonics and enough high for the fundamental frequency. As a result there must be one filter for each harmonic range to be eliminated [35]. The equivalent circuit of the resonant filter with the harmonic source and grid impedance is shown in Figure 2.7.

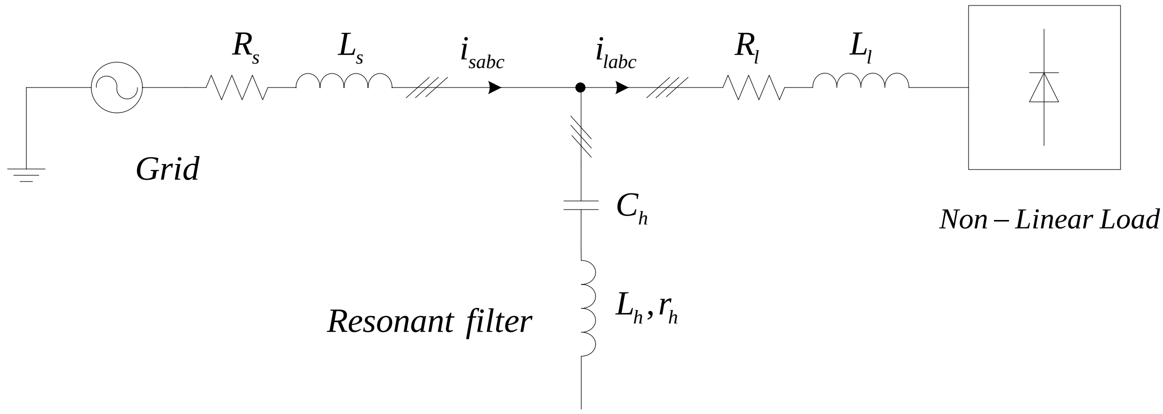

Figure 2.6: Resonant filter in parallel with non-linear load [35].

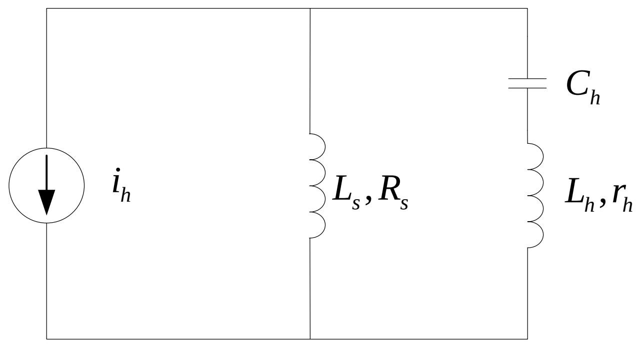

Figure 2.7: Harmonic equivalent circuit of passive filter with the grid impedance [12, 35].

2.4.3.2 Amortized Filter or High Pass Filter of Second Order

The second order high pass filter is constructed of passive elements RLC as shown in figure 2.8. The aim of this filter is to eliminate the harmonics in a large band. It is usually used in the elimination of high order harmonics which are enough away from the fundamental of the system.

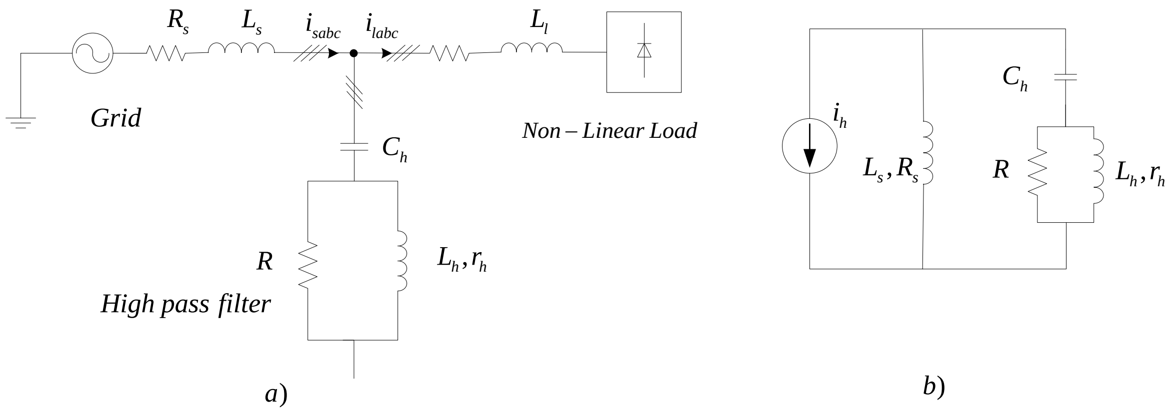

Figure 2.8: a) Diagram of the high pass filter. b) Equivalent circuit of the HPF.

2.4.3.3 Resonant Amortized Filter

These filters are composed of resonant filters for certain harmonic ranges, connected in parallel with high pass filter to eliminate the higher harmonics. Figure 2.9 shows the connection of resonant filter for 5th and 7th harmonics with high pass filter.

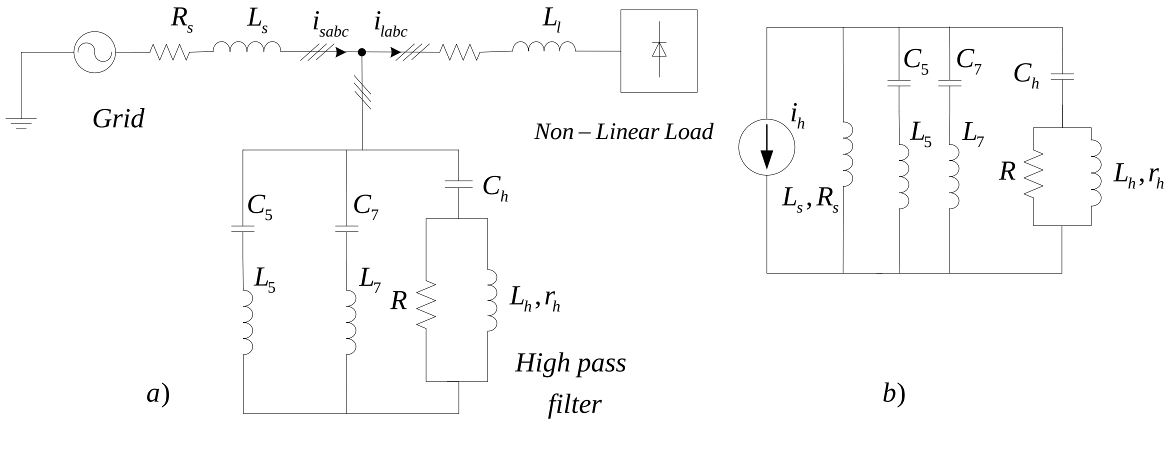

Figure 2.9: a) Diagram of the connection of amortized resonant filters. b) Equivalent circuit diagram. [12]

The traditional solutions generally used for harmonics reduction and power factor correction are composed of passive filters connected in parallel to trap the harmonic currents. These are composed of resonant filters or high pass filters of the second degree or amortized. These solutions extremely simple and widely used have at the same time important problems [35]:

- ✓ The construction of filter needs a brief knowledge of the configuration of the electric grid.
- ✓ The sizing of the filter is dependent on the harmonic specter and the grid impedance.
- ✓ Due to the existence of voltage harmonics, some current harmonics can be generated by the passive filters and injected into the grid.
- ✓ The variation of the source frequency affects the passive filter's compensation characteristics. In power systems we consider a high variation of frequency with about 0.5 Hz.
- ✓ Any modifications in the grid (restructuring, new clients,… etc) can affect the adaptation of the passive filter. That is, any modifications in the grid must be accompanied with modifications in the passive filter.
- ✓ There is a risk of resonance between the grid and the passive filters at specified frequencies. To solve this problem the quality factor of the filter is reduced which provoke the consumption of active power.
- ✓ These circuits are capacitive for the fundamental frequency and they are considered as reactive power sources.

These problems make the use of passive filters difficult and useless in many cases. The grid parameters are dynamically changing and the harmonic specter is variable. The construction of passive filters in accordance with specified harmonics is not sufficient to eliminate grid harmonics.

2.5 Modern Solutions for Harmonics' Problems

Modern solutions were proposed as efficient solutions for the elimination of electric grid harmonics in order to defeat the disadvantages of the traditional methods like passive filters [20]. Between these solutions we find two categories which are the most used:

- ✓ Active filters (series, parallel, or a combination of both of them in Unified Power Quality Conditioner (UPQC)).
- ✓ Hybrid filters composed of active and passive filters at once.

2.5.1 Active Power Filters

The function of the active power filters (APF) is to generate either harmonic currents or voltages in a manner such that the grid current or voltage waves conserve the sinusoidal form. The APFs can be connected to the grid in series (Series APF), shunt (SAPF) to compensate voltage harmonics or current harmonics respectively. Or can be associated with passive filters to construct the hybrid filters (HAPF).

Active filters are relatively new types of devices for eliminating harmonics. This kind of filter is based on power electronic devices and is much more expensive than passive filters. They have the distinct advantage that they do not resonate with the power system and they work independently with respect to the system impedance characteristics. They are used in difficult circumstances where passive filters don't operate successfully because of resonance problems and they don't have any interference with other elements installed anywhere in the power system [38].

The active filters present many other advantages over the traditional methods for harmonic compensation such as [33]:

- ✓ Adaptation with the variation of the loads.
- ✓ Possibility of selective harmonics compensation.
- ✓ Limitations in the compensation power.
- ✓ Possibility of reactive power compensation.

2.5.1.1 Series Active Power Filter (series APF)

The aim of the series APF is to locally modify the impedance of the grid. It is considered as harmonic voltage source which cancel the voltage perturbations which come from the grid or these created by the circulation of the harmonic currents into the grid impedance. However, series APFs can't compensate the harmonic currents produced by the loads.

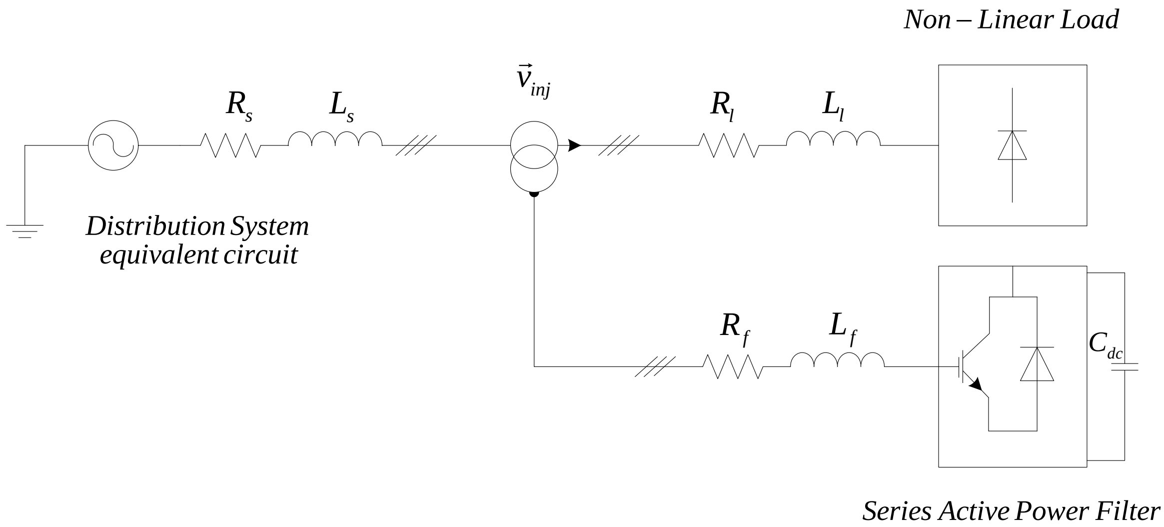

Figure 2.10: Series active power filter connected to the grid [20].

2.5.1.2 Shunt Active Power Filter (SAPF)

The SAPFs are connected in parallel with the harmonic producing loads. They are expected to inject in real time the harmonic currents absorbed by the pollutant loads. Thus, the grid current will become sinusoidal.

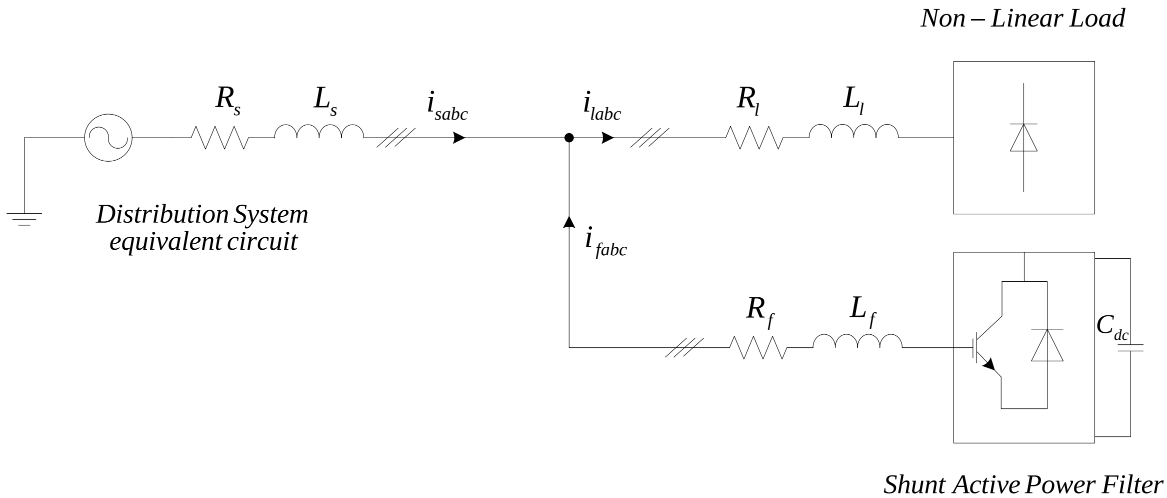

Figure 2.11: Shunt APF connected in parallel with non-linear load [20].

2.5.1.3 Combination of Parallel and Series APF (UPQC)

Figure 2.12 explains the combination of two APFs parallel and series, called also (Unified Power Quality Conditioner). This structure combines the advantages of the two APF type's series and parallel. So it allows simultaneously achieving sinusoidal source current and voltage [20].

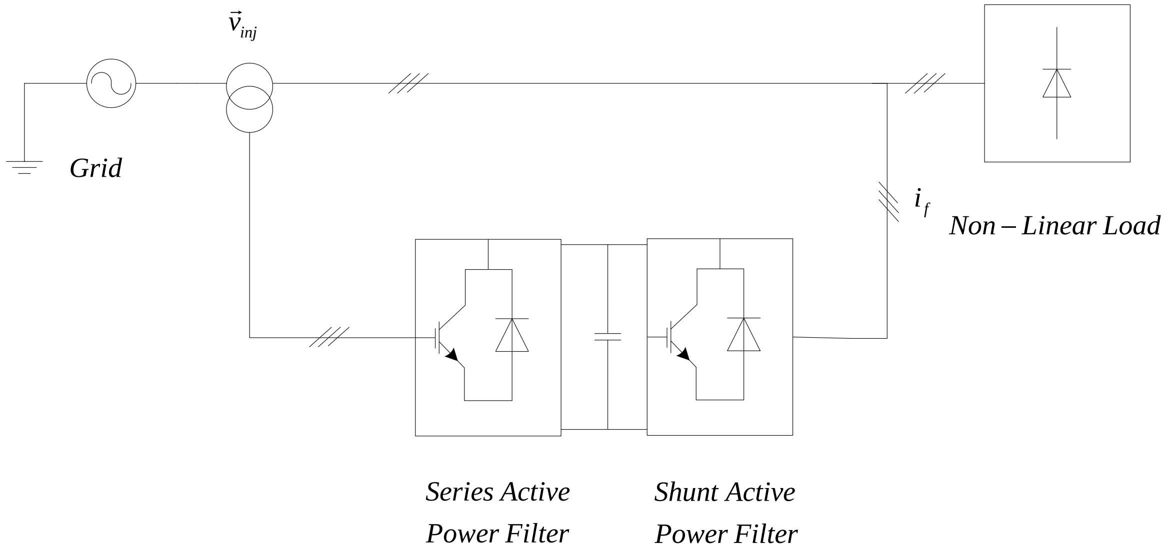

Figure 2.12: Unified Power Quality Conditioner's Diagram [20].

2.5.2 Hybrid Filters

Hybrid filter is a filter topology which combines the advantages of the passive and active filters. For this reason, it is considered as the best solution to eliminate the harmonic currents from the grid. The principal reason for the use of hybrid filters is the development of the power semiconductors like MOSFETs and IGBTs. Over more, from an economical point of view, the hybrid power filters allow reducing the cost of APF [39].

Hybrid power filters can be classified according to the number of elements used in the topology, the treated system (single phase, three phase three legs or four legs) and the used inverter type (current source inverter or voltage source inverter) [20].

2.5.2.1 Series Association of Active Filter with Passive Filter

In this configuration the active and passive filters are connected together directly in series. Then the system is connected in parallel with the grid as shown in figure 2.13.

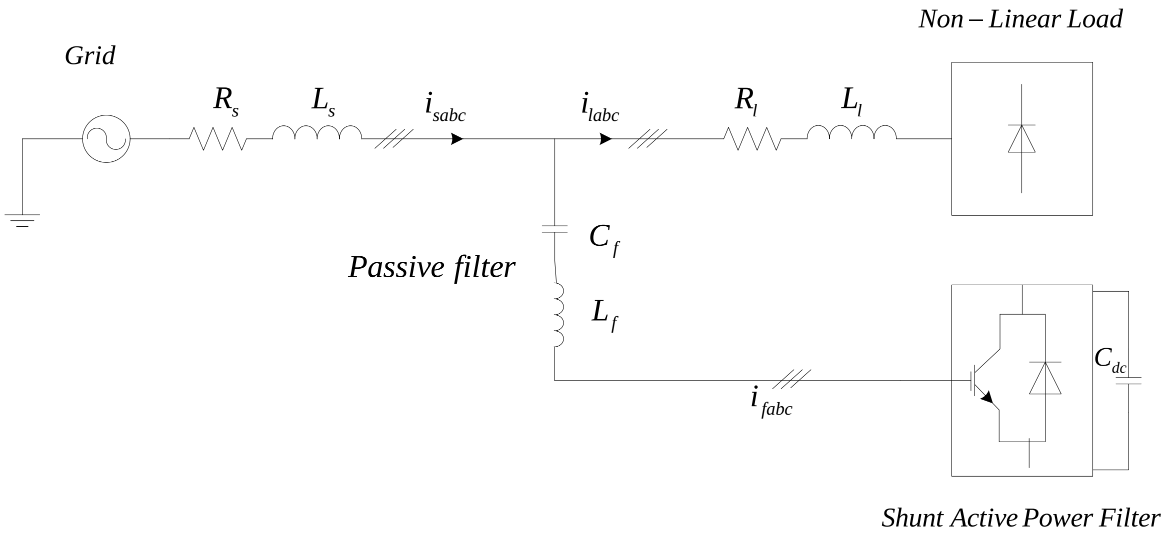

Figure 2.13: Series association of SAPF and passive filter [35].

2.5.2.2 Parallel Association of SAPF with Passive Filters

In this topology, the active filter is connected in parallel with the passive filter. Both of them are shunted with the load as shown in figure 2.14. The passive filters compensate certain harmonic ranges, while the active filter compensates the rest of the grid harmonics.

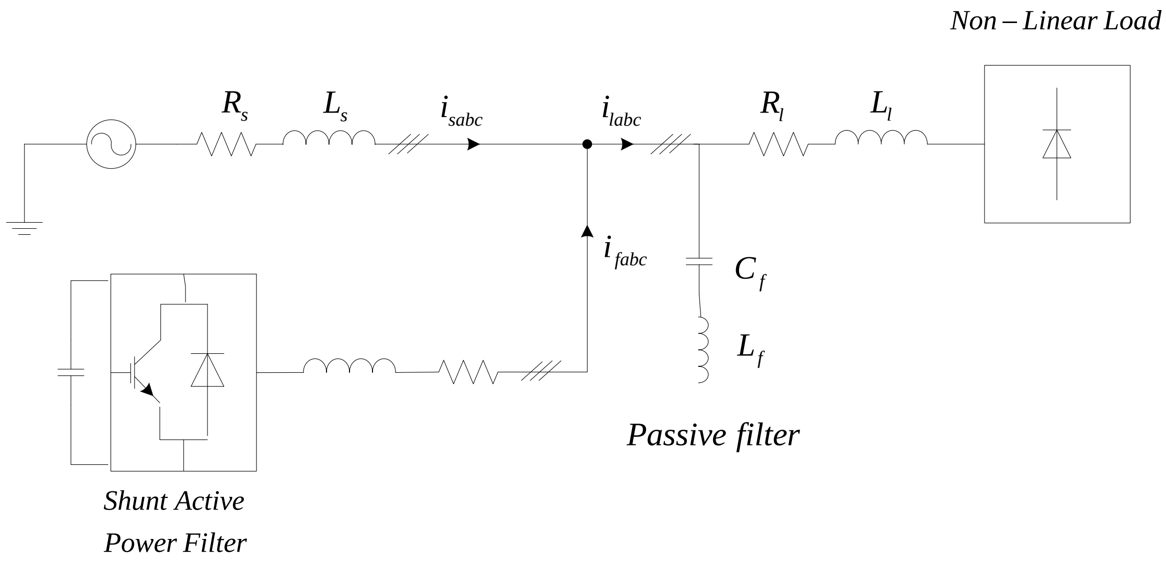

Figure 2.14: Parallel association of SAPF and passive filters [35].

2.5.2.3 Series Active Filter with Passive Filter

This structure shown in figure 2.15 allows the reduction of the risk of anti-resonance between the elements of passive filter and the grid impedance. In this case, the series active filter plays the role of a resistance against the harmonic currents and forces them to pass toward the passive filter without affecting the fundamental [20].

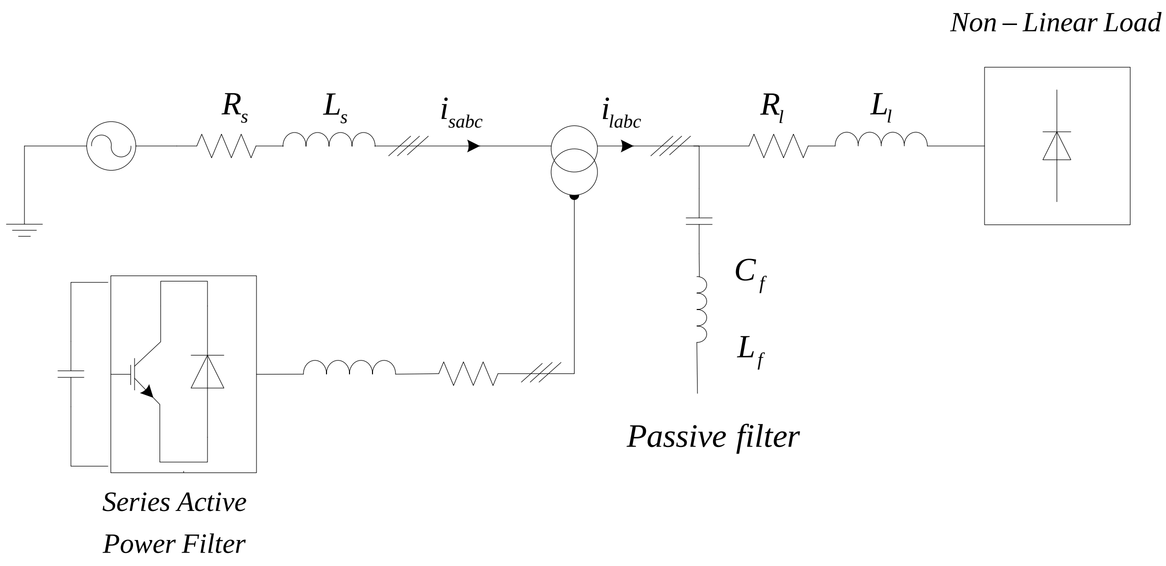

Figure 2.15: Series active power filter with passive filter [20].

2.6 Non-Linear Loads

When the input current into the electrical equipment does not follow the impressed voltage across the equipment, then the equipment is said to have a nonlinear relationship between the input voltage and input current [35 , 37, 40]. All equipments that employ some sort of rectification are examples of nonlinear loads. Nonlinear loads generate voltage and current harmonics that can have adverse effects on equipment designed for operation as linear loads. Transformers that bring power into an industrial environment are subject to higher heating losses due to harmonic generating sources (nonlinear loads) to which they are connected [40].

2.6.1 Modeling of the Non-Linear Load (Diode Bridge with Inductive Load)

The non-linear load is a three phase bridge rectifier connected to the grid by the means of line inductor (L_l, R_l) feeding an inductive load (R_{dc}, L_{dc}) as shown in figure 2.16.

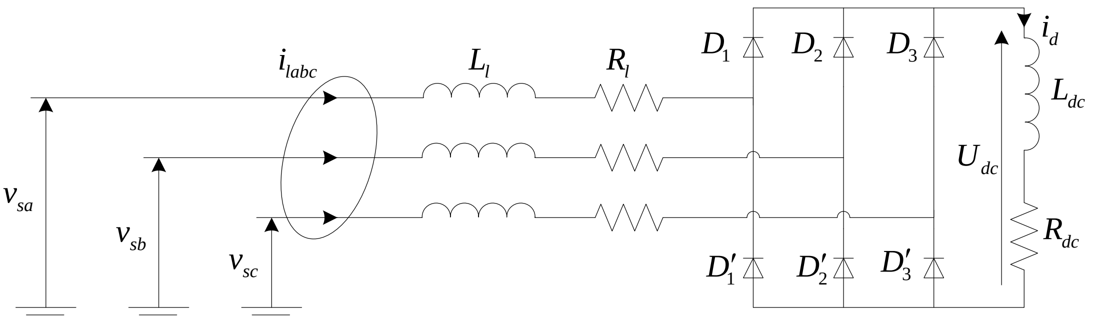

Figure 2.16: Diode bridge rectifier with RL load.

For the reason of simplification we suppose that the rectifier is ideal. Two diodes on the same leg of the rectifier can't have the same state at the same time. If D_1 is closed, one of the two diodes D_5 or D_6 is closed also. It is well known that D_1 is passing when the voltage v_{sa} is more than v_{sb} and v_{sc} or:

$$v_{sa} = \text{Max}(\text{v}_{sj}) \ ; \qquad j = 1,2,3 \qquad (2.12)$$

The same condition is applied on the other diodes and we find:

$$
\begin{aligned}
&D_i \text{ passes if } v_{si} = \mathrm{Max}(v_{sj}) \;\;;\;\; i, j = 1,2,3 \\
&D_{i+3} \text{ passes if } v_{si} = \mathrm{Min}(v_{sj}) \;\;;\;\; i, j = 1,2,3
\end{aligned}
\tag{2.13}
$$

The output voltage is given then by:

$$
U_{dc} = \mathrm{Max}(v_{sj}) - \mathrm{Min}(v_{sj}); \qquad j = 1,2,3 \tag{2.14}
$$

From where we can calculate the average of the output voltage, it is given by:

$$
\bar{U}_{dc} = \frac{3\sqrt{3}}{\pi} v_{peak} = \frac{3\sqrt{3}}{\pi} \sqrt{2} v = 1.654\sqrt{2} v \tag{2.15}
$$

Figure 2.17 shows the output voltage of the three phase diode rectifier and the line voltage on the PCC.

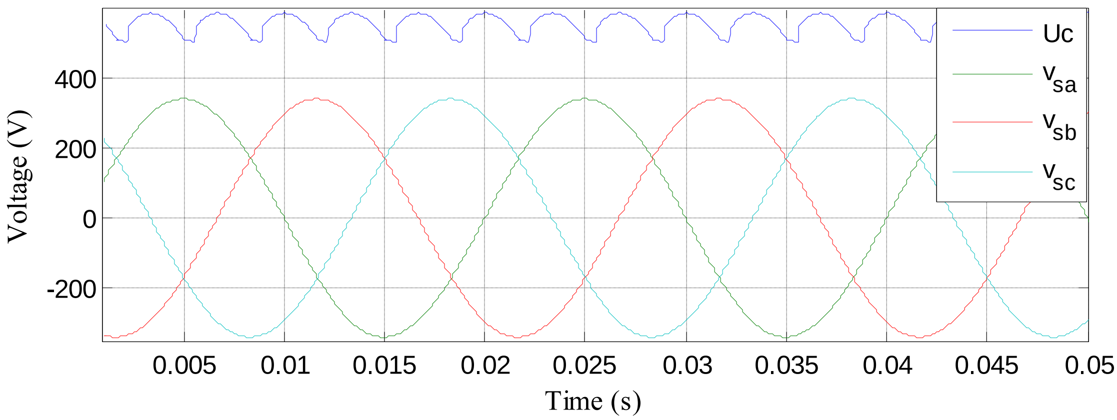

Figure 2.17: Input and output voltage of three phase bridge rectifier.

2.7 Shunt Active Power Filter

The concept of using active power filters to mitigate harmonic problems and to compensate reactive power was proposed more than two decades ago [41]. It has proven its ability to control the grid current and to ameliorate the power quality. The theories and applications of active power filters have become more popular and have attracted great attention. Without the drawbacks of passive harmonic filters, such as component aging and resonant problems, the active power filter appears to be a viable solution for reactive power compensation as well as for eliminating harmonic currents. As we mentioned earlier, the SAPF is connected in parallel with the non-linear load to behave as another controlled non-linear load. The system of the non-linear load and the SAPF will be seen by the grid as a linear load connected to the PCC. In the case of compensation of reactive power this load will be resistive. Otherwise it will be either inductive or capacitive linear load.

The general structure of the SAPF is composed of a two level, three level, or multilevel voltage source inverter with a DC power stock capacitor, input low pass filter, in addition to the associated control circuit. The construction of the SAPF and its control theories will be discussed in the next chapter of this work.

CHAPTER 3

SHUNT ACTIVE POWER FILTER

3.1 Overview

Shunt active power filter compensates current harmonics by injecting equal-but-opposite harmonic compensating currents into the grid. In this case the shunt active power filter operates as a current source injecting the harmonic components generated by the load but phase shifted by 180° [42]. This principle is applicable to any type of load considered as harmonic source. Moreover, with an appropriate control scheme, the active power filter can also compensate the load power factor. In this way, the power distribution system sees the non linear load and the active power filter as an ideal resistor. The current compensation characteristics of the shunt active power filter is shown in Figure 3.1 [43].

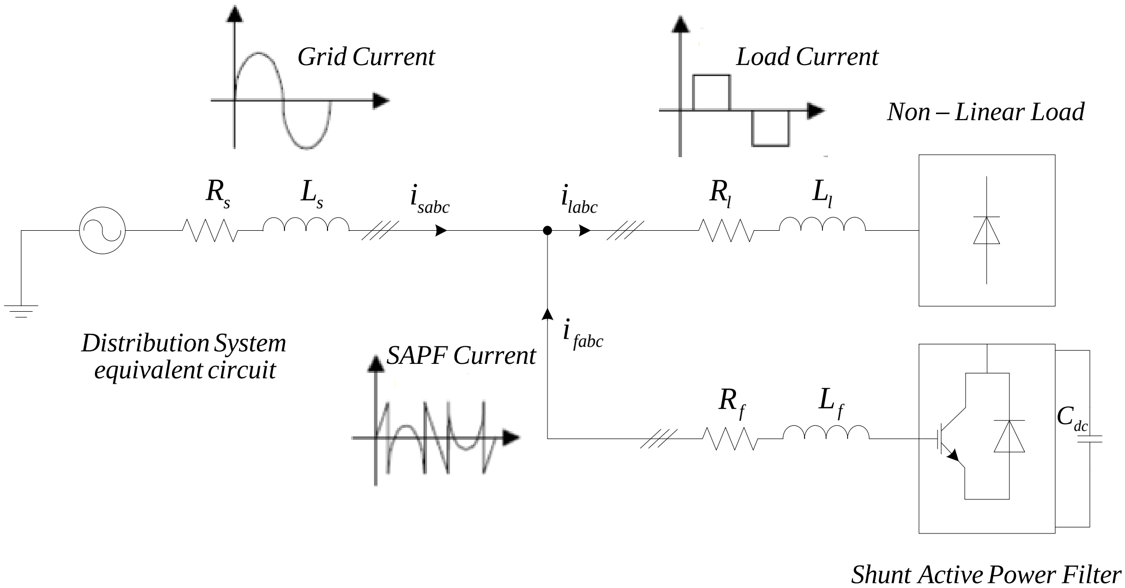

Figure 3.1 : Compensation characteristic of shunt active power filter [43].

3.2 Harmonic Current Extraction Methods

The aim of active power filtering is to compensate the harmonic currents produced by the non-linear loads, and to ensure the sinusoidal form of grid currents and voltages. The first step in active filtering is the harmonic currents extraction to be injected into the grid. The good extraction of harmonics is a keyword for a good active power filtering. Many extraction methods were proposed in literary. They can be divided into two families: the first family uses the Fast Fourier Transform (FFT) in the frequency domain to extract the current harmonics [44, 45]. The main disadvantages of this method are the bad results in transient, the heavy amount of calculations, and the use of considerable memory [45]. In addition to a delay in the extraction of harmonics which can be at least one period.

The second family is based on the time domain calculations in the extraction of harmonics. Some of its methods are based on the instantaneous active and reactive power. Others are based on the calculation of direct and indirect current components. Recently, the neural networks and the adaptive linear neural networks have been used in the extraction of harmonic components of current and voltage.

The time domain methods allow a faster response and less calculation and memory use [45].

3.2.1 Instantaneous Active and Reactive Power Theory

This method offers a good precision and ease of implementation. Its main disadvantage is that it can't be applied in the case of unbalanced grid voltage [44, 45]. In this case, A Self Tuning Filter (STF) can be used after the measurement of the grid voltages to extract the fundamental balanced three phase voltage components of the distorted unbalanced one. The study of the STF will be discussed later in appendixes.

Most APFs have been designed on the basis of instantaneous active and reactive power theory (p-q), first proposed by Akagi et al in 1983 [46, 47]. Initially, it was developed only for three-phase systems without neutral wire, being later worked by *Watanabe* and *Aredes* for three-phase four wires power systems [47]. The method uses the transformation of distorted currents from three phase frame *abc* into bi-phase stationary frame $\alpha\beta$. The basic idea is that the harmonic currents caused by nonlinear loads in the power system can be compensated with other nonlinear controlled loads. The p-q theory is based on a set of instantaneous powers defined in the time domain. The three-phase supply voltages (u_a, u_b, u_c) and currents (i_a, i_b, i_c) are transformed using the Clarke (or α-β) transformation into a different coordinate system yielding instantaneous active and reactive power components. This transformation may be viewed as a projection of the three-phase quantities onto a stationary two-axis reference frame. The Clarke transformation for the voltage variables is given by [4]:

$$\begin{bmatrix} u_\alpha \\ u_\beta \\ u_0 \end{bmatrix} = \sqrt{\frac{2}{3}} \begin{bmatrix} 1 & -\frac{1}{2} & -\frac{1}{2} \\ 0 & \frac{\sqrt{3}}{2} & -\frac{\sqrt{3}}{2} \\ \frac{1}{\sqrt{2}} & \frac{1}{\sqrt{2}} & \frac{1}{\sqrt{2}} \end{bmatrix} \begin{bmatrix} u_a \\ u_b \\ u_c \end{bmatrix} \tag{3.1}$$

Similarly, this transform can be applied on the distorted load currents to give:

$$\begin{bmatrix} i_{l\alpha} \\ i_{l\beta} \\ i_{l0} \end{bmatrix} = \sqrt{\frac{2}{3}} \begin{bmatrix} 1 & -\frac{1}{2} & -\frac{1}{2} \\ 0 & \frac{\sqrt{3}}{2} & -\frac{\sqrt{3}}{2} \\ \frac{1}{\sqrt{2}} & \frac{1}{\sqrt{2}} & \frac{1}{\sqrt{2}} \end{bmatrix} \begin{bmatrix} i_{la} \\ i_{lb} \\ i_{lc} \end{bmatrix} \tag{3.2}$$

The instantaneous active power *p(t)* is defined by:

$$p(t) = u_a i_{la} + u_b i_{lb} + u_c i_{lc} \tag{3.3}$$

This expression can be given in the stationary frame by:

$$\begin{cases} p(t) = u_\alpha i_{l\alpha} + u_\beta i_{l\beta} \\ p_0(t) = u_0 i_{l0} \end{cases} \tag{3.4}$$

Where, $p(t)$ is the instantaneous active power, $p_0(t)$ is the instantaneous homo-polar sequence power. Similarly the instantaneous reactive power can be given by:

$$q(t) = -\frac{1}{\sqrt{3}}[(u_a - u_b)i_{lc} + (u_b - u_c)i_{la} + (u_c - u_a)i_{lb} = u_\alpha i_{l\beta} - u_\beta i_{l\alpha} \tag{3.5}$$

It is important to notice that the instantaneous reactive power *q(t)* signify more than the simple reactive power. The instantaneous reactive power take in consideration all the current and voltage harmonics, where as the habitual reactive power consider just the fundamentals of current and voltage [4].

From eqns. 3.4 and 3.5 the instantaneous active and reactive power can be given in matrix form by:

$$\begin{bmatrix} p \\ q \end{bmatrix} = \begin{bmatrix} u_\alpha & u_\beta \\ -u_\beta & u_\alpha \end{bmatrix} \begin{bmatrix} i_{l\alpha} \\ i_{l\beta} \end{bmatrix} \tag{3.6}$$

In general, each one of the active and reactive instantaneous power contains a direct component and an alternating component. The direct component of each presents the power of the fundamentals of current and voltage. The alternating term is the power of the harmonics of currents and voltages.

In order to separate the harmonics from the fundamentals of the load currents, it is enough to separate the direct term of the instantaneous power from the alternating one. A Low Pass Filter (LPF) with feed-forward effect can be used to accomplish this task. Figure 3.2 shows the principle of this extraction filter.

Figure 3.2 : Diagram of the low pass filter with feed-forward.

After the separation of the direct and alternating terms of instantaneous power, the harmonic components of the load currents can be given using the inverse of equation (3.6) which gives:

$$\begin{bmatrix} i_{l\alpha} \\ i_{l\beta} \end{bmatrix} = \frac{1}{v_{s\alpha}^2 + v_{s\beta}^2} \begin{bmatrix} v_{s\alpha} & -v_{s\beta} \\ v_{s\beta} & v_{s\alpha} \end{bmatrix} \begin{bmatrix} \tilde{p}_l \\ \tilde{q}_l \end{bmatrix} \tag{3.7}$$

Where, the ˜ sign points to the alternating term and the ¯ sign points to the direct component of each active and reactive power. The APF reference current can be then given by:

$$\begin{bmatrix} i_{fa}^* \\ i_{fb}^* \\ i_{fc}^* \end{bmatrix} = \sqrt{\frac{2}{3}} \begin{bmatrix} 1 & 0 \\ -\frac{1}{2} & \frac{\sqrt{3}}{2} \\ -\frac{1}{2} & -\frac{\sqrt{3}}{2} \end{bmatrix} \begin{bmatrix} \tilde{i}_{l\alpha} \\ \tilde{i}_{l\beta} \end{bmatrix} \tag{3.8}$$

Figure 3.3 presents the principle of the active and reactive instantaneous power. This method offers the advantage of the possibility of harmonic compensation and/or reactive power compensation. In the case of reactive power compensation it is enough to send the reactive power q(t) directly to the reference current calculation bloc without the use of any extraction filter.

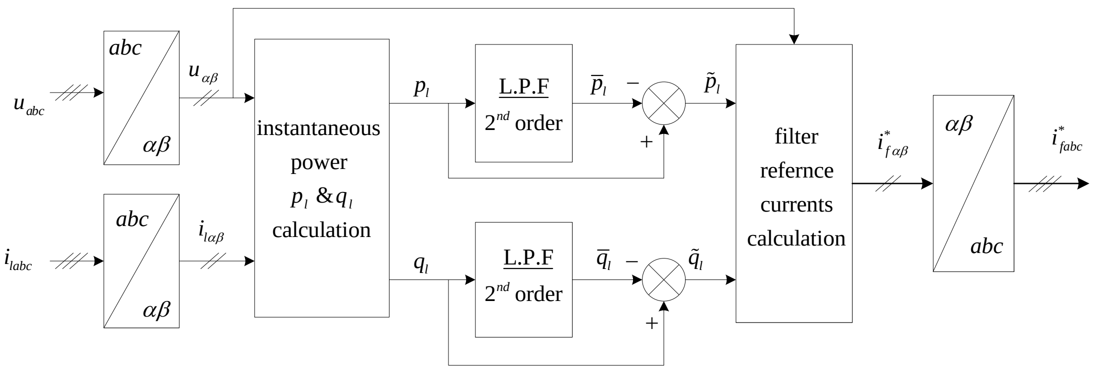

Figure 3.3 : Principle of instantaneous active and reactive power theory.

3.2.2 Synchronous Reference d-q Method

In this method, called also the method of instantaneous currents i_d, i_q, the load currents are transformed from three phase frame reference *abc* into synchronous reference in order to separate the harmonic contents from the fundamentals [7]. It gives better performance even in the case where the three phase voltage is not ideal. Fig. c presents the diagram bloc of this extraction method. The transform is defined by [45]:

$$\begin{bmatrix} i_{ld} \\ i_{lq} \\ i_{l0} \end{bmatrix} = \sqrt{\frac{2}{3}} \begin{bmatrix} \cos\theta & \cos(\theta - \frac{2\pi}{3}) & \cos(\theta + \frac{2\pi}{3}) \\ -\sin\theta & -\sin(\theta - \frac{2\pi}{3}) & -\sin(\theta + \frac{2\pi}{3}) \\ \frac{1}{\sqrt{2}} & \frac{1}{\sqrt{2}} & \frac{1}{\sqrt{2}} \end{bmatrix} \begin{bmatrix} i_{la} \\ i_{lb} \\ i_{lc} \end{bmatrix} \tag{3.9}$$

Where, θ is the angular position of the synchronous reference. It is a linear function of the fundamental frequency. This reference is turning in a synchronous constant speed with the three phase voltage [7]. The harmonic reference current can be extracted from the load currents using a simple LPF with feed-forward effect. The currents in the synchronous reference can be decomposed into two terms as:

$$\begin{cases} i_{ld} = \bar{i}_{ld} + \tilde{i}_{ld} \\ i_{lq} = \bar{i}_{lq} + \tilde{i}_{lq} \end{cases} \tag{3.10}$$

Only the alternating terms -which are related to the harmonic contents - will be seen at the output of the extraction system. Moreover, using the extraction system just on the d axe, all the q axe component will be used as compensation reference. This way, the reactive power consumed by the load will be compensated in addition to the harmonics. The APF reference currents will be then:

$$\begin{bmatrix} i_{fd}^{*} \\ i_{fq}^{*} \end{bmatrix} = \begin{bmatrix} \tilde{i}_{ld} \\ i_{lq} \end{bmatrix} \tag{3.11}$$

In order to find the APF currents in three phase system, the inverse Park transform can be used as follow:

$$\begin{bmatrix} i_{fa}^{*} \\ i_{fb}^{*} \\ i_{fc}^{*} \end{bmatrix} = \sqrt{\frac{2}{3}} \begin{bmatrix} \cos\theta & -\sin\theta \\ \cos(\theta - \frac{2\pi}{3}) & -\sin(\theta - \frac{2\pi}{3}) \\ \cos(\theta + \frac{2\pi}{3}) & \sin(\theta + \frac{2\pi}{3}) \end{bmatrix} \begin{bmatrix} i_{fd}^{*} \\ i_{fq}^{*} \end{bmatrix} \tag{3.12}$$

The determination of the angular position of the synchronous reference requires the use of a Phase Locked Loop (PLL).

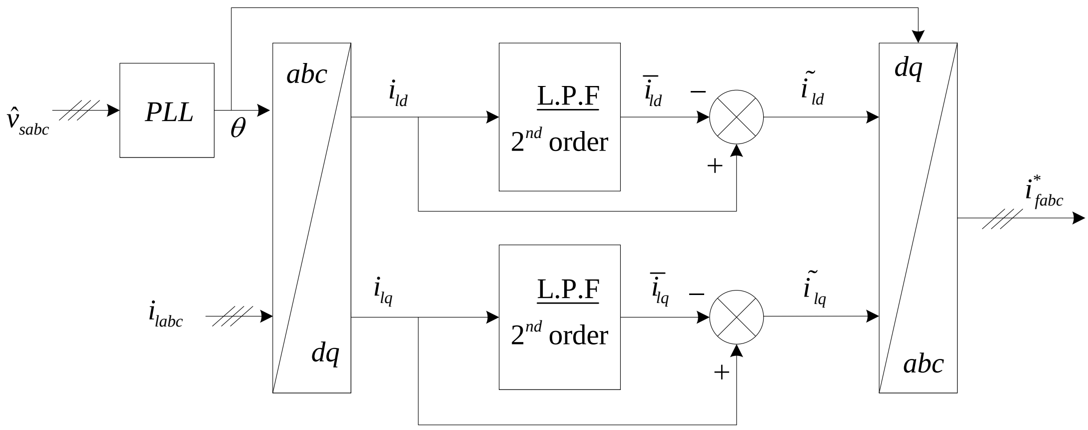

Figure 3.4 : Principle of the synchronous reference method [7].

3.2.3 RMS Value Based Algorithm

The analysis of the new reference current generation technique is based on the block diagram which is shown in Figure 3.5. For a three-phase three wire electrical power system, the load currents (i_{la}, i_{lb}, i_{lc}) are measured and transformed into stationary reference system. According to this method the high order harmonics, both in the phase and the magnitude of the load's current vector, are eliminated from the load currents. Then Eqn. 3.13 is used to calculate the magnitude of the reference current vector [48].

$$\left|I_{ref}\right| = \sqrt{i_{l\alpha}^{2} + i_{l\beta}^{2}} \tag{3.13}$$

To reduce the ripples of $|I_{ref}|$, a low pass filter is used. Also, a low pass filter is used to reduce the ripples from the vector I_{ref} angle. The currents i_α and i_β pass from a low pass filter and Eqn. 3.14 is used to calculate the new angle (gamma).

$$gamma = \tan^{-1}\left(\frac{i_{l\beta}}{i_{l\alpha}}\right) \tag{3.14}$$

From Eqn. 3.15 the sinusoidal mains current in α axis of αβ reference frame will be calculated and the sinusoidal mains current in a-axis of a-b-c reference frame will be calculated in Eqn. 3.16.

$$i_{s\alpha} = I_{ref}\cos(gamma) \tag{3.15}$$

$$i_{sa} = \sqrt{\frac{2}{3}} i_{f\alpha} \tag{3.16}$$

Where, i_{sa} is the rms value of the sinusoidal current of the phase a. In order to generate the three phase sinusoidal grid reference currents, the peak value of these currents can be given using Eqn. 3.17. Then the grid reference current can be generated using the angular position of the three phase reference generated by a PLL as in Eqn. 3.18.

$$I_{sa\max} = \sqrt{2} i_{sa} \tag{3.17}$$

$$\begin{aligned} i_{sa}^{*} &= I_{s\max}\sin(\omega t) \\ i_{sb}^{*} &= I_{s\max}\sin(\omega t - \frac{2\pi}{3}) \\ i_{sc}^{*} &= I_{s\max}\sin(\omega t + \frac{2\pi}{3}) \end{aligned} \tag{3.18}$$

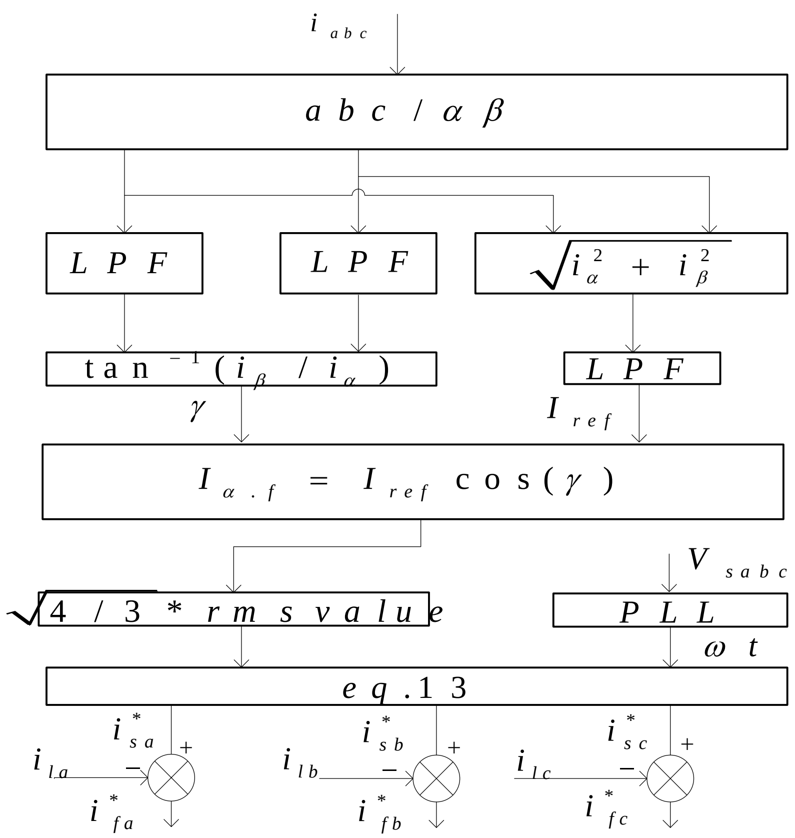

Figure 3.5 : RMS value based algorithm bloc diagram [48].

3.2.4 Active and Reactive Currents Method

In this method, instead of using the clarck transform to calculate instantaneous active and reactive power, it calculates directly the active and reactive parts of the load current. The currents are determined under the constraint that they must transport the same power absorbed by the load [49].

The reactive instantaneous current in the system is a component that doesn't contribute in the active energy transfer. But, it increases the current amplitude and the losses. This current can be determined using the Lagrange method.

If we suppose that the load current i_{Lk} with k=a, b, c is composed of active i_{Lka} and reactive i_{Lkr} parts as:

$$i_{Lk} = i_{LKa} + i_{Lkr} \tag{3.19}$$

The principle of this method is to determine the active current in the load current with the constraint that the reactive current doesn't produce any instantaneous active power. The task is then to minimize the function L given by:

$$L(i_{La}, i_{Lb}, i_{Lc}) = i_{La}^2 + i_{Lb}^2 + i_{Lc}^2 \tag{3.20}$$

With the constraint that:

$$p = v_a i_{La} + v_b i_{Lb} + v_c i_{Lc} \tag{3.21}$$

The problem can be solved using Lagrange method which leads to:

$$\begin{bmatrix} 2 & 0 & 0 \\ 0 & 2 & 0 \\ 0 & 0 & 2 \end{bmatrix} \begin{bmatrix} i_{La} \\ i_{Lb} \\ i_{Lc} \end{bmatrix} = -\lambda \begin{bmatrix} v_a \\ v_b \\ v_c \end{bmatrix} \tag{3.22}$$

In this equation, λ is given by:

$$\lambda = -\frac{2\mathrm{p}}{v_a^2 + v_b^2 + v_c^2} \tag{3.23}$$

From Eqns. 3.22 and 3.23 the currents can be given by:

$$\begin{bmatrix} i_{Laa} \\ i_{Lba} \\ i_{Lca} \end{bmatrix} = \frac{\mathrm{p}}{v_a^2 + v_b^2 + v_c^2} \begin{bmatrix} v_a \\ v_b \\ v_c \end{bmatrix} \tag{3.24}$$

The active currents obtained by Eqn. 3.24 and the original load currents produce the same instantaneous active power. This means that the load currents are equal to the active currents from the power point of view. The difference is that the active currents don't produce any reactive power and they have less root mean squared value than the original currents.

As in the PQ theory, the active instantaneous power has two components in addition to the zero components. The first direct represents the fundamentals of current and voltage and the second alternative represents the harmonics.

$$P = \bar{P} + \tilde{P} + P_0 \tag{3.25}$$

If we use the direct component of the power, the active fundamental currents will be achieved.

$$\begin{bmatrix} i_{Laaf} \\ i_{Lbaf} \\ i_{Lcaf} \end{bmatrix} = \frac{\bar{P}}{v_a^2 + v_b^2 + v_c^2} \begin{bmatrix} v_a \\ v_b \\ v_c \end{bmatrix} \tag{3.26}$$

A low pass filter of the second order can be used to extract the direct component of the power.

3.3 Voltage Source Inverter

Voltage source inverters (VSI) are one of the most important applications of power electronics. The main purpose of these devices is to provide a three-phase voltage source, where the amplitude, phase, and frequency of the voltages should always be controllable [49]. The important development of VSI is a result, from the one hand to the development of fast, controllable, powerful, and robust semi-conductors, from the other hand to the use of the so-called pulse width modulation (PWM) techniques. In the high power applications, the three level VSIs are the most adopted in comparison with two levels ones. Because the THD of the output voltage and current of the three levels VSI is clearly lower [50].

The standard three-phase VSI topology is shown in Figure 3.6. It is composed of three legs with current reversible switches, controlled for the open and close. These switches are realized by controlled switches (GTO or IGBT) with anti-parallel diodes to allow the flow of the free-wheeling currents [4, 6, and 51].

The eight valid switch states are given in Table 3.1. The switches of any leg of the inverter (T_1 and T_4, T_2 and T_5, T_3 and T_6) cannot be switched on simultaneously because this would result in a short circuit across the dc link voltage supply. Similarly, in order to avoid undefined states in the VSI, and thus undefined ac output line voltages, the switches of any leg of the inverter cannot be switched off simultaneously as this will result in voltages that will depend upon the respective line current polarity.

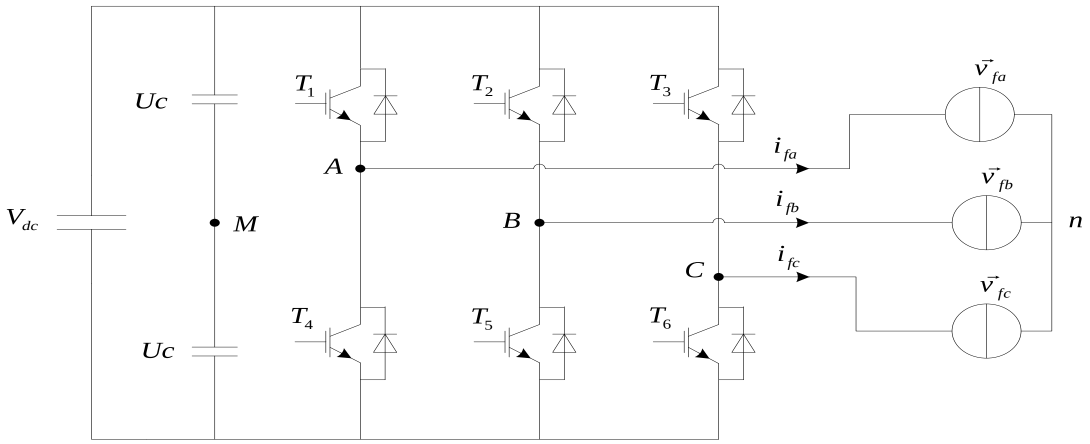

Figure 3.6 : Three-phase two levels VSI topology [49].

3.3.1 Modeling of Voltage Source Inverter

The output of the VSI which is shown in Figure 3.6 can take two levels of voltage ($+V_{dc}$, $-V_{dc}$) dependent on the dc source voltage and the switches states. Actually, the control of the two switches on the same leg is complementary: the conduction of one of them implies the blocking of the other.

The state of each one of the switches is defined by the control signals (S_a, S_b, and S_c) as follow:

$$S_a = \begin{cases} 1 \;\; if \;\; T_1 \, close \, \& T_4 \, open \\ 0 \;\; si \;\; T_1 \, open \, \& T_4 \, close \end{cases}$$

$$S_b = \begin{cases} 1 \ \ if \ \ T_2 \ close \ \& T_5 \ open \\ 0 \ \ if \ \ T_2 \ open \ \& T_5 \ close \end{cases}$$

$$S_c = \begin{cases} 1 \ \ if \ \ T_3 \ close \ et \ T_6 \ open \\ 0 \ \ if \ \ T_3 \ open \ \& T_6 \ close \end{cases}$$

From figure 3.6 the voltages of the points A, B, and C to the imaginary point M can be given by:

$$\begin{cases} V_{AM} = Uc.(2S_a - 1) \\ V_{BM} = Uc.(2S_b - 1) \\ V_{CM} = Uc.(2S_c - 1) \end{cases} \qquad ,with \ Uc = \frac{V_{dc}}{2}. \tag{3.27}$$

After the simplification of derivation the simple voltages of the VSI can be given by:

$$\begin{cases} v_{fa} = V_{An} = 2Uc \dfrac{2S_a - S_b - S_c}{3} = V_{dc} \dfrac{2S_a - S_b - S_c}{3} \\ v_{fb} = V_{Bn} = 2Uc \dfrac{2S_b - S_a - S_c}{3} = V_{dc} \dfrac{2S_b - S_a - S_c}{3} \\ v_{fc} = V_{Cn} = 2Uc \dfrac{2S_c - S_a - S_b}{3} = V_{dc} \dfrac{2S_c - S_a - S_b}{3} \end{cases} \tag{3.28}$$

Table 3.1 : VALID SWITCH STATES FOR A THREE-PHASE TWO LEVEL VSI

state	S_a	S_b	S_c	V_{fa}	V_{fb}	V_{fc}	α+jβ
0	0	0	0	0	0	0	0+j0
1	1	0	0	2/3	-1/3	-1/3	0,8+j0
2	0	1	0	-1/3	2/3	-1/3	-0.4+j0.7
3	1	1	0	1/3	1/3	-2/3	0.4+j0.7
4	0	0	1	-1/3	-1/3	2/3	-0.4-j0.7
5	1	0	1	1/3	-2/3	1/3	0.4-j0.7
6	0	1	1	-2/3	1/3	1/3	-0.81+j0
7	1	1	1	0	0	0	0+j0

3.3.2 Modeling of Active Power Filter

The connection of the shunt active power filter to the point of common coupling of the grid is done mostly by the mean of a RL low pass filter as shown in figure 3.7. The voltage equation for each phase can be given by:

$$\begin{aligned} v_{sk} &= v_{fk} - v_{L_{fk}} - v_{R_{fk}} \\ &= v_{fk} - L_f \frac{di_{fk}}{dt} - R_f i_{fk} \qquad ,k = a,b,c \end{aligned} \tag{3.29}$$

The three phase equations are then given by:

$$L_f \frac{d}{dt}\begin{bmatrix} i_{fa} \\ i_{fb} \\ i_{fc} \end{bmatrix} = -R_f \begin{bmatrix} i_{fa} \\ i_{fb} \\ i_{fc} \end{bmatrix} + \begin{bmatrix} v_{fa} \\ v_{fb} \\ v_{fc} \end{bmatrix} - \begin{bmatrix} v_{sa} \\ v_{sb} \\ v_{sc} \end{bmatrix} \tag{3.30}$$

And for the dc side:

$$C_{dc} \frac{dV_{dc}}{dt} = S_a i_{fa} + S_b i_{fb} + S_c i_{fc} \tag{3.31}$$

The equation system defining the SAPF in the three phase frame is then given by:

$$\begin{cases} L_f \dfrac{di_{fa}}{dt} = -R_f i_{fa} + v_{fa} - v_{sa} \\ L_f \dfrac{di_{fb}}{dt} = -R_f i_{fb} + v_{fb} - v_{sb} \\ L_f \dfrac{di_{fc}}{dt} = -R_f i_{fc} + v_{fc} - v_{sc} \\ C_{dc} \dfrac{dV_{dc}}{dt} = S_a i_{fa} + S_b i_{fb} + S_c i_{fc} \end{cases} \tag{3.32}$$

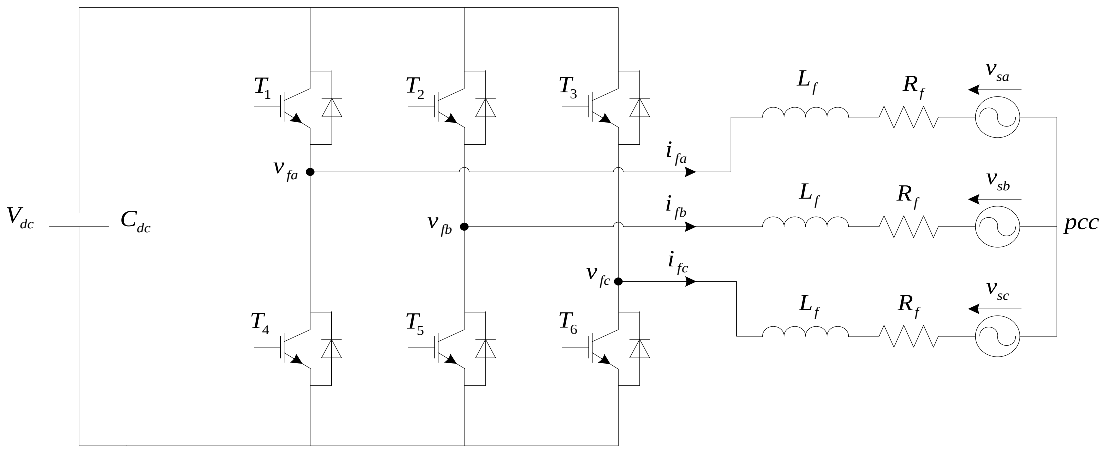

Figure 3.7 : SAPF connection to the PCC [49].

Applying the Park Transform on the system given by Eqn. 3.9, the modeling of the APF can be defined in the synchronous reference frame as follow:

$$\begin{cases} L_f \dfrac{di_{fd}}{dt} = -R_f\, i_{fd} - L_f\, \omega i_{fq} + v_{fd} - v_{sd} \\ L_f \dfrac{di_{fd}}{dt} = -R_f\, i_{fq} + L_f\, \omega i_{fd} + v_{fq} - v_{sq} \\ C \dfrac{dV_{dc}}{dt} = S_d i_{fd} + S_q i_{fq} \end{cases} \tag{3.33}$$

Where

$$S_d = S_\alpha \cos \omega t + S_\beta \sin \omega t$$
$$S_q = -S_\alpha \sin \omega t + S_\beta \cos \omega t$$
$$S_\alpha = \frac{1}{\sqrt{6}}(2S_a - S_b - S_c)$$
$$S_\beta = \frac{1}{\sqrt{2}}(S_b - S_c)$$

The modeling of the SAPF in the stationary reference frame can be derived by applying Concordia Transform on the system (3. 33) which gives:

$$\begin{cases} L_f \dfrac{di_{f\alpha}}{dt} = -R_f i_{f\alpha} + v_{f\alpha} - v_{s\alpha} \\ L_f \dfrac{di_{f\beta}}{dt} = -R_f i_{f\beta} + v_{f\beta} - v_{s\beta} \\ C_{dc} \dfrac{dV_{dc}}{dt} = S_\alpha i_{f\alpha} + S_\beta i_{f\beta} \end{cases} \tag{3.34}$$

3.3.3 Control Methods of VSI

The aim of the control of the VSC is to force the output currents of the inverter to follow their predefined reference currents. The main principle is based on the comparison between the actual current of the filter with the reference currents generated by the different extraction methods. In the next section, we are going to discuss some different methods in VSC control.

3.3.3.1 Hysteresis Control Method

The current control strategy plays an important role in fast response current controlled inverters such as the active power filters. The hysteresis current control method is the most commonly proposed control method in time domain. This method provides instantaneous current corrective response, good accuracy and unconditioned stability to the system. Besides that, this technique is said to be the most suitable solution for current controlled inverters.

Hysteresis current control is a method of controlling a voltage source inverter so that an output current is generated which follows a reference current waveform [9].

The basic structure of PWM voltage source inverter with hysteresis controller is shown in Figure 3.8. The hysteresis control strategy aims to keep the controlled current inside a defined rejoin around the desired reference current. The status of the switches is determined according to the error. When the current is increasing and the error exceeds a certain positive value, the status of the switches changes and the current begins to decrease until the error reaches a certain negative value, then the switches status changes again [23, 52, and 53].

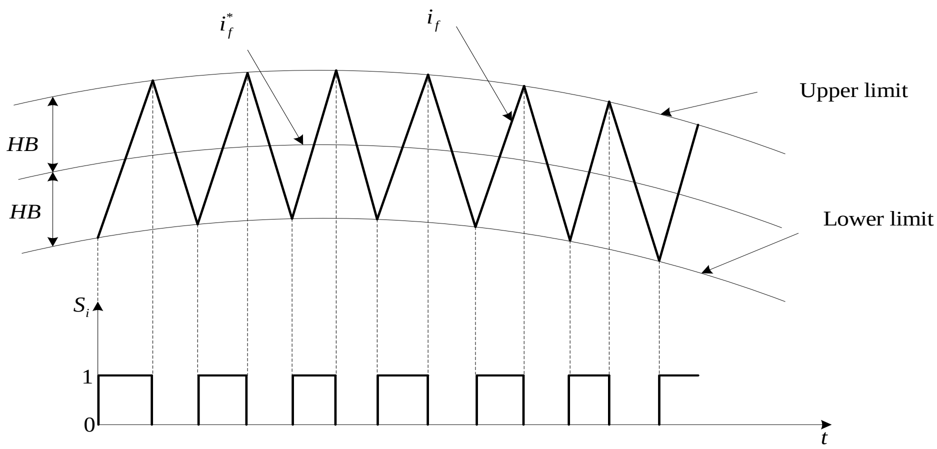

Figure 3.8 : Hysteresis control principle [23].

In the fix hysteresis band control of the VSI, the switching frequency is a function of the derivative of the output current. This one depends on the value of the inductance of the decoupling filter and the voltage drop around it. It is important to notice that the coupling filter affects the switching frequency and the dynamic behavior of the active filter. The simple implementation procedure is the main advantage of this control method. However, the variable switching frequency is the major draw-back of this method [4, 9, and 54]. This variable frequency affects mainly the function of power electronic elements which can't support high switching frequency in high power applications. In order to solve the problem of variable switching frequency, a new hysteresis control strategies like "modulated hysteresis control" [55, 56] and "variable hysteresis band" [41, 57] were proposed. In the modulated hysteresis control it is difficult to define the hysteresis band width. Over more, the fix switching frequency achieved using this method affects the rapidity obtained by hysteresis control [4].

3.3.3.2 Sinusoidal Pulse Width Modulation (SPWM) Control

The control techniques based on the PWM solve the problem of switching frequency of the VSI. They use a fix switching frequency which makes it easier to cancel the switching harmonics [4]. The PWM can be realized using different techniques such as carrier based PWM, PWM with harmonics minimization, and space vector PWM. The carrier PWM can be natural PWM, symmetric PWM, and asymmetric PWM [23].

The most simple and well known PWM technique is the sinusoidal PWM. This technique uses a controller which determines the voltage reference of the inverter from the error between the measured current and its reference. This reference voltage is then compared with a triangular carrier signal (with high frequency defining the switching frequency). The output of this comparison gives the switching function of the VSI [4]. The choice of the ratio between the frequency of the reference signal and the frequency of the carrier signal is very important in the case of symmetric and periodic reference. As a consequence, in the case of sinusoidal reference, the ratio between the two frequencies must be integer to synchronize the carrier with the reference. Over more, it is preferable that the carrier frequency be odd to conserve the reference symmetry. In all cases this ratio must be sufficiently high to ensure the fast switching [23] and to take the switching harmonics away from the fundamental produced by the inverter.

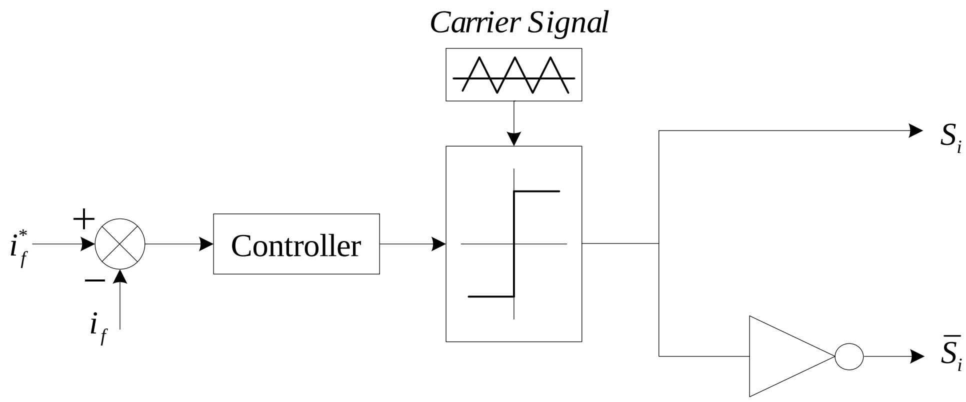

Figure 3.9 : The principle of sinusoidal PWM control method [23].

Recently, new control techniques called space vector PWM were implemented. The difference between this technique and the sinusoidal technique is that it doesn’t use carrier signal to define switching orders.

3.3.3.3 Space Vector PWM Control (SVPWM)

Space vector modulation technique was first introduced by German researchers in the mid of 1980s. This technique showed several advantages over the traditional PWM technique and has been proven to inherently generate superior PWM waveforms. By implementing the SVM technique, the number of switching is reduced to about 30% at the same carrier frequency of the sinusoidal pulse width modulation (SPWM) method. It offers better DC bus utilizations with lower THD in the AC current and reduces of switching losses too. The maximum modulation index for the SPWM method is 0.785 with the sinusoidal waveform between the phase and the neutral current of the system. However, the modulation index can be increased to 0.907 for the SVPWM [9].

The basic principle of the SVM technique is that it treats the inverter as a whole unit, which is different when compared to PWM technique. This technique is based on the decomposition of a reference voltage vector into voltage vector realizable on a six pulse inverter.

The SVPWM technique is widely used in inverter and rectifier controls. Compared to the sinusoidal pulse width modulation (SPWM), SVPWM is more suitable for digital implementation and can increase the obtainable maximum output voltage with maximum line voltage approaching 70.7% of the DC link voltage (compared to SPWM's 61.2%) in the linear modulation range. Moreover, it can obtain a better voltage total harmonic distortion factor. There are different algorithms for using SVPWM to modulate the inverter or rectifier. Many SVPWM schemes have been investigated extensively in literatures. The goal in each modulation strategy is to lower the switching losses, maximize bus utilization, reduce harmonic content, and still achieve precise control [58, and 59].

The output voltage of a VSI can be given in the stationary frame reference as shown in Tab. A. In the SVPWM scheme, the 3-phase output voltage is represented by a reference vector which rotates at an angular speed of $\omega = 2\pi f$. The task of SVM is to use the combinations of switching states to approximate the reference vector. To approximate the locus of this vector, the eight possible switching states of the inverter are represented as 2 null vectors and 6 active vectors.

These vectors can be used to frame the vector plane, which is illustrated in Figure 3.10. The rotating reference vector can be approximated in each switching cycle by switching between the two adjacent active vectors and the zero vectors. In order to maintain the effective switching frequency at a minimal value, the sequence of the toggling between these vectors is organized in such way that only one leg is affected in every step.

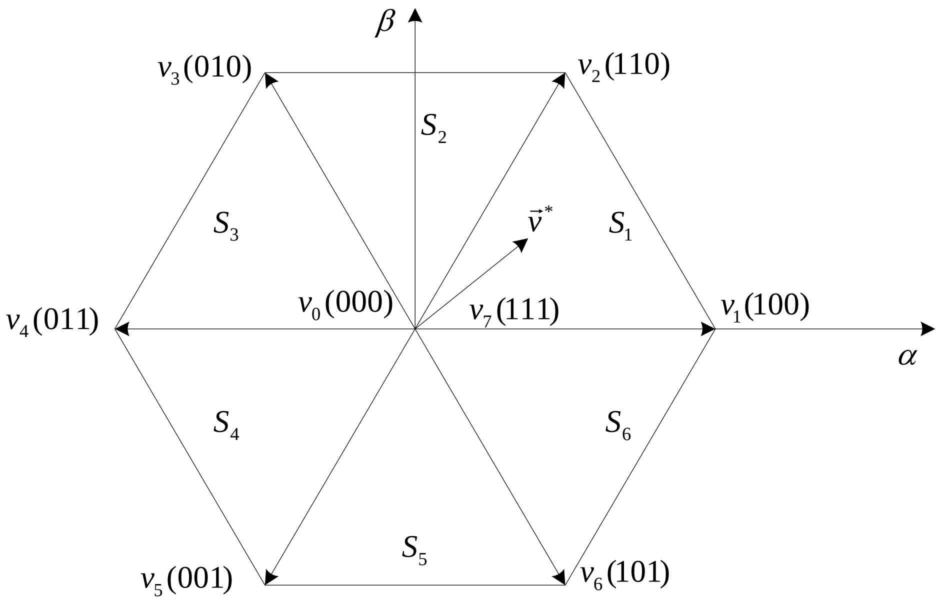

Figure 3.10 : Space vector representation of the inverter output voltage [58].

The choice of the null vector determines the SVM scheme. There are a few options: the null vector v_0 only, the null vector v_7 only, or a combination of the null vectors. A popular SVM technique is to alternate the null vector in each cycle and to reverse the sequence after each null vector. This will be referred to as the symmetric 7-segment technique. In the case where the reference vector appears in the sector S_1 as shown in Figure 3.10, we use the sequence v_0, v_1, v_2, and v_7 in the first half period $T_s/2$, and the sequence v_7, v_2, v_1, and v_0 in the second half period. In this case, the sequences are symmetrical [58].

To determine the sequence that corresponds to the reference vector, we must determine the modulus and the angle of this vector as given in Eqn. 3.35 and 3.36.

$$\mathrm{m} = |\vec{v}^*| = \sqrt{v_\alpha^2 + v_\beta^2} \tag{3.35}$$

$$\gamma = \arctan\left(\frac{v_\beta}{v_\alpha}\right) \tag{3.36}$$

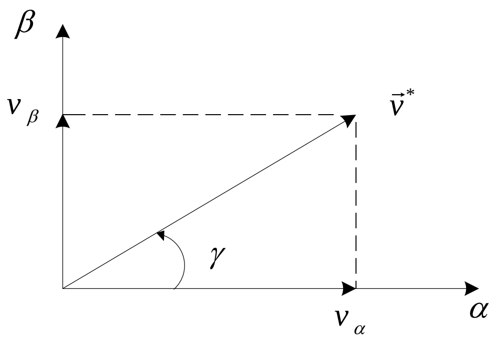

Figure 3.11 : Reference vector presentation in stationary frame [58].

To determine the conduction times for each sector during the period T_s, the mean value of the reference vector must be equal to the mean value of the three voltage vectors defining that sequence. This is defined by:

$$\frac{1}{T_s}\int_0^{T_{com}} \vec{v}^* dt = \frac{1}{T_s}\left[\int_0^{t_0} \vec{v}_{0,7} dt + \int_{t_0}^{t_0+t_1} \vec{v}_i dt + \int_{t_0+t_1}^{t_0+t_1+t_2} \vec{v}_{i+1} dt\right] \tag{3.37}$$

Where, we can find:

$$T_s \vec{v}^* = t_1 v_i + t_2 v_{i+1} + t_0 v_{0,7} \qquad (i = 0,1,...,5) \tag{3.38}$$

$$\text{with } v_i = \sqrt{\frac{2}{3}} V_{dc} \quad \text{is the modulus of vector } \vec{v_i} \quad i = 1,..,5$$

As an example, the case of the first sector is given and the conduction times of each one of the consecutive vectors are calculated. The reference vector is defined in S_1, the two adjacent active vectors are v_1 and v_2. The projection of these two vectors and the reference vector on the stationary plan gives:

$$\begin{cases} T_s \left|v^*\right| \cos\gamma = t_1 v_1 \cos(0) + t_2 v_2 \cos(60) \\ T_s \left|v^*\right| \sin\gamma = t_1 v_1 \sin(0) + t_2 v_2 \sin(60) \end{cases} \tag{3.39}$$

The solution of these equations gives the periods of application of each one of the two active vectors, defined by:

$$t_1(v_1) = \frac{\sqrt{3}}{2}\frac{T_s.m}{V_{dc}}(-\sin(\gamma) + \sqrt{3}.\cos(\gamma))$$

$$t_2(v_2) = \sqrt{3}\frac{T_s.m}{V_{dc}}.\sin(\gamma) \tag{3.40}$$

The null vectors are then applied on the rest of the period, defined by:

$$t_0 = T_s - (t_1 + t_2) \tag{3.41}$$

The same way we can determine the conduction periods for each one of the sectors defined by the sex active vectors in Figure 3.10.

3.3.3.3.1 Determination of Conduction Periods

In order to determine the duration of application of each pulse, the symmetric method of zero vectors was chosen. In this method, the time of application of the null vector is divided equally between the two null states $v_0(000)$ and $v_7(111)$ in order to minimize the switching losses. The sequences are chosen in a manner that ensures the switching of one interrupter in each transition between the sequences. To explain the idea let us take the case of the reference voltage in the second sector S_2, in this case, the vectors $v_2(110)$, $v_0(000)$, $v_7(111)$, and $v_3(010)$ can be applied. With the condition of minimum switching, the vector $v_0(000)$ can be applied for the period of $t_0/4$. Then we choose –from the three other vectors- the one that needs the minimum transitions. This one will be applied for the period of $t_1/2$ or $t_2/2$, in this example we find $v_3(010)$. Using the same manner until $T_s/2$, after $T_s/2$ we apply the same sequences symmetrically until T_s, the fig. L shows the conduction periods for each sector.

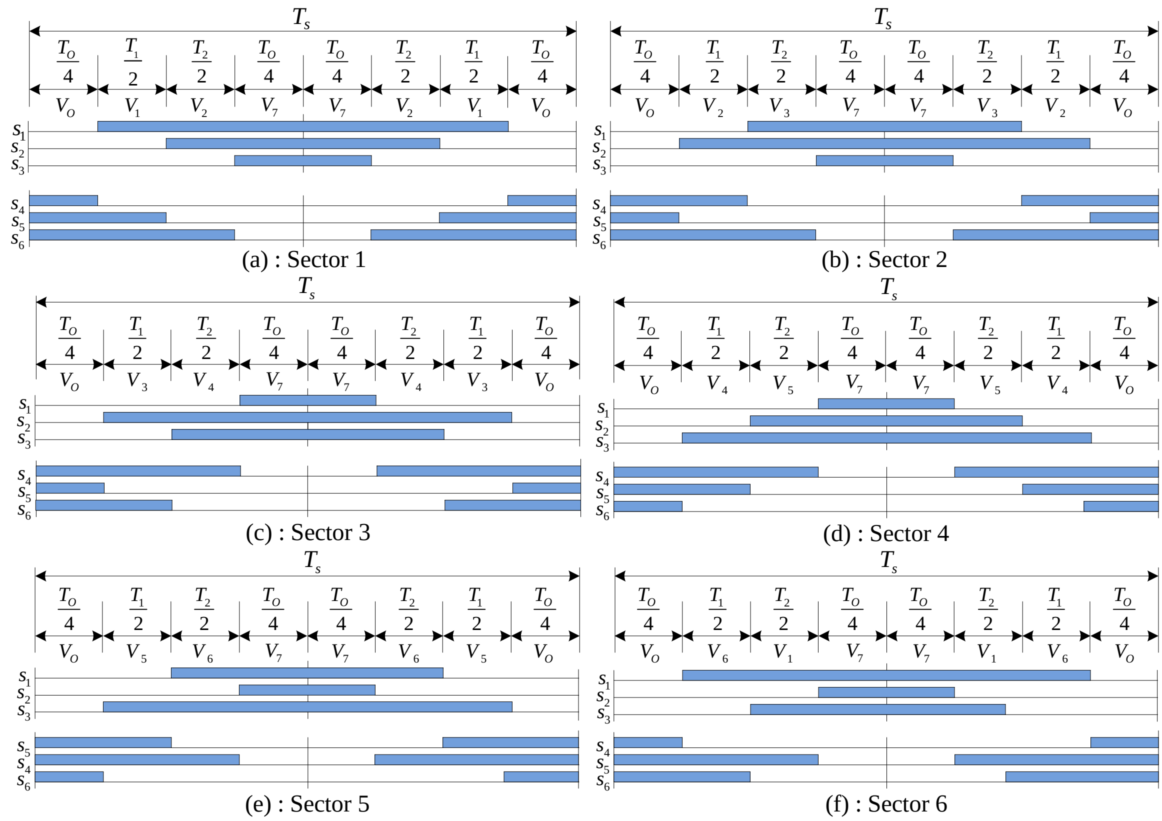

Figure 3.12 : Conduction periods for each voltage vector in the different sectors.

3.4 Control of the Active Power Filter

The researchers are always at the point of the research to ameliorate the control methods of the SAPF to achieve better results either from the point of view of better perturbation extraction methods, the amelioration of the dynamic regimes, decreasing the value of the THD,…etc, or the development of new control methods to ameliorate the performance of the APF with the different non-linear loads. There are principally two methods for the compensation of the harmonic currents dependent on the measured current:

- ✓ **Direct Control Method.**

In this method the load currents are measured and the harmonic currents are extracted from the load currents [21]. Figure 3.13 shows the diagram of the direct control method. Using this method, the SAPF injects the harmonic currents without any information about the grid currents. All the errors in the system like the parameters uncertainty, the measurement or control errors will appear in the grid current as unfiltered harmonic contents. The main advantage of this method is the system stability. However, this method needs an expanded control algorithm with large number of sensors [60].

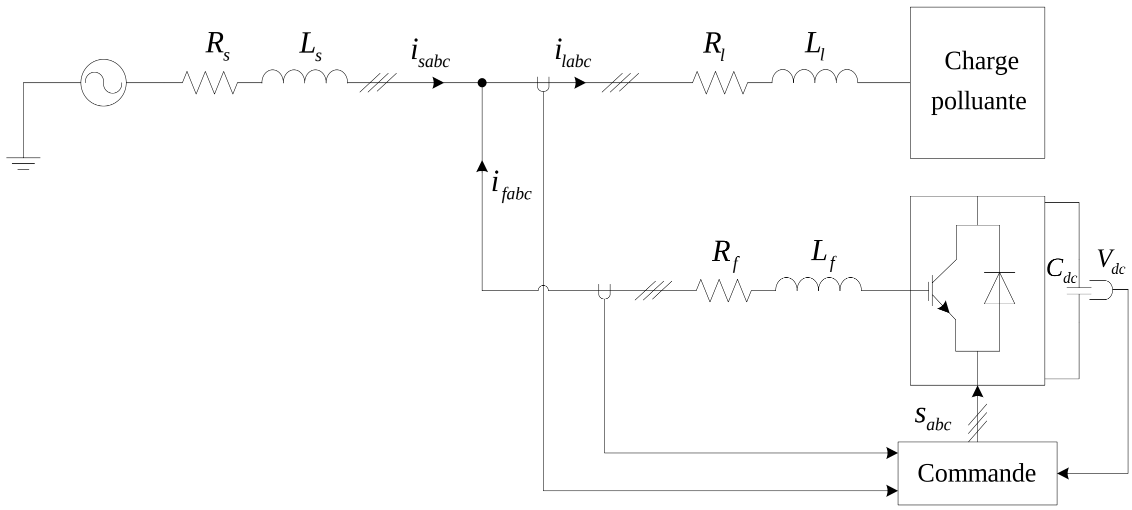

Figure 3.13 : Direct control method diagram [60].

- ✓ **Indirect Control Method.**

This method based on the measurement of the source currents, and then to impose the sinusoidal form on these currents. The control algorithm is less complicated and needs fewer sensors than the direct control. Figure 3.14 shows the diagram of the indirect control method of the SAPF.

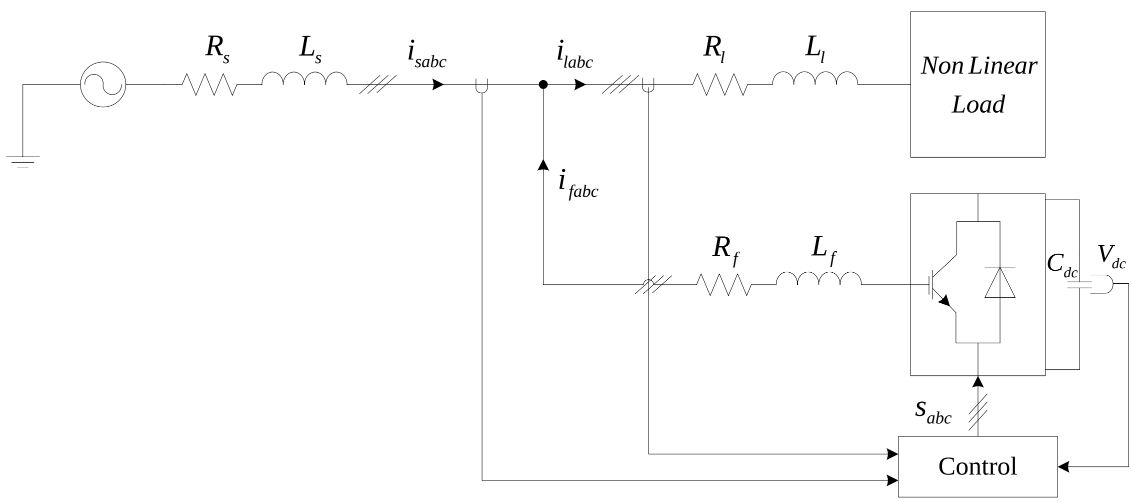

Figure 3.14 : Indirect control method diagram [60].

3.4.1 Direct Control Method

Figure 3.15 presents the global diagram of the direct control method of parallel active power filter. Applying the Laplace transform on the equation of the APF voltages we can find:

$$V_f(S) = V_s(S) + SL_f I_f(S) + R_f I_f(S) \tag{3.42}$$

Where we can describe the filter current by:

$$I_f(S) = \frac{V_f(S) - V_s(S)}{L_f S + R_f} \tag{3.43}$$

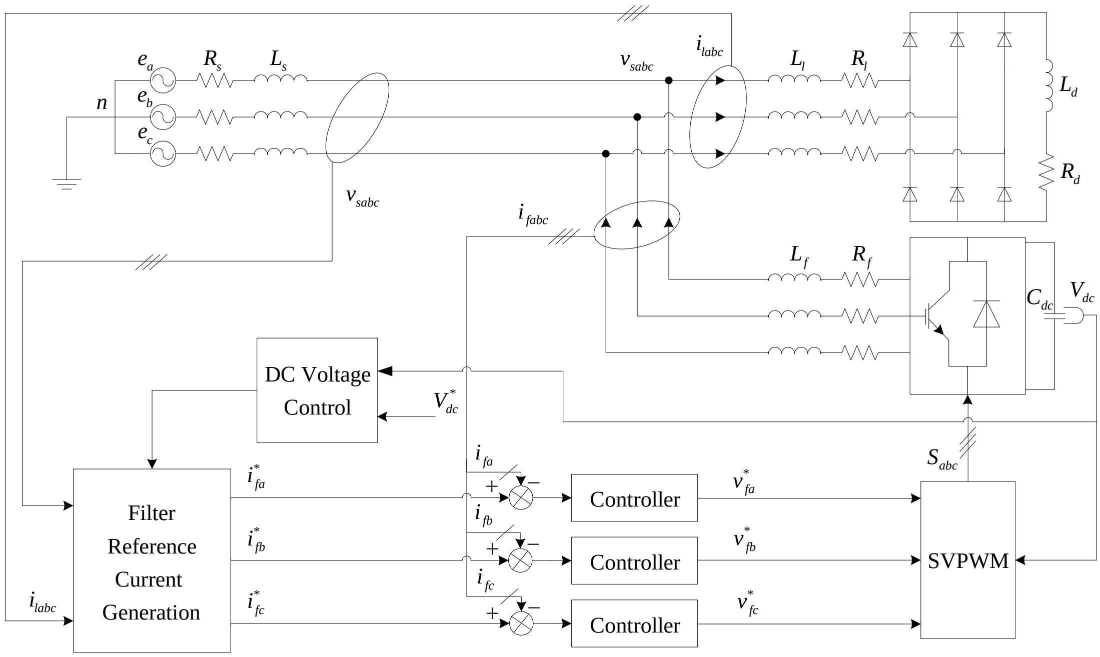

Figure 3.15 : Direct control of shunt active power filter.

The voltage V_f given by eqn. 3.42 is composed of two different frequency parts. The first is the grid voltage –at the PCC- which is a measurable quantity. The second part is the voltage across the coupling filter L_f when the reference current passes through it [6]. This component is compensated by the current controllers. Figure 3.16 shows the structure of the control loop with the voltage source inverter [61].

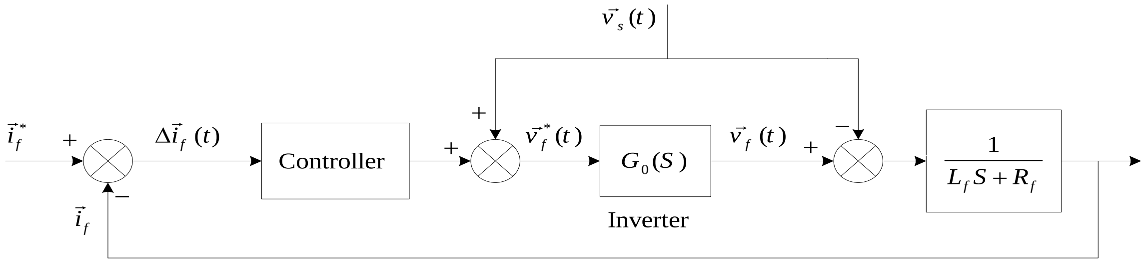

Figure 3.16 : Structure of current control loop [4, 6, 61].

In order that the output voltage of the VSI is equal to its reference, a good choice of the transfer function which represents the inverter is to be 1 [4, 6].

Control of Filter Current Using PI Controllers

3.4.1.1 Control in the Three Phase Reference

The PI controller is the most classical controller used in the current regulation due to its simplicity. The simplified diagram of the current regulation using PI controller is shown in figure 3.17. Transfer function in closed loop for this diagram is given by:

$$H_{CL} = \frac{k_{pi} S + k_{ii}}{L_f S^2 + (R_f + k_{pi}) S + k_{ii}} \tag{3.44}$$

It can be written in the next form:

$$H_{CL} = \frac{(2\xi\omega_c - \frac{R_f}{L_f}) S + \omega_c}{S^2 + 2\xi\omega_c S + \omega_c^2} \tag{3.45}$$

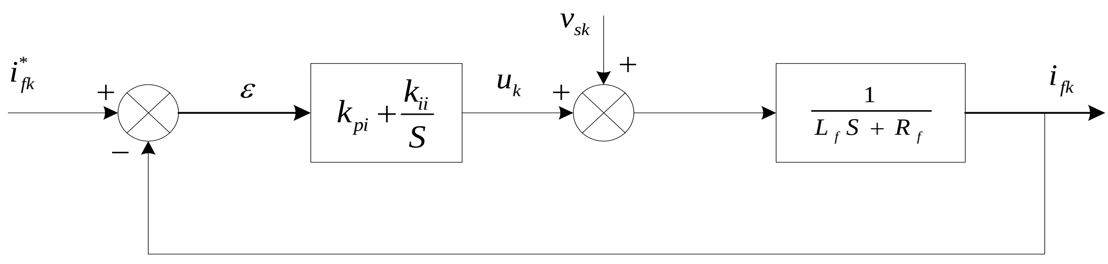

Figure 3.17 : Diagram of PI current controller loop [6].

The value of the damping factor is chosen to be 0.707 for a good dynamic response. In order to reject the harmonics due to the switching, the cut off frequency of the system must be away from the PWM switching frequency [4, 61]. The constants of the controller are given by:

$$\begin{aligned} k_{pi} &= 2\xi\omega_c L_f - R_f \\ k_{ii} &= L_f \omega_c^2 \qquad\qquad \omega_c = 2\pi f_c \end{aligned} \tag{3.46}$$

The output of the regulator is added to the voltage of the PCC to cancel the effect of this voltage on the static behavior of the filter [4, 6].

3.4.1.2 Control in the Synchronous Frame Reference d-q

The structure of the direct control of the SAPF in the synchronous reference is shown in Figure 3.18. In this control the PI controllers are constructed to control the currents in the synchronous reference instead of controlling them in the three phase reference.

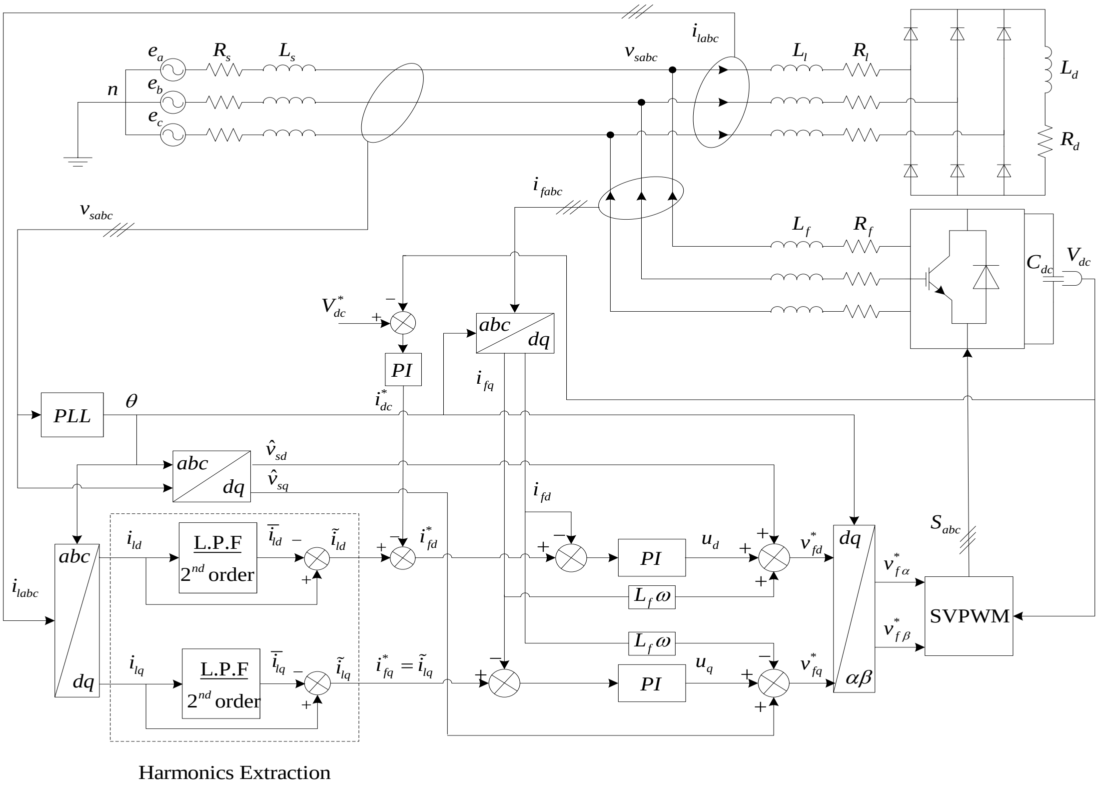

Figure 3.18 : Direct control by PI controllers in the synchronous reference.

From the model of the inverter given by the Eqn. 3.33, we can write:

$$\begin{aligned}
v_{sd} &= v_{fd} - R_f i_{fd} - L_f \frac{di_{fd}}{dt} - L_f \omega i_{fq} \\
v_{sq} &= v_{fq} - R_f i_{fq} - L_f \frac{di_{fq}}{dt} + L_f \omega i_{fd} \\
C\frac{dV_{dc}}{dt} &= S_d i_{fd} + S_q i_{fq}
\end{aligned} \tag{3.47}$$

3.4.1.2.1 Control of the Currents i_d and i_q

As it is clear from Eqn. 3.33, the currents on the axes *d* and *q* are coupled. To simplify the control of these two components, it is enough to separate them, by introducing new terms in the first and the second equation of the system 3.33, we define:

$$\begin{aligned}
u_d &= L_f \frac{di_{fd}}{dt} + R_f i_{fd} \\
u_q &= L_f \frac{di_{fq}}{dt} + R_f i_{fq}
\end{aligned} \tag{3.48}$$

It becomes then:

$$\begin{aligned}
v_{fd}^* &= u_d + v_{sd} + L_f \omega i_{fq} \\
v_{fq}^* &= u_q + v_{sq} - L_f \omega i_{fd}
\end{aligned} \tag{3.49}$$

Applying the Laplace transform on the first and the second system, we find:

$$G_{dq}(S) = \frac{I_{fd}(S)}{V_d(S)} = \frac{I_{fq}(S)}{V_q(S)} = \frac{1}{R_f + L_f S} \tag{3.50}$$

Figure 3.19 shows the diagram of the closed loop current control in the synchronous frame. The transfer function of the currents and the PI controller are indicated in this figure. The closed loop transfer function is given by [62]:

$$G_{CLdq}(S) = \frac{G_{PIdq}.G_{dq}}{1 + G_{PIdq}.G_{dq}} = \frac{\dfrac{k_{I_{id,iq}}}{L_f} + \dfrac{k_{p_{id,iq}}}{L_f} S}{S^2 + \dfrac{R_f + k_{p_{id,iq}}}{L_f} S + \dfrac{k_{I_{id,iq}}}{L_f}} \tag{3.51}$$

Where: $G_{PIdq} = k_{p_{id,iq}} + \dfrac{k_{I_{id,iq}}}{S}$

Comparing this transfer function with the canonic form of second order transfer function, we find:

$$k_{p_{id,iq}} = 2L_f \xi \omega_c - R_f \qquad and \quad k_{I_{id,iq}} = L_f \omega_c^2 \tag{3.52}$$

At last, the control lows in closed loop of the currents are given by:

$$\begin{aligned} v_{fd}^* &= v_{sd} + L_f \omega i_q + u_d \\ v_{fq}^* &= v_{cq} - L_f \omega i_d + u_q \end{aligned} \tag{3.53}$$

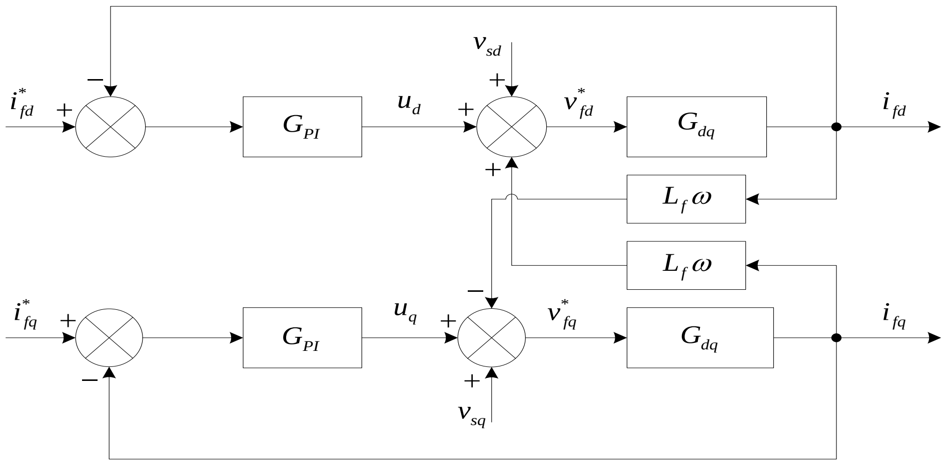

Figure 3.19 : Bloc diagram of the current controllers in synchronous reference.

3.4.1.3 Control of DC voltage of the capacitor V_{dc}

The DC voltage around the capacitor of the VSI must be kept constant [4, 6, and 63]. The cause of its variation is the power exchange between the grid and the capacitor [6], In addition to the losses in the switches and the filter inductance. The variations of this voltage must be small in order not to exceed the voltage limits of the semi-conductors from the one hand, and in order not to affect the performance of the filter from the other hand [63]. To ensure the regulation of the dc capacitor voltage, a PI controller can be used. If we neglect the losses in the inverter and the output filter, the relation between the absorbed power by the filter and the voltage around the capacitor can be given by:

$$p_{dc} = \frac{d}{dt}\left(\frac{1}{2} C_{dc} V_{dc}^2\right) \tag{3.54}$$

Applying the Laplace transform, we can achieve:

$$p_{dc}(S) = \frac{1}{2} S C_{dc} V_{dc}^2 (S) \tag{3.55}$$

The voltage of the capacitor is then given by:

$$V_{dc}^2(S) = \frac{2 p_{dc}(S)}{C_{dc} S} \tag{3.56}$$

From Eqn. 3.56 and considering the use of PI controller, the control loop of the dc voltage can be represented by Figure 3.20. The choice of the parameters k_{vi} and k_{vp} is restrained by a minimal response time and a stable dynamic behavior that doesn't affect the performance of the APF. It is important to notice at this stage that high cut-off frequency ameliorates the control of the direct voltage and minimize the response time of the system. But it leads to errors in the generation of APF's reference currents and then reduces the filtering efficiency.

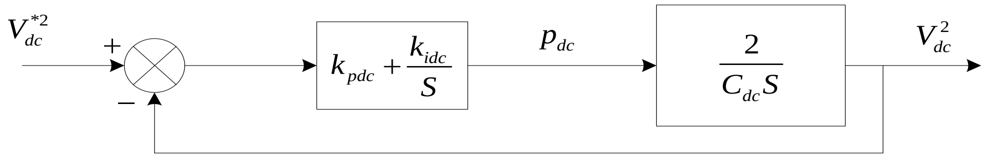

Figure 3.20 : Control loop of the DC voltage.

From Figure 3.20, the closed loop transfer function of the system with the controller can be given by:

$$\frac{(1+\frac{k_{pdc}}{k_{idc}}S)}{S^2+2\frac{k_{pdc}}{C_{dc}}S+2\frac{k_{idc}}{C_{dc}}} \tag{3.57}$$

From where we can find the different parameters of the controller as:

$k_{idc}=\frac{1}{2}C_{dc}\omega_c^2$, $\omega_c=2\pi f_c$ And $k_{pdc}=\xi\sqrt{2C_{dc}k_{idc}}$

3.4.2 Indirect Control of the Active Power Filter

In the indirect control method of the active power filter, we interest in the control of the grid currents without looking at the filter currents. Sinusoidal current reference for the grid is generated using appropriate methods. These currents are then compared with the measured grid currents. The error is fed to a hysteresis current controller which generates the pulses to control the switches of the SAPF.

3.4.2.1 Grid Current Reference Generation

The generation of the grid reference currents is similar to that used for the generation of filter current reference. In literature one can find different methods for the identification of the grid currents. From these methods we can find the method based on the PQ theory, the method based on the d-q theory [21], and the method based on the DC voltage controller [27, 28, 29, 42, 64, and 65]. In the next section, we are going to discuss these different methods in the generation of the grid current reference.

3.4.2.1.1 PQ Theory Based Algorithm

This method utilize the theory proposed by *Akagi*, however, on contrary to the direct method; the indirect method uses just the instantaneous active power. In addition, in the indirect control, the alternative components of the instantaneous active power P are eliminated. The direct components are then used to generate grid currents. The reactive power is imposed to be zero. This method allows the compensation of the current harmonics and the reactive power at the same time [21]. The principle is explained as follow:

In three phase system without neutral, the simple voltages of the PCC v_{sa}, v_{sb},v_{sc} and the load currents i_{La}, i_{Lb}, i_{Lc} are given in the stationary frame reference by:

$$\begin{bmatrix} \hat{v}_{s\alpha} \\ \hat{v}_{s\beta} \end{bmatrix} = \sqrt{\frac{2}{3}} \begin{bmatrix} 1 & -\frac{1}{2} & -\frac{1}{2} \\ 0 & \frac{\sqrt{3}}{2} & -\frac{\sqrt{3}}{2} \end{bmatrix} \begin{bmatrix} \hat{v}_{sa} \\ \hat{v}_{sb} \\ \hat{v}_{sc} \end{bmatrix} \tag{3.58}$$

$$\begin{bmatrix} i_{l\alpha} \\ i_{l\beta} \end{bmatrix} = \sqrt{\frac{2}{3}} \begin{bmatrix} 1 & -\frac{1}{2} & -\frac{1}{2} \\ 0 & \frac{\sqrt{3}}{2} & -\frac{\sqrt{3}}{2} \end{bmatrix} \begin{bmatrix} i_{la} \\ i_{lb} \\ i_{lc} \end{bmatrix} \tag{3.59}$$

Neglecting the voltage harmonics, the instantaneous active power is given by:

$$p_l = v_{s\alpha} i_{l\alpha} + v_{s\beta} i_{l\beta} \tag{3.60}$$

This active power can be decomposed into two components, the first direct representing the power of the fundamentals of the voltage and current. The second component is alternative due to the harmonics of the current and voltage.

$$p_l = \overline{p}_l + \tilde{p}_l \tag{3.61}$$

The reference power on the source side is given by:

$$p_s^* = \overline{p}_l + p_{dc}^* \tag{3.62}$$

The direct component of the active power can be extracted using low pass filter of the second or third order to filter the instantaneous active power.

Where; p_{dc}^{*} is the amount of power used to compensate the losses in the filter and to keep its voltage constant. This term is generated using the direct voltage controller. The reference currents of the grid are given by:

$$i_{s\alpha}^{*} = \frac{v_{s\alpha}}{v_{s\alpha}^{2} + v_{s\beta}^{2}} p_{s}^{*} \tag{3.63}$$

$$i_{s\beta}^{*} = \frac{v_{s\beta}}{v_{s\alpha}^{2} + v_{s\beta}^{2}} p_{s}^{*} \tag{3.64}$$

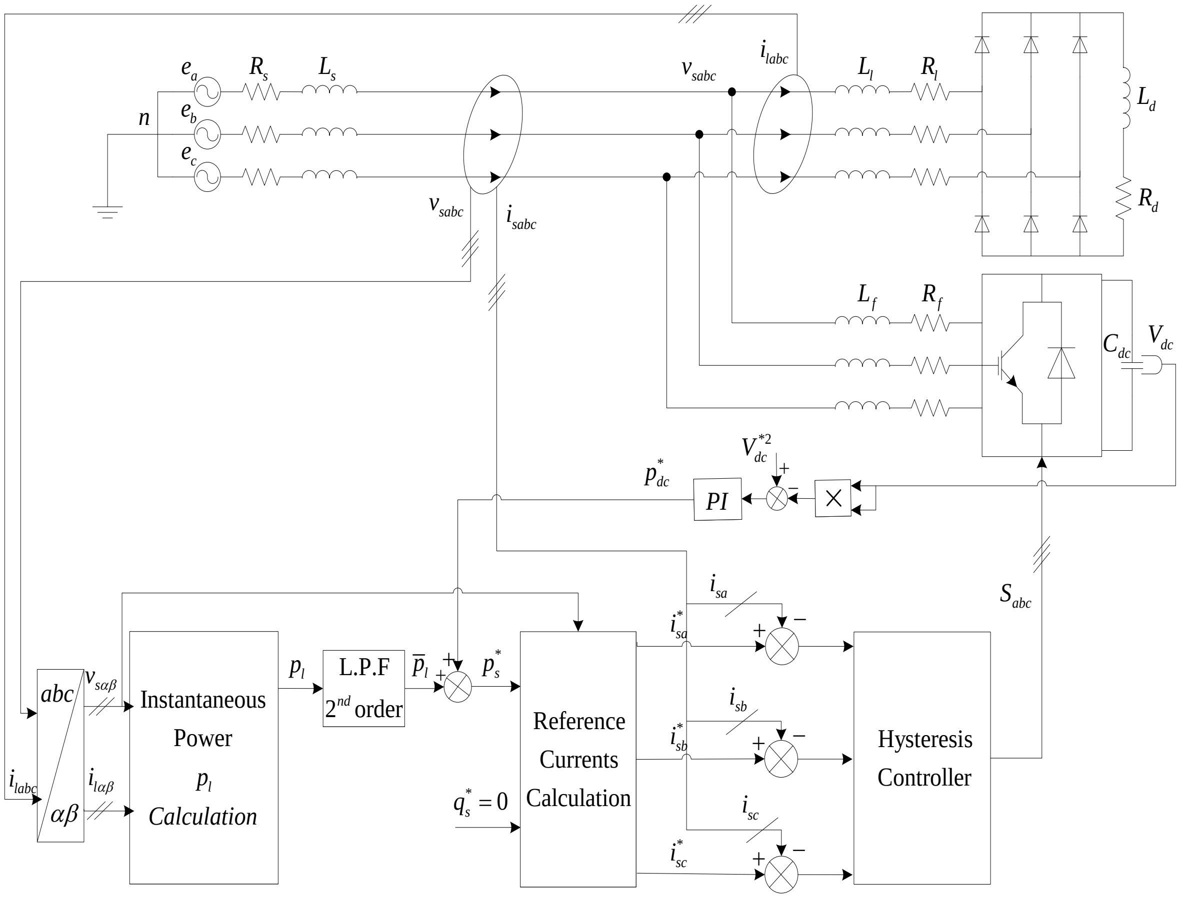

Figure 3.21 : Indirect control based on the instantaneous power theory [21].

The reference currents in the three phase frame are then given by:

$$\begin{bmatrix} i_{sa}^* \\ i_{sb}^* \\ i_{sc}^* \end{bmatrix} = \sqrt{\frac{2}{3}} \begin{bmatrix} 1 & 0 \\ -\frac{1}{2} & \frac{\sqrt{3}}{2} \\ -\frac{1}{2} & -\frac{\sqrt{3}}{2} \end{bmatrix} \begin{bmatrix} i_{s\alpha}^* \\ i_{s\beta}^* \end{bmatrix} \tag{3.65}$$

Figure 3.21 shows the diagram of this control method.

3.4.2.1.2 Synchronous Reference Based Method

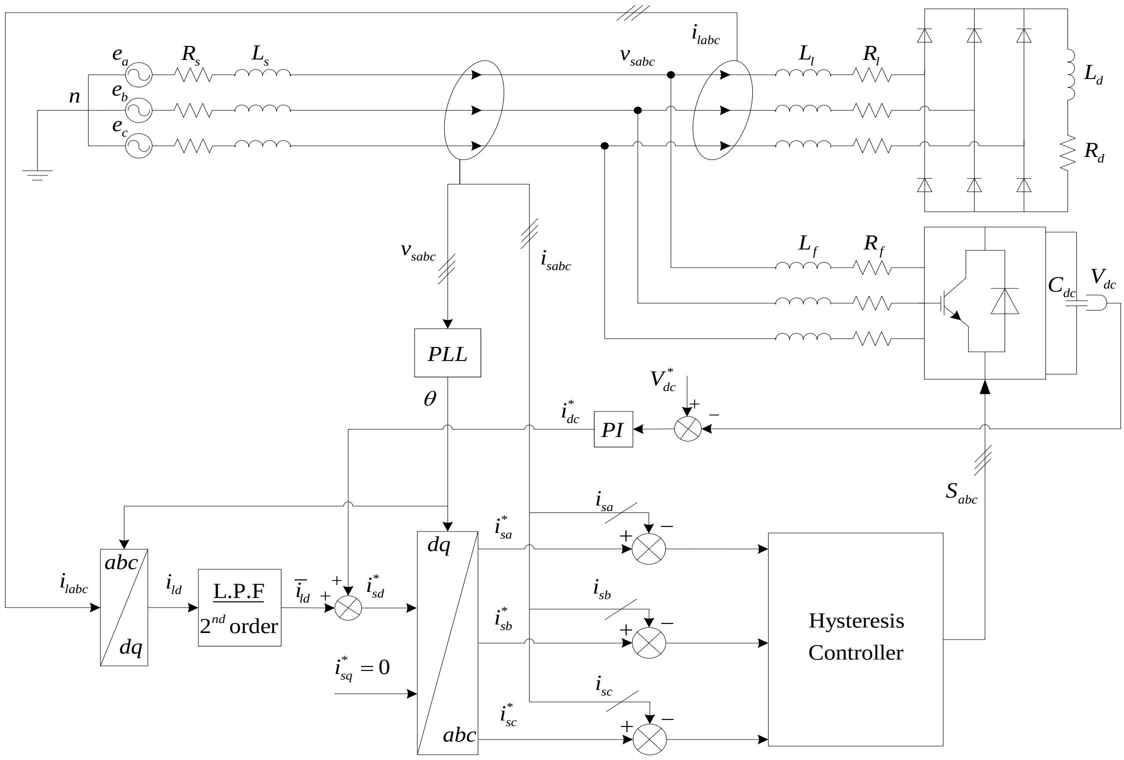

Figure 3.22 : Diagram of indirect control based on the synchronous frame method.

The diagram of this method is shown in Figure 3.22. The principle of this method is similar to the previous method, with the difference that it is based on the synchronous reference currents calculation. Using the load currents and the voltage angular position generated by a PLL circuit, the direct component i_{ld} of the load current can be calculated by:

$$i_{ld} = \sqrt{\frac{2}{3}}(i_{la}\cos(\omega t) + i_{lb}\cos(\omega t - \frac{2\pi}{3}) + i_{lc}\cos(\omega t + \frac{2\pi}{3})) \tag{3.66}$$

This current can be expressed as the sum of two components direct and alternative as given in Eqn. 3.67. Using a low pass filter with appropriate cut-off frequency (we've chosen 20 Hz) we can extract the direct component representing the fundamentals of the grid. The direct current reference of the source side can be given by Eqn. 3.68, where the second term is the output of the DC voltage controller. This term presents the direct current necessary to compensate the losses of the APF. It is important to notice that in this method also we are imposing the value of reactive current i_q to be equal to zero; which means that this method imposes the compensation of harmonics and reactive power at once. The reference currents in three-phase system are then given by equation (3.69).

$$i_{ld} = \overline{i}_{ld} + \tilde{i}_{ld} \tag{3.67}$$

$$i_{sd}^{*} = \overline{i}_{ld} + i_{dc} \tag{3.68}$$

$$\begin{bmatrix} i_{sa}^{*} \\ i_{sb}^{*} \\ i_{sc}^{*} \end{bmatrix} = \begin{bmatrix} \cos(\theta) & -\sin(\theta) \\ \cos(\theta - \frac{2\pi}{3}) & -\sin(\theta - \frac{2\pi}{3}) \\ \cos(\theta + \frac{2\pi}{3}) & -\sin(\theta + \frac{2\pi}{3}) \end{bmatrix} \begin{bmatrix} i_{sd}^{*} \\ i_{sq}^{*} \end{bmatrix} \tag{3.69}$$

3.4.2.1.3 Indirect Control Based on DC Voltage Controller

In this method the peak value of the reference grid current I_{speak}^{*} is determined by the DC voltage regulator. In order to generate the reference currents of the grid, the peak value of the grid current is multiplied simply by the unit vectors of voltage at the PCC. The reference currents are then given by:

$$
\begin{aligned}
i_{sa}^{*} &= I_{speak}^{*}\sin(\theta) \\
i_{sb}^{*} &= I_{speak}^{*}\sin(\theta-\frac{2\pi}{3}) \\
i_{sc}^{*} &= I_{speak}^{*}\sin(\theta+\frac{2\pi}{3})
\end{aligned} \tag{3.70}
$$

Where the angle θ is the angular position generated using a PLL circuit. The diagram of this method is shown in Figure 3.23.

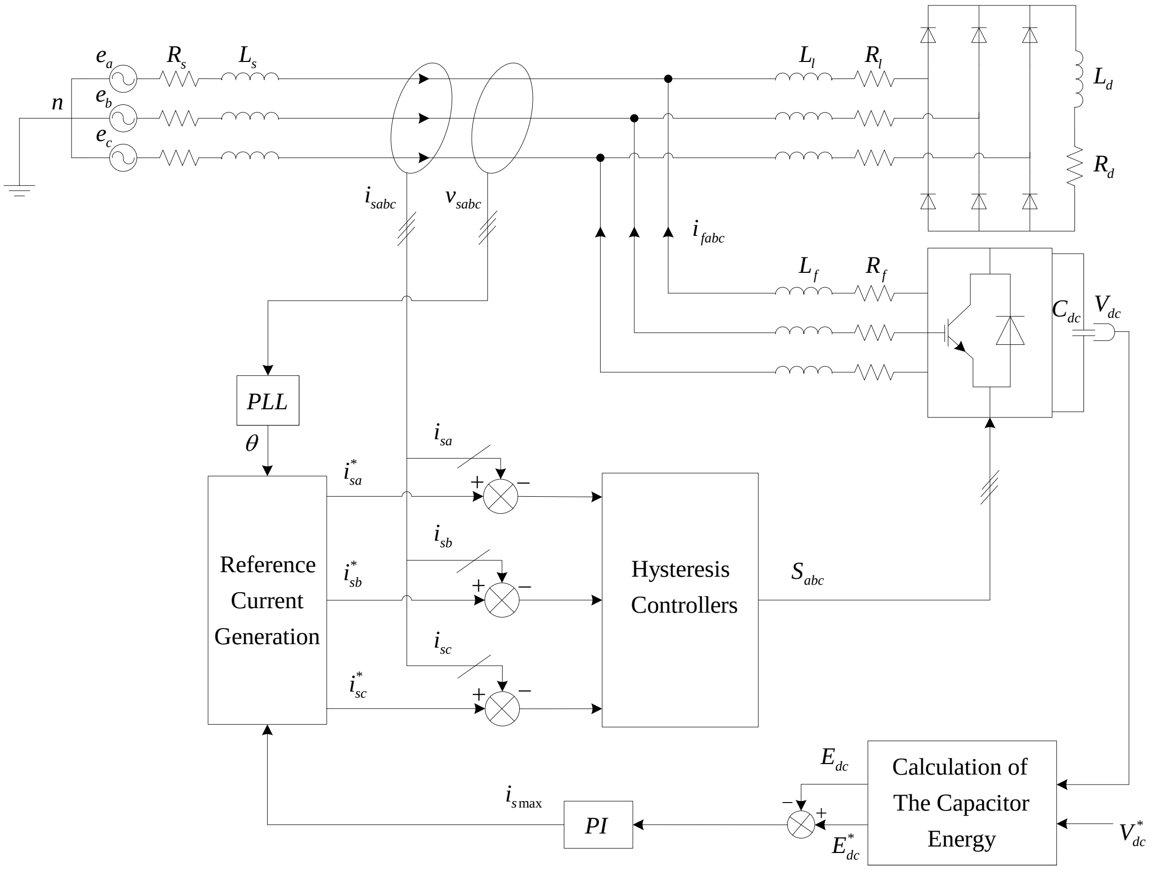

Figure 3.23 : Diagram of the indirect control using DC voltage controller.

3.4.2.2 Design of PI Controller for the Indirect Control Method

In this section, we are going to construct the PI controller which is charged to produce the peak value of the grid current. The input of this controller will be the error between the stored energy in the capacitor and its reference value. Its output represents the reference power of the three-phase system at the PCC defined by Eqn. 3.71. the reference power of the filter p_f^* represents the difference between the grid reference power and the load power, supposing that the filter is able to produce its reference power in each period. This power represents the transmitted power from the source to the filter, neglecting the losses of the filter and the coupling inductance. The integral of the filter power gives the energy stored in the condenser [65]. Figure 3.24 shows the diagram of the voltage regulation.

$$p_s^* = \frac{3V_{speak} i_{speak}}{2} \tag{3.71}$$

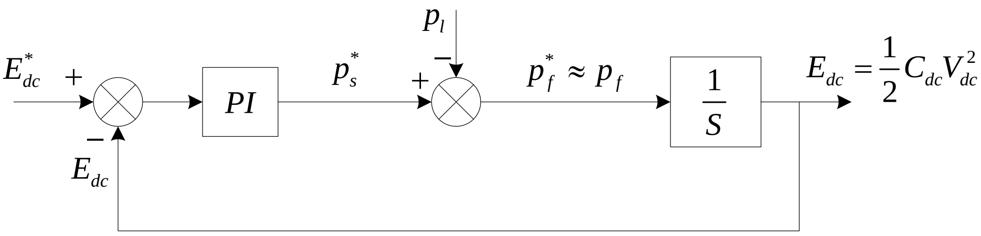

Figure 3.24 : Diagram of DC voltage closed loop control.

From Figure 3.24 we can define the stored energy of the condenser by:

$$p_s^* = G_{PI}(S)(E_{C_{dc}}^* - E_{C_{dc}}) \tag{3.72}$$

$$E_{C_{dc}} = (p_s^* - p_l)\frac{1}{S} \tag{3.73}$$

By substitution of Eqns. 3.72 in 3.74 we achieve:

$$E_{C_{dc}} = \frac{G_{PI}(S)}{S + G_{PI}(S)} E_{C_{dc}}^* - \frac{1}{S + G_{PI}(S)} p_L \tag{3.74}$$

Where,

G_{PI} is the transfer function of the PI controller. This transfer function can be defined by:

$$G_{PI}(S) = k_{pdc} + \frac{k_{idc}}{S} \tag{3.75}$$

By substitution of this transfer function (3.75) in eqn. 3.74, the closed loop transfer function of the system can be given by:

$$E_{C_c} = \frac{k_{pdc}S + k_{idc}}{S^2 + k_{pdc}S + k_{idc}} E_{C_{dc}}^* - \frac{S}{S^2 + k_{pdc}S + k_{idc}} p_l \tag{3.76}$$

Comparing this transfer function with the canonic form of a second order transfer function we find:

$$k_{pdc} = 2\xi\omega_{cdc}$$
$$k_{idc} = \omega_{cdc}^2 \qquad (3.77)$$

Where

ξ is the damping factor, its optimum value is 0.707. the cut-off frequency was chosen to be $f_c = 8$ Hz.

CHAPTER 4

RESULTS AND DISCUSIONS

In the last two chapters, different topologies and control methods of Shunt Active Power Filter (SAPF) were presented and discussed. These methods include the harmonic contents extraction from one part, and the control of SAPF from the other part. Different direct and indirect methods were presented and discussed. The control schemes of these methods were also presented.

This chapter presents the simulation results of different models discussed in this work in addition to different parameters of grid and filter. The simulation results are shown and discussed. Different grid conditions will be discussed and results will be compared. The comparison includes the extraction methods, VSI control theories, DC voltage control, in addition to the function under non ideal system conditions and the use of Self Tuning Filter (STF) for non ideal system.

4.1 System Description

The simulated system is a three phase balanced and non-balanced voltage system, the non-linear load used in this work is a three phase non controlled bridge rectifier discussed in the previous chapters. The parameters of the grid and rectifier in addition to the APF are given in table 4.1.

TABLE 4.I
PARAMETERS OF THE ANALYZED SYSTEM

Symbol	Quantity	Value	Symbol	Quantity	Value
V_s	Ideal grid voltage L-N	240 V	L_f	Filter inductance	0.2 mH
f	Grid frequency	50 Hz	C_{dc}	APF DC capacitor	5 mF
R_s	Grid resistance	3 mΩ	V_{dc}	DC link capacitor	900 V
L_s	Grid inductance	2.6 μH	Load 1	DC Load Resistance	7.5 Ω
R_L	AC load resistance	10 mΩ		DC Load Inductance	2 mH
L_L	AC load inductance	0.3 mH	Load 2	DC Load resistance	10 Ω
R_f	Filter resistor	20 mΩ		DC Load inductance	5 mH

4.2 Non-Linear Load

The DC load voltage and current are shown in figure 4.1.a, while one phase of the AC side distorted load current is shown in Figure 4.1.b.

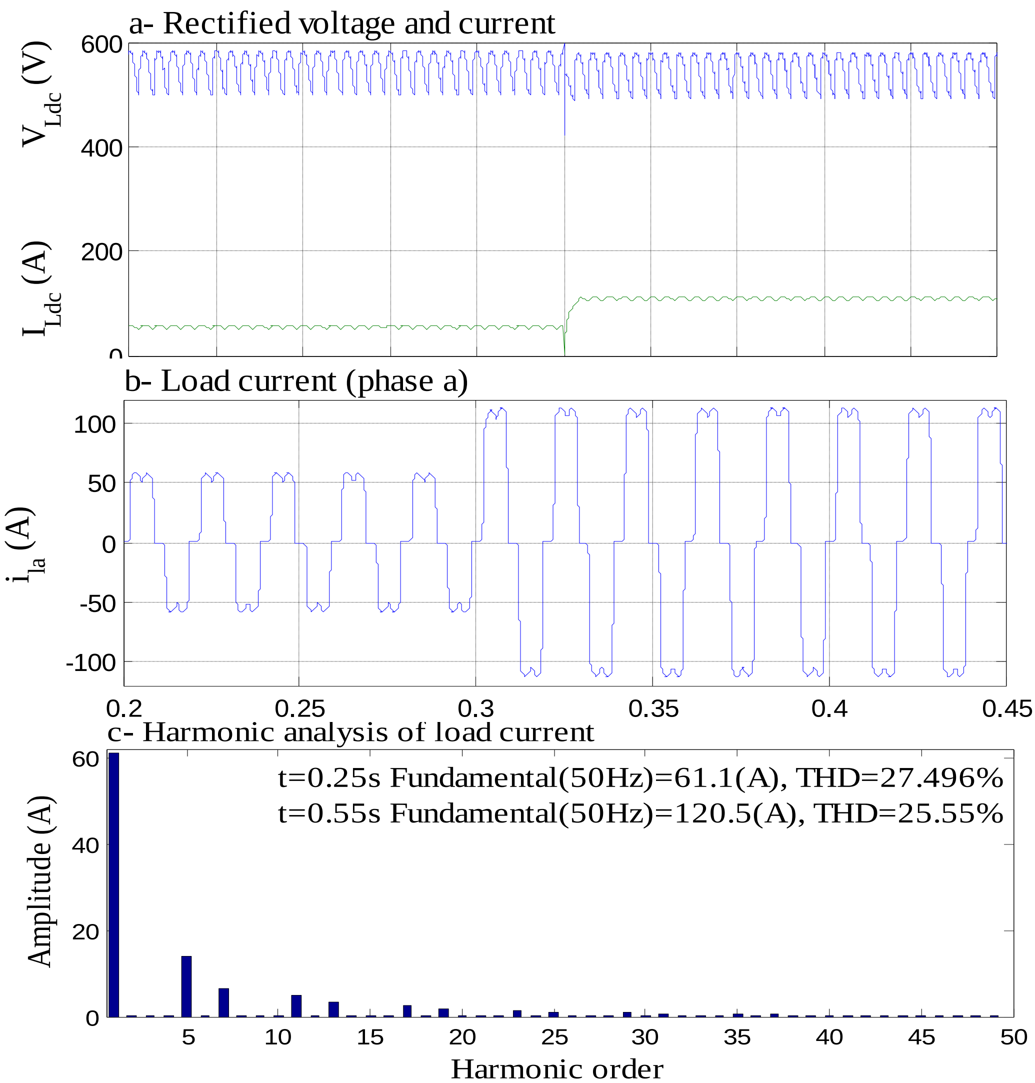

Figure 4. I: a) DC load voltage and current. b) AC load current (phase a). c) Harmonic spectrum of load current.

The harmonic analysis of the load current is given by figure 4.1c. It is will noticed from the harmonic analysis that the AC load current contains large amounts of 5th, 7th, 11th, 13th, and smaller amounts of higher harmonic orders. The total harmonic distortion THD of the current was 27.49% and has changed to 25.55% due to the variation of the load.

As discussed previously, synchronous reference dq theory and instantaneous active and reactive theory PQ are the mostly used and presented in literary due to their simple implementation in addition to their performance. Figure 4.2 presents the d-q and PQ components of load currents before and after filtering by the low pass filter of 3rd order.

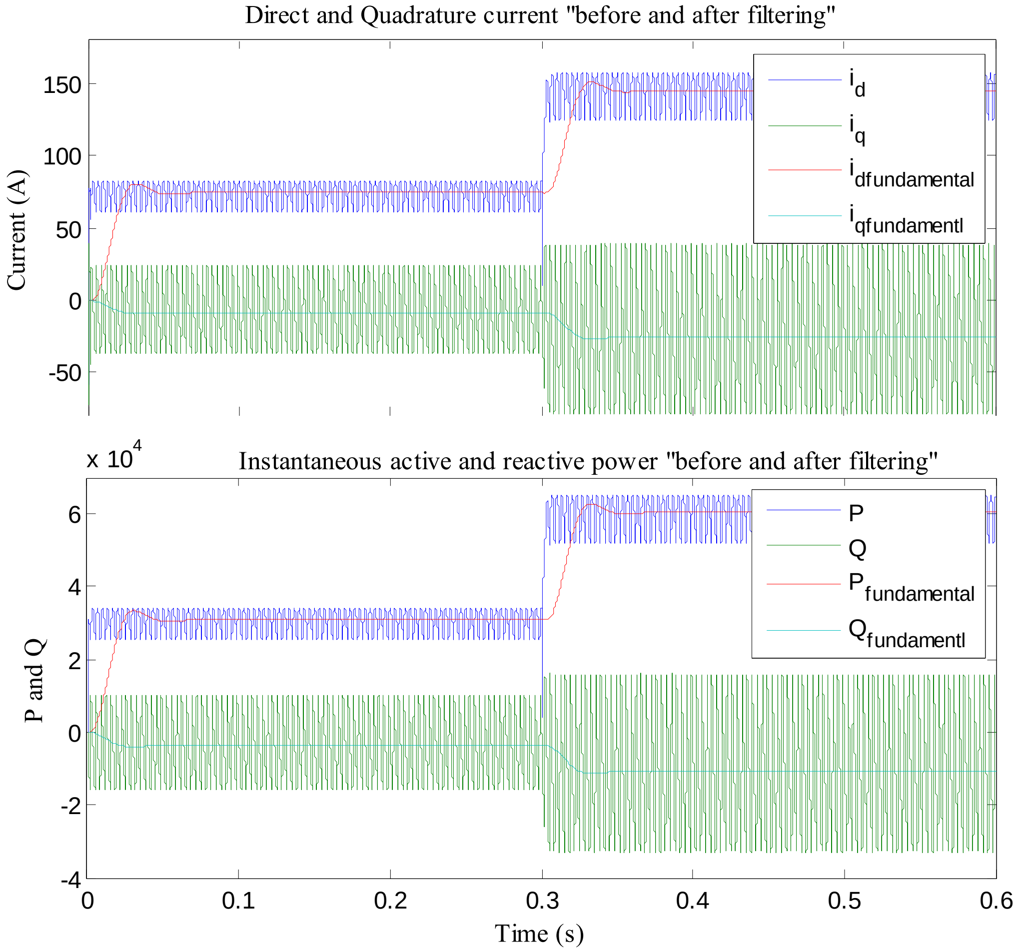

Figure 4. 2: d-q and PQ components of load current before and after filtering by LPF.

4.3 Control of Voltage Source Inverter

4.3.1 Hysteresis Current Control Based on Synchronous Reference d-q Theory

As discussed previously in chapter 2, the hysteresis control is the simplest of the control methods of VSI's current. The main drawback of this control method is the lack of controllability of the switching frequency. The simulation results of a hysteresis based controller are shown in figure 4. 3. A hysteresis band of 2 Amperes was used with reference current extraction based on the synchronous reference dq theory.

It is seen from the figure that the THD of the grid current has been reduced to 2.81% before the variation of the load and 1.86% after load variation.

Figure 4.4 presents the APF current in comparison to its generated reference. We can notice from the figure that the APF follows perfectly its reference. The switching frequency in this case was less than 20 kHz.

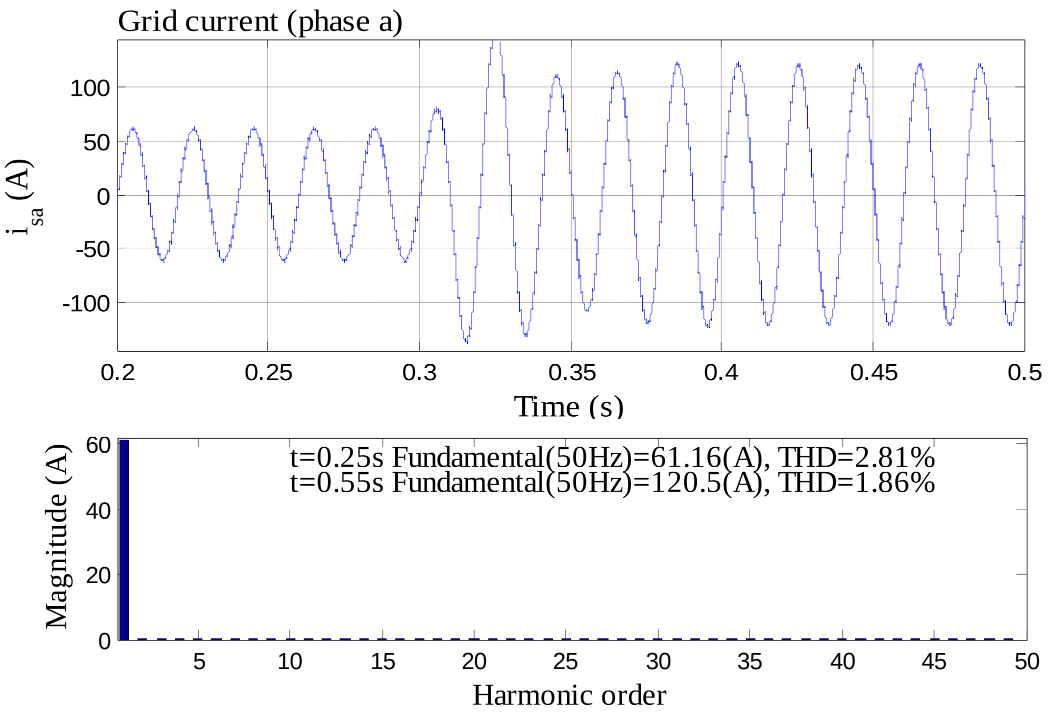

Figure 4.3: Grid current and its harmonic spectrum analysis after compensation.

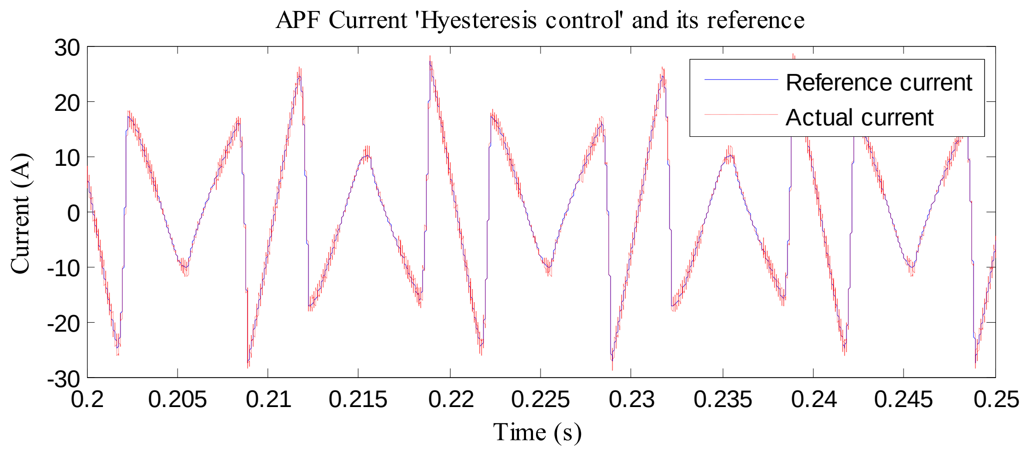

Figure 4.4: APF current and its reference (Hysteresis control).

4.3.2 Sinusoidal PWM Control Based on d-q Theory

In this part, the sinusoidal pulse width (SPWM) modulation control of VSI is applied in combination with linear PI controller. The controller is responsible to generate voltage reference of the VSI dependent on the error between the actual current and the reference current of the APF. The SPWM generates then the switching orders after comparing the reference voltage with a fix frequency triangular signal or carrier signal. The carrier frequency was chosen to be 12.5 kHz. The cutoff frequency of the current PI controller is 6000 with 0.707 damping factor. The DC voltage controller has a cutoff frequency of 20 with 0.707 damping factor. Figure 4.5 shows the simulation results of SPWM_dq. The grid current is sinusoidal with 2.18% of THD before the variation of the DC load. After the variation of the load, the grid current passes by a transient phase of less than 0.08s before arriving its steady state performance with THD of 1.27%. It is important to notice here that this transient is not related to the PI controller performance, but it is a normal result of the delay caused by the LPF, in addition to the variation of the voltage of DC link capacitor which occurred after load variation. This load variation causes the change of power rate of APF. The APF current follows ideally its extracted reference as shown in Figure 4.6.

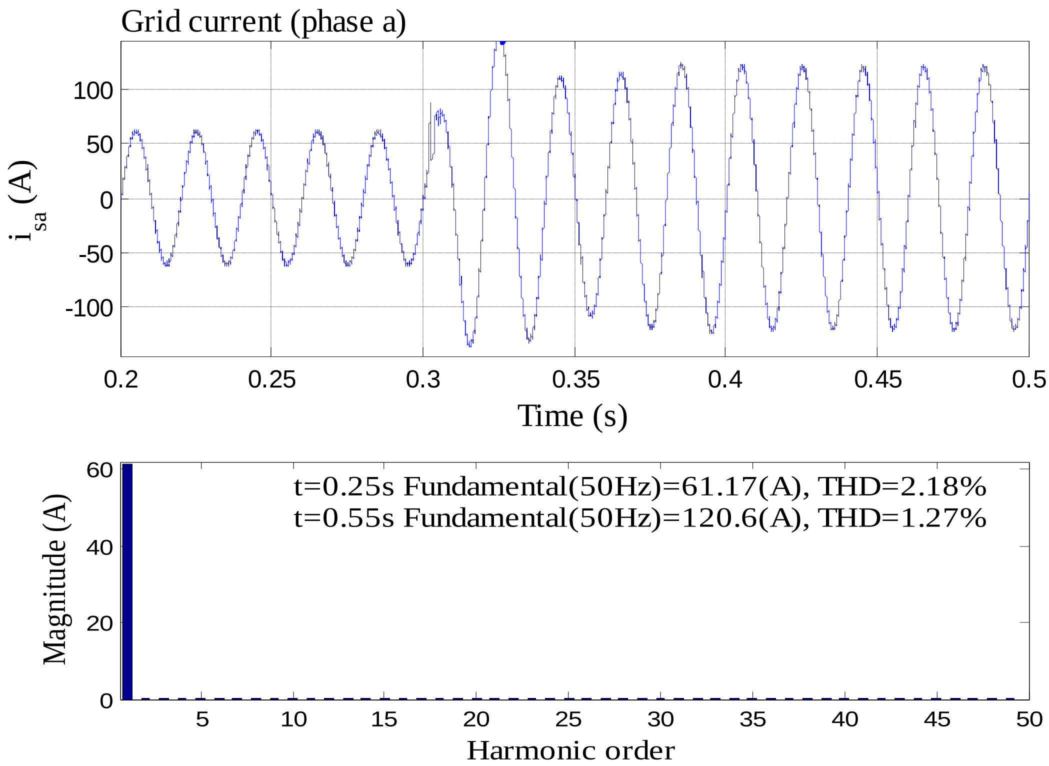

Figure 4.5: Grid current and its harmonic spectrum after compensation.

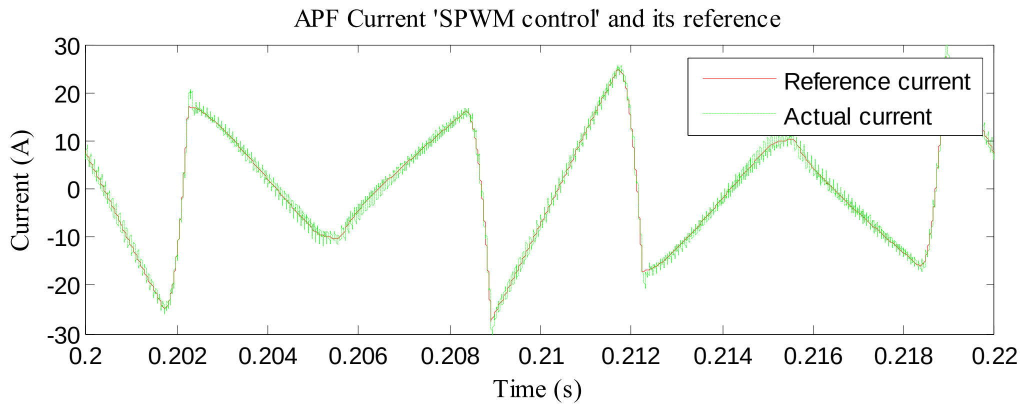

Figure 4.6: APF current and its reference (case of SPWM-PI control).

4.3.3 Space Vector Pulse Width Modulation SVPWM

Figure 4.7 shows the simulation results of the SVPWM control on the VSI. The dq reference theory was used in harmonic current extraction. The grid current is sinusoidal with short time transient follows the load variation. The THD was 2.1% before the load variation and it has decreased to 1.2% after the variation of the load as shown in the harmonic analysis of the grid current. A switching frequency of 12.5 kHz was adapted to this control strategy.

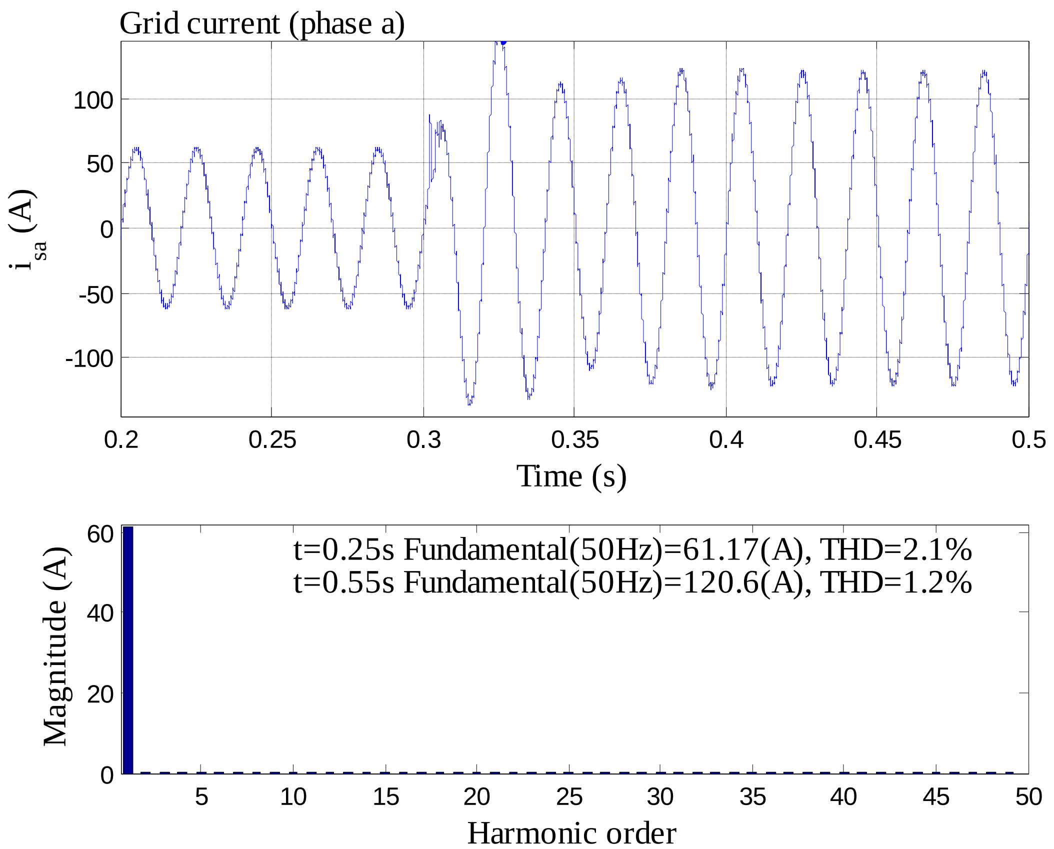

Figure 4.7: Grid current and Harmonic analysis with SVPWM-PI control.

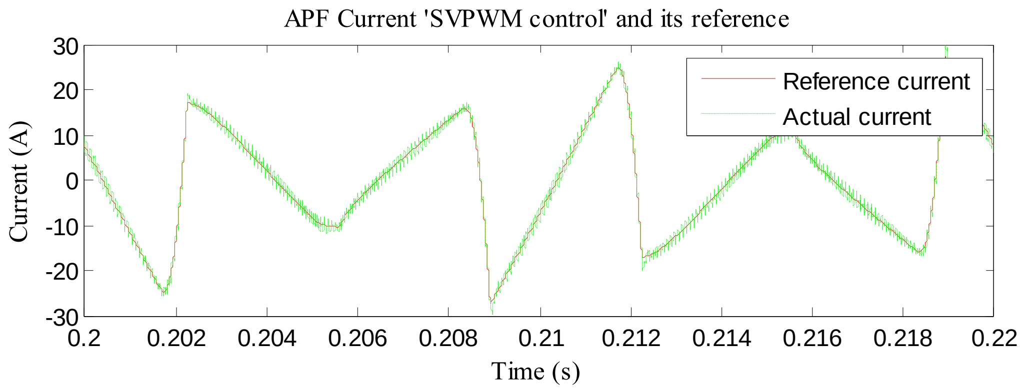

Figure 4.8: APF current and its reference in the case of SVPWM-PI control.

The results shown in the previous sections of this chapter shows that the best compensation results in terms of THD were obtained in the case of SVPWM control with THD of 2.1% (1.2%) before (after) the variation of the load. The SPWM based control gives better results than the hysteresis control with THD of 2.18% (1.27%) before (after) load variation, compared to 2.73% before load variation and 2.01% after load variation with hysteresis control.

Although of the design simplicity of the hysteresis controller, the fact that it is using a non fix switching frequency presents the most important drawback of this controller type. That is, the variable or high switching frequency is not adequate for power applications because of the limitations on power electronic elements. As a result, the next section will be concentrated on the SVPWM control with the different control and extraction theories discussed previously in chapter 3 of this work.

4.4 Case of Balanced Voltage System

4.4.1 SVPWM Control with d-q Theory and Two Current Controllers (d-q)

In this section, the controllers were designed to generate voltage reference directly in the d-q frame reference. Two controllers were used in this method instead of three controllers. The extraction of harmonic currents was achieved using the synchronous reference theory. The grid current and its spectrum analysis are shown in figure 4.9. The THD was decreased until 2.1% before and 1.19% after load variation. The parameters of current controllers were (k_{pi}=105, k_{ii}=2.8x10^6).

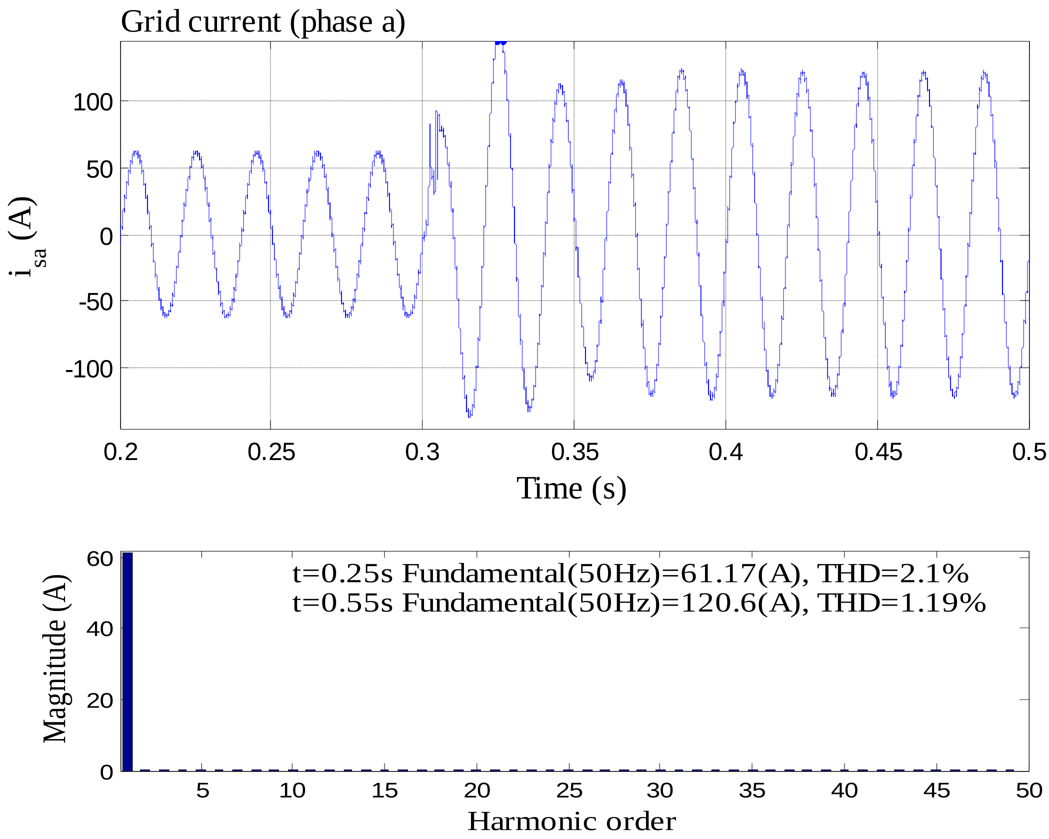

Figure 4.9: Grid current and its harmonic spectrum analysis.

4.4.2 SVPWM Control Based on PQ Theory

In this part, the SVPWM control of APF based on the instantaneous active and reactive power theory is applied and the results are shown. PI current controllers were designed in the three phase abc frame and in the alpha-beta frame. Figure 4.10 shows the results in the case of three PI controllers for a, b, and c phases and its spectrum analysis. Figure 4.11 presents the results in the case of two PI controllers in the alpha-beta frame reference.

As seen from the results in figures 4.10 and 4.11, the control of APF currents in the alpha-beta frame using two controllers gives better results than the control in the three phase reference. The THD of the grid current was 2.1% before the variation of the load compared to 1.9% in case of alpha-beta currents control. After load variation, the THD has been reduced to 1.19% in three phase control and 1.08% in the case of two phase control.

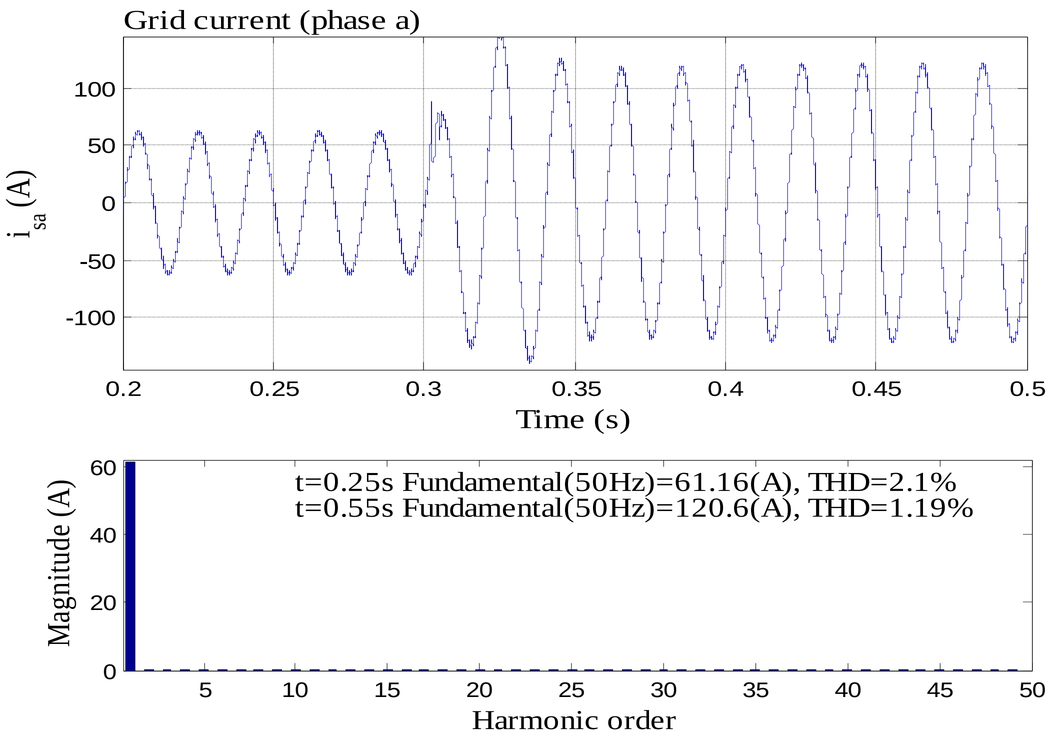

Figure 4.10: Grid current and its harmonic analysis (PQ with three PI controllers).

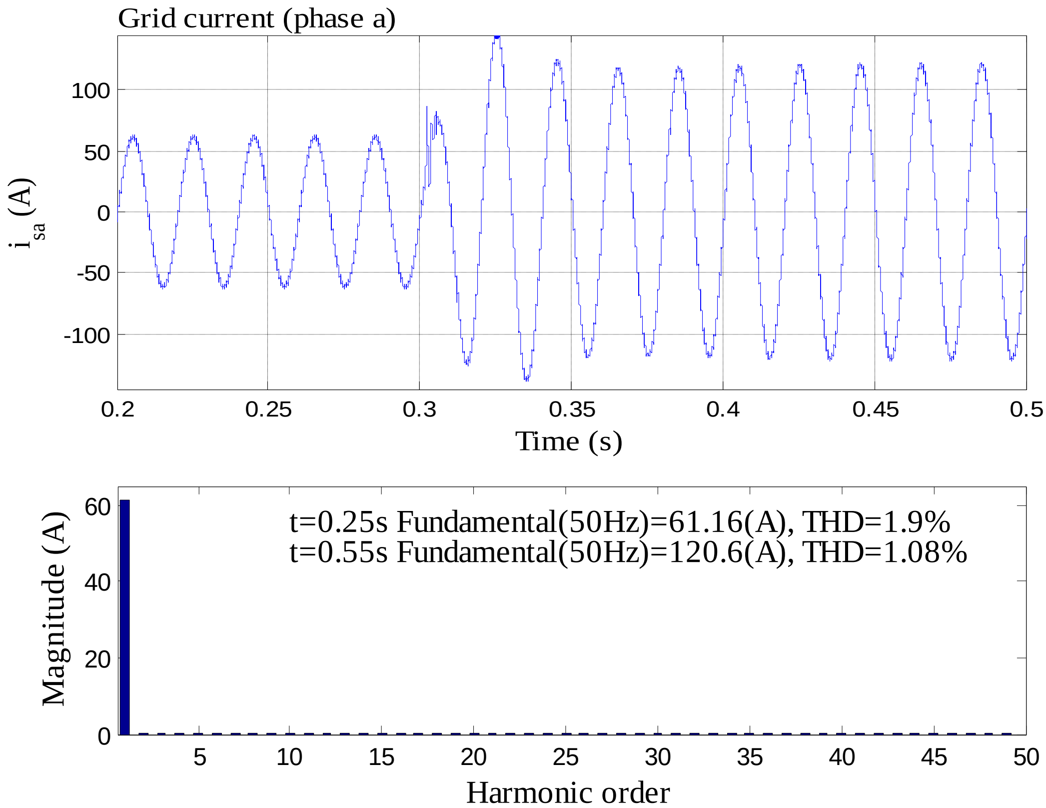

Figure 4.11: Grid current and its harmonic analysis (PQ with two PI controllers).

4.4.3 RMS Value Based APF

Figure 4.12 presents the simulation results of the previously discussed extraction method based on the RMS value algorithm. The results include the grid current and its harmonic analysis. The grid current has the shape of perfect sinusoidal wave with THD of 2.08% before the load variation and 1.58% after its variation. The grid current passes by a 60 ms transient after load variation before it returns to its steady state as seen in figure 4.12.

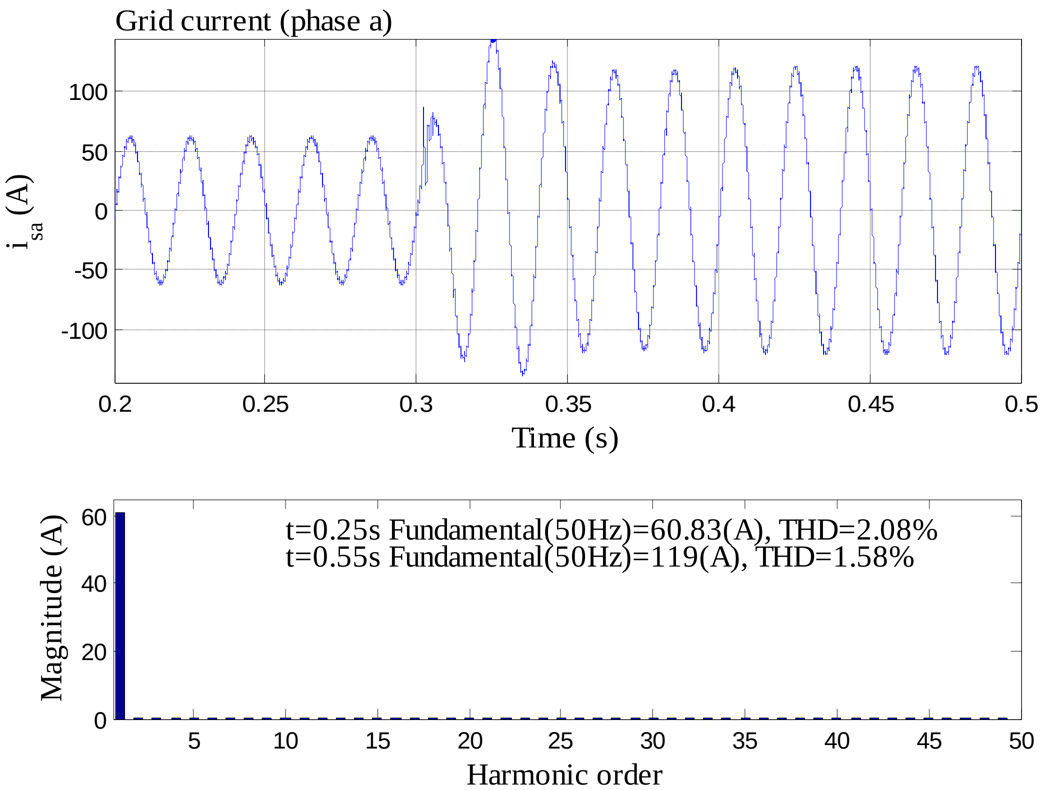

Figure 4.12: Grid current and its harmonic analysis (RMS based algorithm).

4.4.4 Active and Reactive Currents Method

The Active and Reactive currents algorithm was built and simulated in combination with the non-linear load. The simulation results are shown in figure 4.13. The grid current is perfectly sinusoidal with a short transient time after load variation. The THD has decreased from 2.13% to 1.39% after the load variation.

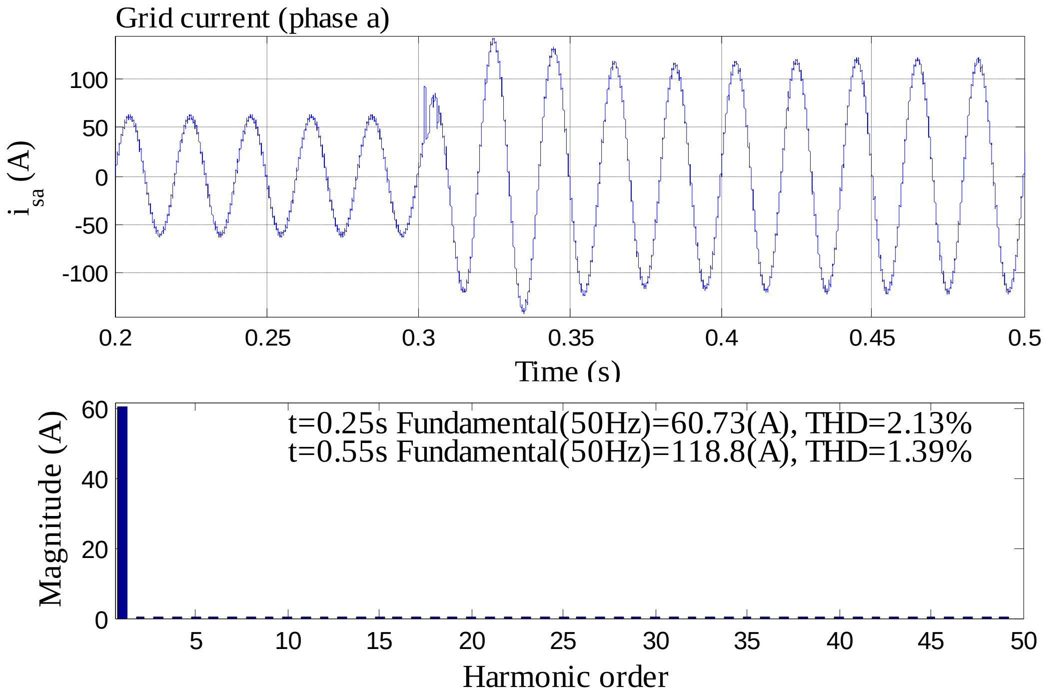

Figure 4.13: Grid current and its harmonics (Active and Reactive currents algorithm).

4.4.5 Proportional Integral Based Reference Generation Method

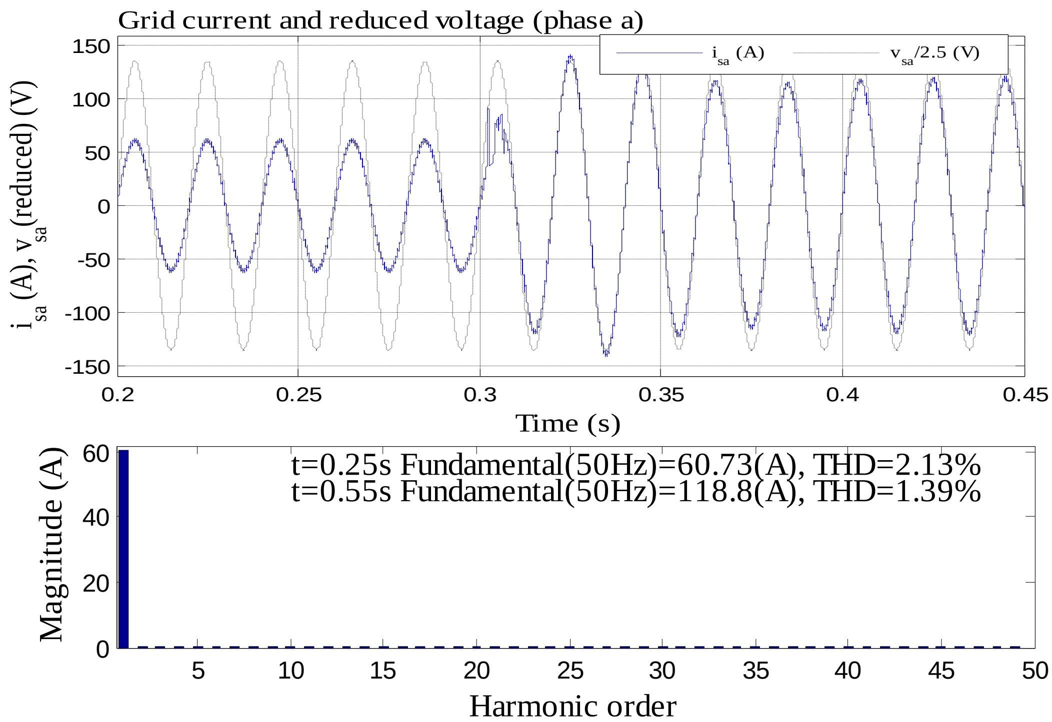

Figure 4.14: Grid voltage and current (after compensation) and the current harmonics.

In this method, the grid refernce current was generated dependent on the DC-link capacitor voltage controller. This controller is supposed to generate the peak value of the grid current which will be then multiplied by the unit vector of grid voltage for each phase.

The reference grid current is now generated, this current can either be used directly in the indirect control of SAPF or the filter reference current can be generated by subtraction of measured load current from grid reference current. In this part, the second method is applied and the simulation results are presented in figure 4.14. The figure shows the grid voltage and current in addition to the harmonic spectrum of grid current. It is noticed that the grid current is sinusoidal in phase with its voltage. The harmonic analysis shows low harmonic contents with THD of 2.13% decreased to 1.39% after load variation.

4.4.6 DC Side Voltage Control

The control of the DC voltage of the APF is of great importance because of its main effect on the stability of the compensation system and the harmonic compensation effeciency. The DC voltage must be kept within certein limits to ensure the control of energy transfert between the grid and the APF. Figures 4.15, 16, and 17 presents the DC link capacitor voltage and its reference with the three studied controllers: the direct current based controller, the instantaneous active power controller, and the grid current peak generating controller.

It was noticed from figures 4.15, 16, and 17 that the DC voltage of the APF follows perfectly with fluctuation its reference. The fluctuation is due to the energy exchange between the grid and the APF. The DC voltage passes by a transient after load variation because of changing of the power transfer between the filter and the grid. This transient is a function of the controller parameters and the load variation. It was noticed from the results that the DC voltage convergs again to its reference which prove the efficiency of the discussed controllers.

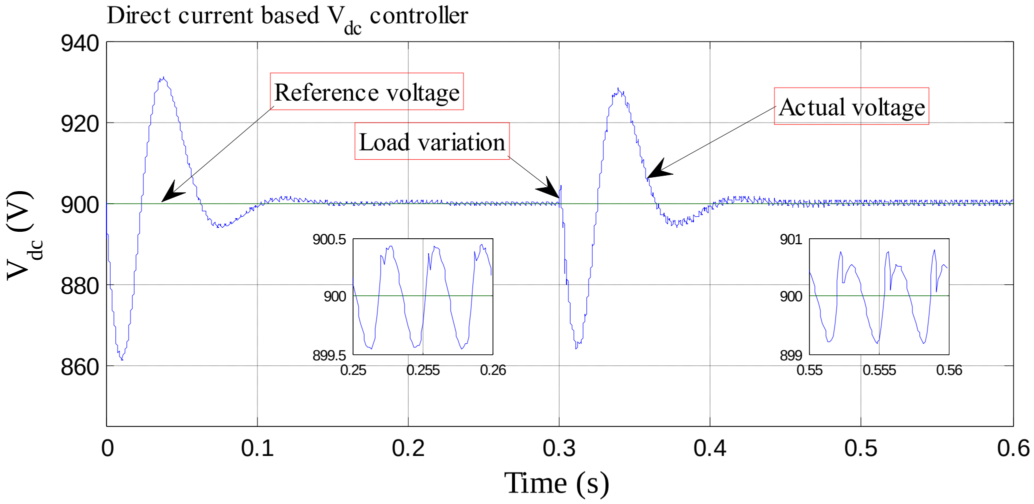

Figure 4.15: DC link voltage and its reference (Direct current method).

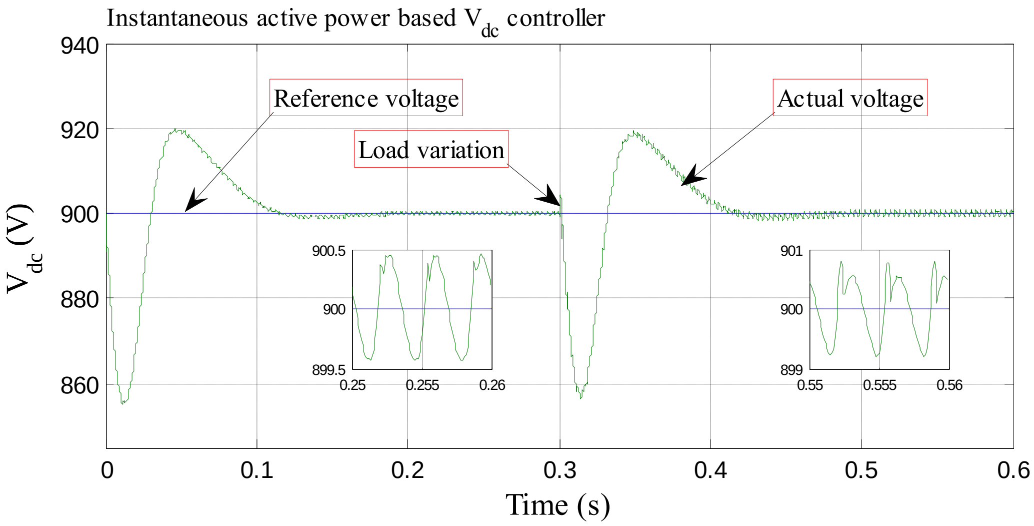

Figure 4.16: DC voltage and its reference (Instantaneous active power method)

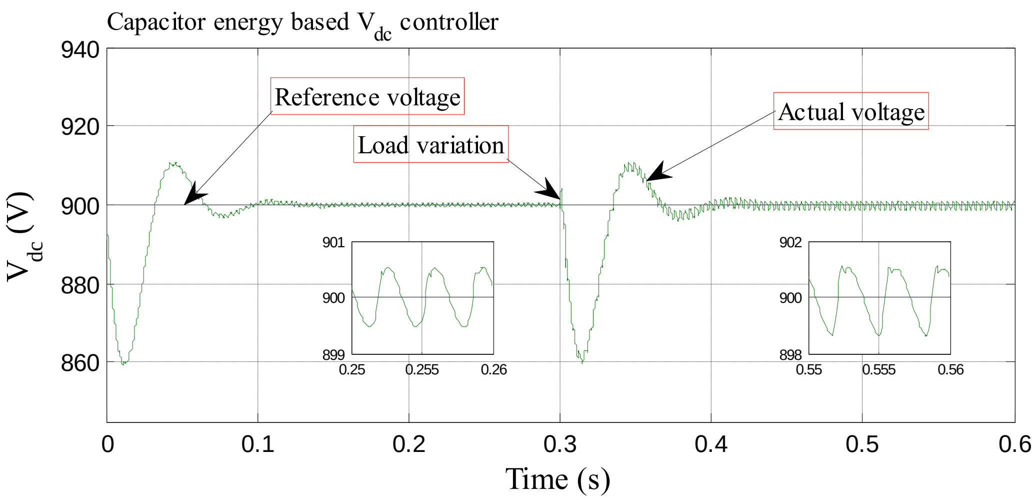

Figure 4.17: DC voltage and its reference (peak generation method).

4.5 Case of Unbalanced Distorted Grid Voltage

In the last section, the SAPF efficiency has been examined under ideal system parameters. These parameters are rarely encountered in practice, that is, the power systems' voltages are usually unbalansed and contains certein amounts of voltage harmonics. These unbalanced or distorted system voltage conditions can affect negatively the normal function of SAPF.

The different studied control strategies will be tested in the case of three phase distorted and unbalanced system. The parameters of the three phase system are given in table 4.2. this voltage contains in addition to the unbalanced fundamental voltages, some different amounts of 3rd, 5th, 7th, and 11th harmonics. Figure 4.18 presents the three phase distorted grid voltage used in the simulation.

TABLE 4.2: DISTORTED UNBALANCED VOLTAGE SYSTEM PARAMETERS.

f (Hz)	50	150	250	350	550	THD%
Phase a(rms)	226	21	14	12	5	12.5
Phase b(rms)	240	17.6	15.5	12	7	11.2
Phase c(rms)	233	19.5	12.7	10	9	11.5

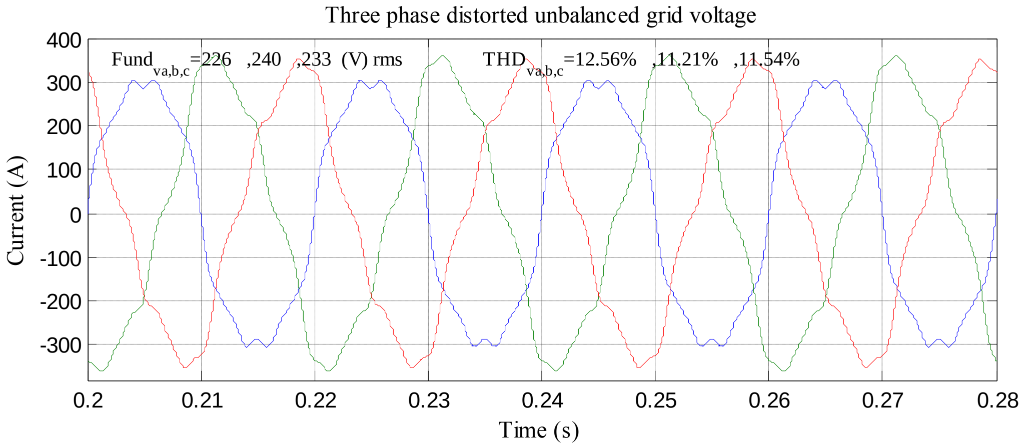

Figure 4.18: Distorted unbalanced grid voltage used in the test of SAPF.

Figure 4.19 shows the three phase load current in the case of non-ideal system voltage condition. It is seen from the figure that the currents are also unbalanced and contain different amounts of harmonics in each phase. That which is proved in figure 4.20 presenting the harmonic spectrum of the three phases of the load current. It shows that each phase of load current contains different harmonics with different magnitudes each.

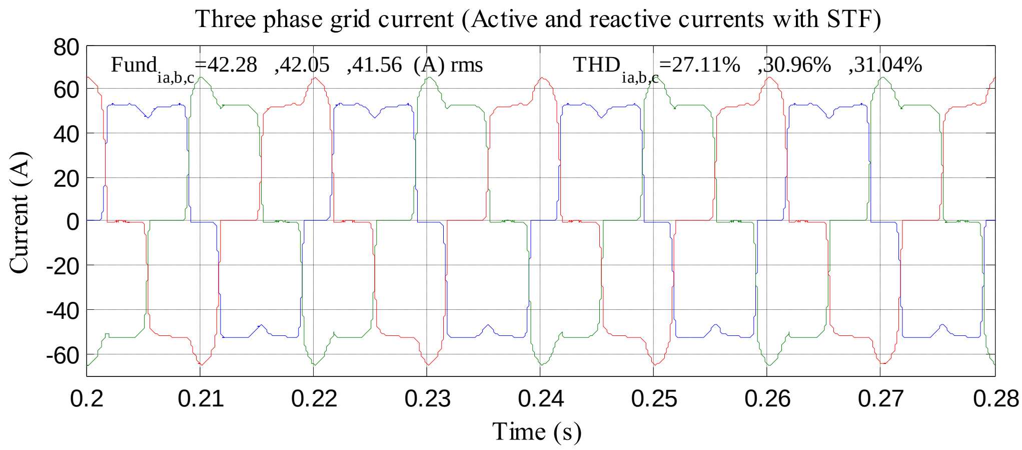

Figure 4.19: Three phase load current under non-ideal grid conditions.

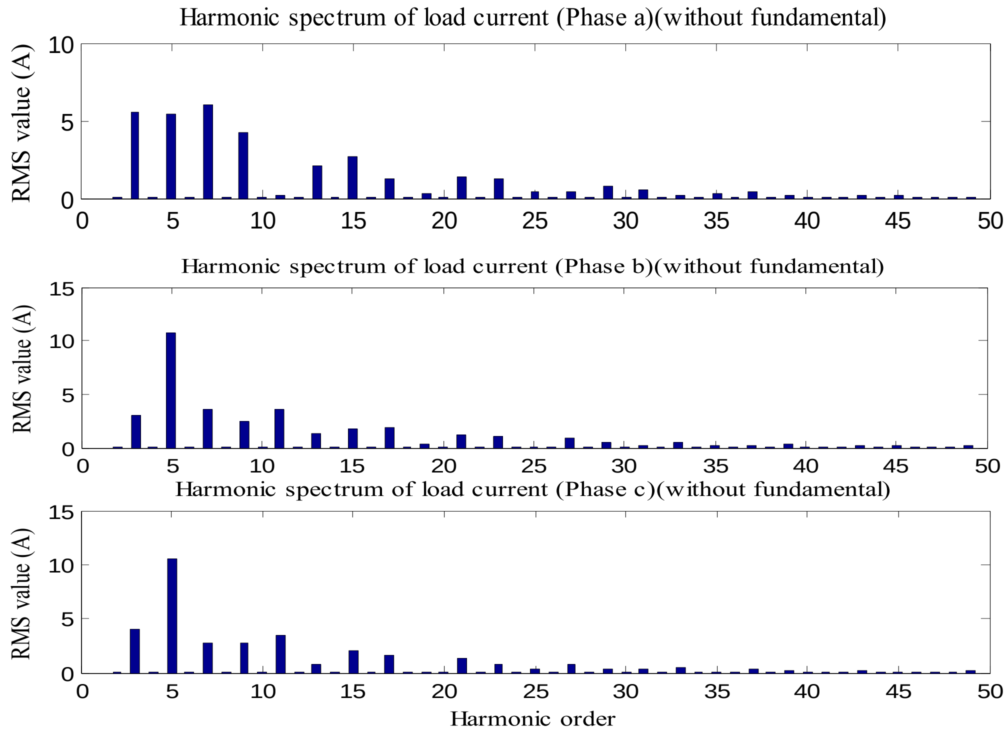

Figure 4.20: Harmonic spectrum of load current (case of non ideal grid voltage).

Figure 4.21 presents the three phase grid current waveforms obtained in this case. It was noticed from the waveforms of the grid current that all of the control strategies were affected by the grid voltage distortion. The currents were no more perfect sinusoids and they contain higher amounts of harmonics. The THD values of these currents in addition to their fundamentals were obtained and tabulated in table 4.3.

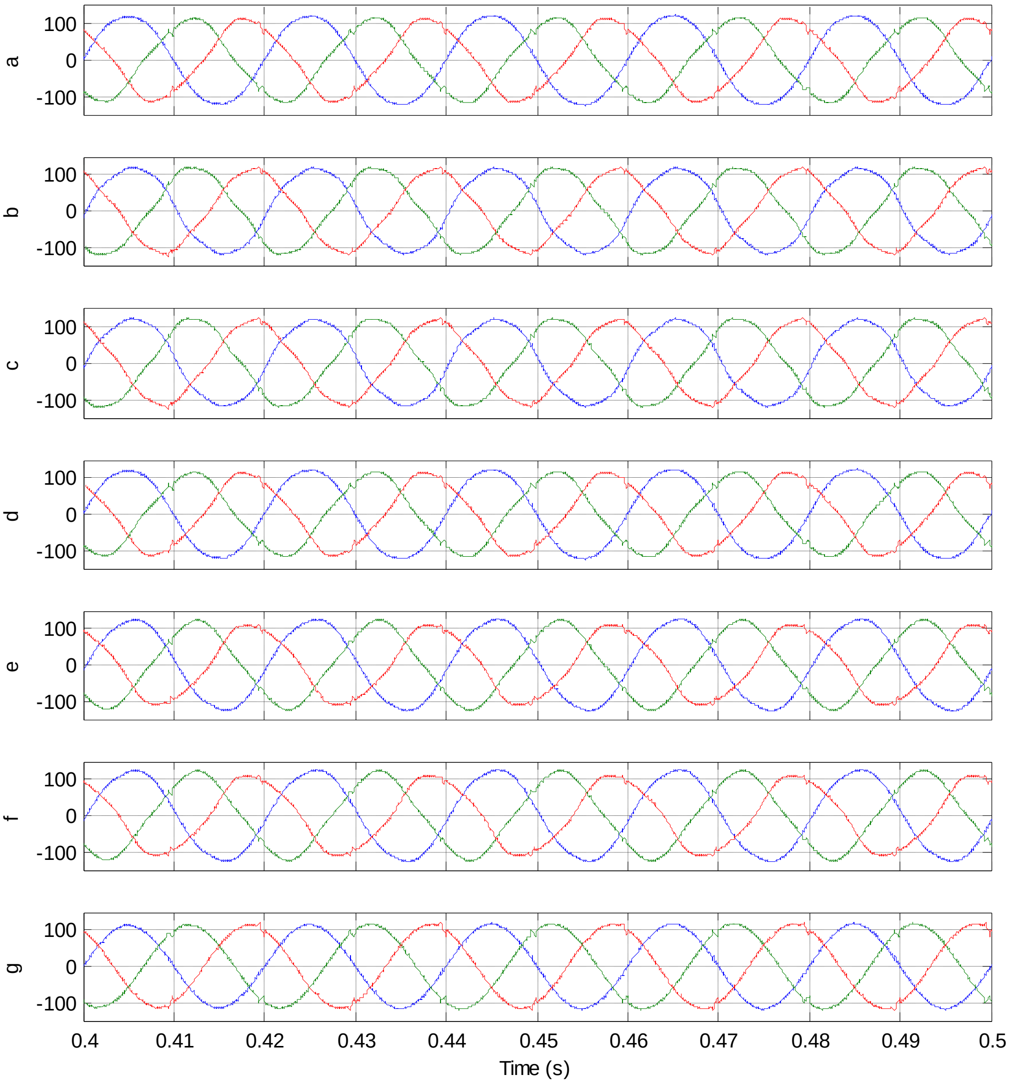

Figure 4.21: Three phase grid currents after compensation in case of distorted unbalanced grid voltage. a) Active and reactive currents. b) d-q method with 2 PIs. c) d-q method with 3 PIs. d) PI based peak detection. e) PQ method with 3 PIs. f) PQ method with 2 PIs. g) RMS current value based algorithm.

The results presented in figure 4.21 and table 4.214 shows that the grid currents are not balanced after compensation. The efficiency of harmonic compensation has been reduced because of the non ideal voltage conditions. In terms of THD it was noticed that the ability of all the studied control strategies has been affected by the voltage distortion. The THD values of the current were in the most of cases more than the international regulation limits. These results imply the necessity of the improvement of efficiency of these strategies under non ideal voltage conditions, which represents the subject of the next section of our study.

TABLE 4.3: THD VALUES AND FUNDAMENTAL PEAK VALUES OF CURRENTS FOR THE DIFFERENT USED CONTROL STRATEGIES.

	Case	Phase 'a'		Phase 'b'		Phase 'c'	
		THD	Peak value	THD	Peak value	THD	Peak value
Before Load Variation	a	4.01	64.93	7.29	58.07	7.37	56.94
	c	7.2	61.9	5.79	59.8	4.93	57.9
	d	11	58.2	10.15	59.8	10.13	59.3
	e	4.17	65.17	6.47	59.63	7.61	56.46
	g	7.39	61.49	5.52	58.92	5.33	57.96
After Load Variation	a	3.58	126.9	7.45	113.1	7.85	111.4
	c	6.92	121.9	5.51	117.9	4.79	113.9
	d	10.91	113.9	9.88	116.6	10.19	115.6
	e	3.98	128.2	6.22	118.2	7.97	110.5
	g	7.2	120	5.32	114.8	5.71	113.3

4.6 The Use of Self Tuning Filter (STF)

This section was dedicated for the study and discussion of the use of STF in the SAPF to ameliorate the performance of the SAPF in the case of non ideal grid voltage. The STF which is presented in the third chapter of this work is used in the generation of three phase balanced non distorted voltage system from non ideal voltage. it was implemented with the different studied control strategies. The performance of the SAPF with STF was examined and the simulation results are presented in Figures 4.22-4.27.

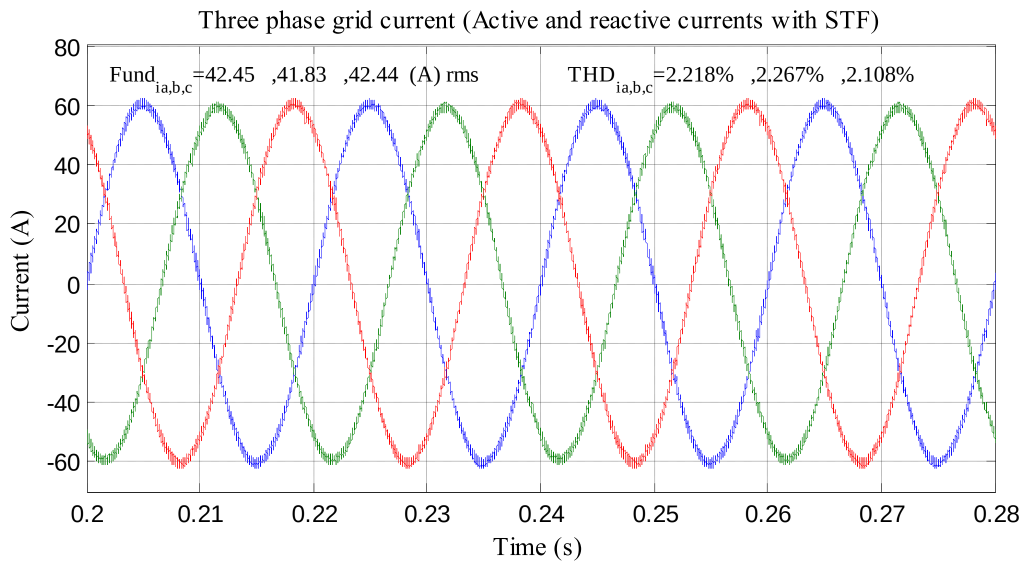

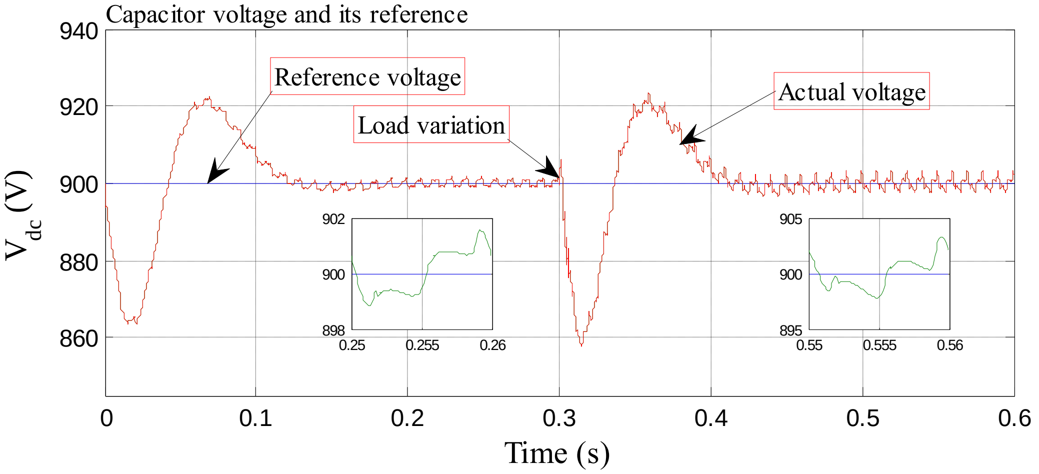

Figure 4.22: Grid current and DC capacitor voltage (active and reactive currents method with STF).

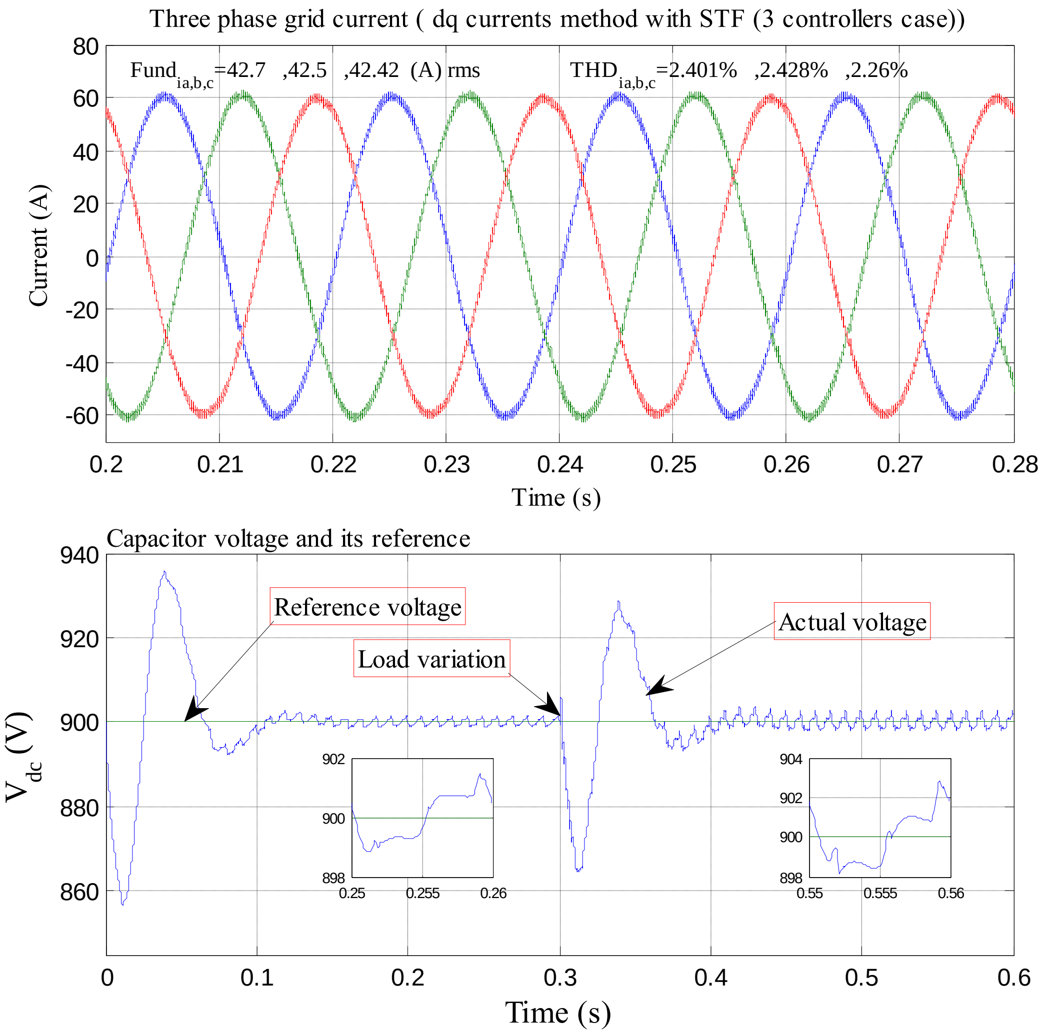

Figure 4.23: Grid current and DC voltage (d-q method, STF and 3 current controllers).

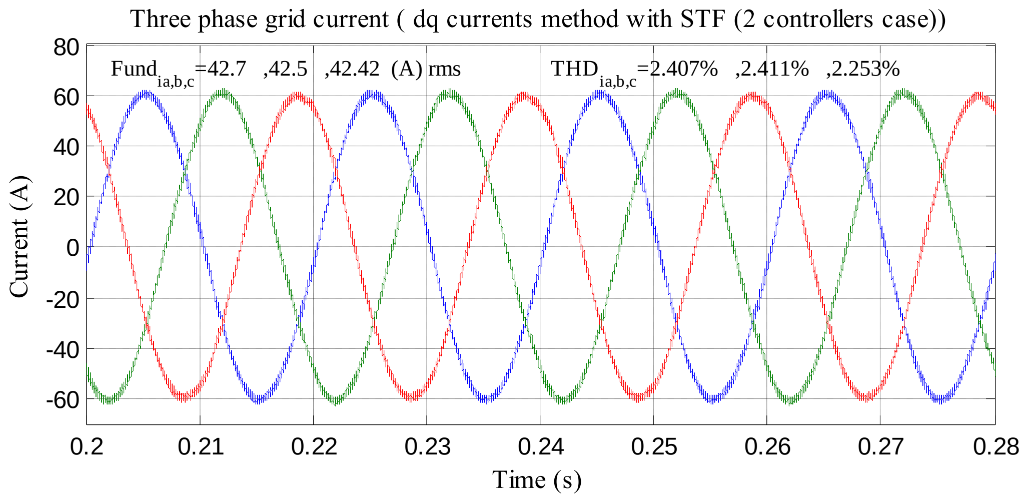

Figure 4.24: Grid currents and DC (d-q, STF, and 2 current controllers).

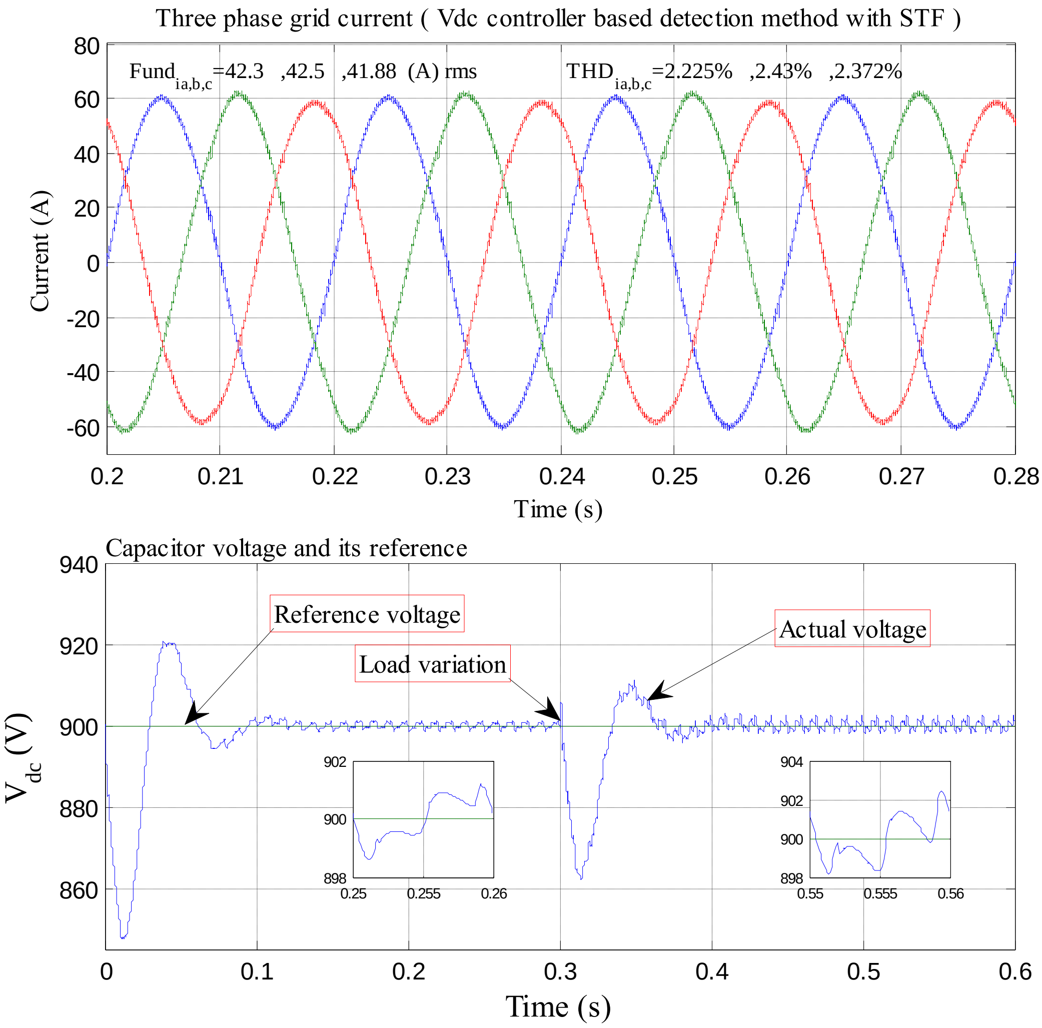

Figure 4.25: Grid current and DC voltage (PI based grid reference generation).

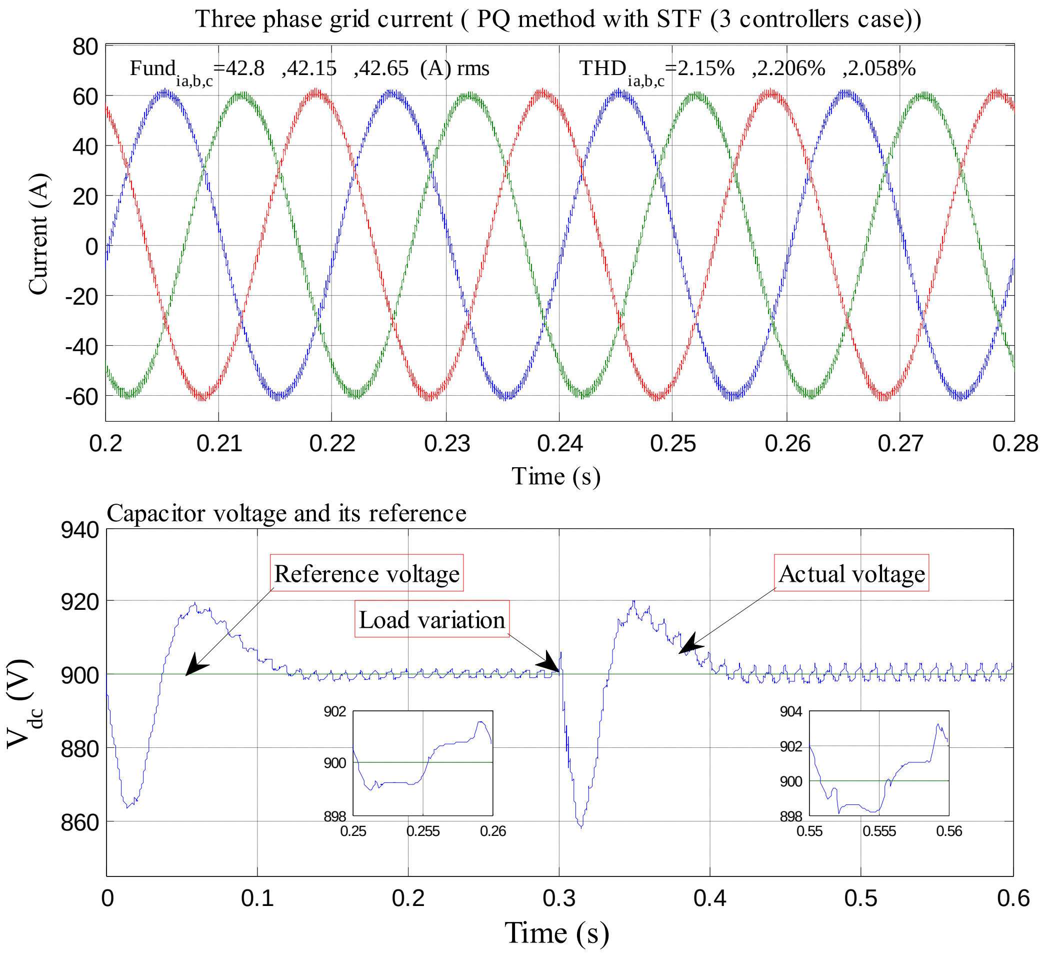

Figure 4.26: Grid current and DC voltage (PQ, STF, and 3 current controllers).

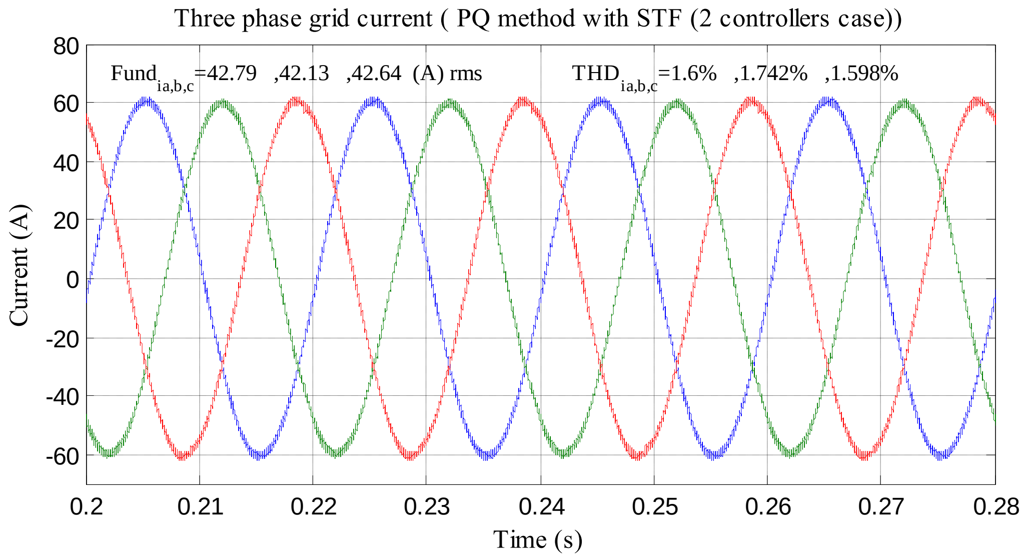

Figure 4.27: Grid current (PQ, STF, and 2 current controllers).

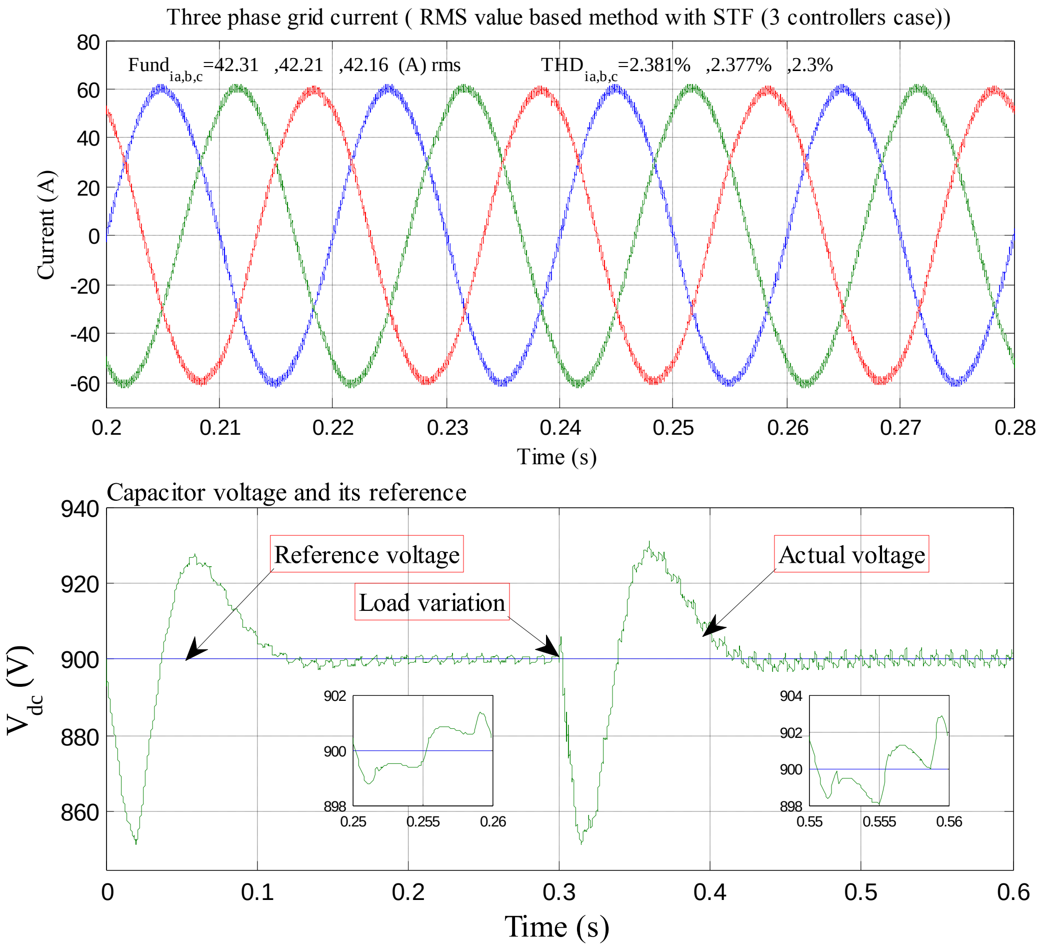

Figure 4.28: Grid current and DC voltage (RMS based algorithm).

Figure 4.22-28 shows the three phase grid currents and the DC voltage of APF obtained using the different control strategies of APF with STF. It is seen that the use of STF has increased significantly the efficiency of SAPF with distorted system voltage. The three phase grid currents are balanced and sinusoidal with perfectly reduced harmonic contents. The THD values of these currents after compensation were all less than 5%. PQ based extraction strategy was the best in term of harmonic compensation. Three current controllers case reduced the THD to a maximum of 2.2%, where the use of two controllers has ameliorated the compensation with THD of 1.7%. Active and reactive currents method gave better results than the d-q method with 2.26% THD. PI based reference generation and d-q method came in the last and showed similar efficiency with maximum THD of 2.4% compared to 2.38% obtained with RMS based reference extraction.

DC voltage of SAPF shown in the figures proves the efficiency of the different PI voltage controllers in the control of the capacitor voltage. It is clear that the capacitor voltage follows its defined reference with fluctuation dependent on the power exchange between the grid and SAPF. The steady state fluctuation was always less than 0.4% of the reference voltage.

4.7 Reactive Power Compensation.

This section presents a study of the performance of SAPF in the compensation of current harmonics in addition to the system reactive power. A linear inductive load is connected in parallel with the non-linear load. The power of the inductive load was 14 kVA with power factor of 0.71. The SAPF will be responsible for the compensation of harmonics and reactive power. System models were built in MATLAB/Simulink and simulation results were obtained and presented.

Figure 4.29 shows the three phase load current with the grid voltage. Load currents are distorted and not in phase with grid voltage. The THD levels of load current are between 19.8% and 24.38%.

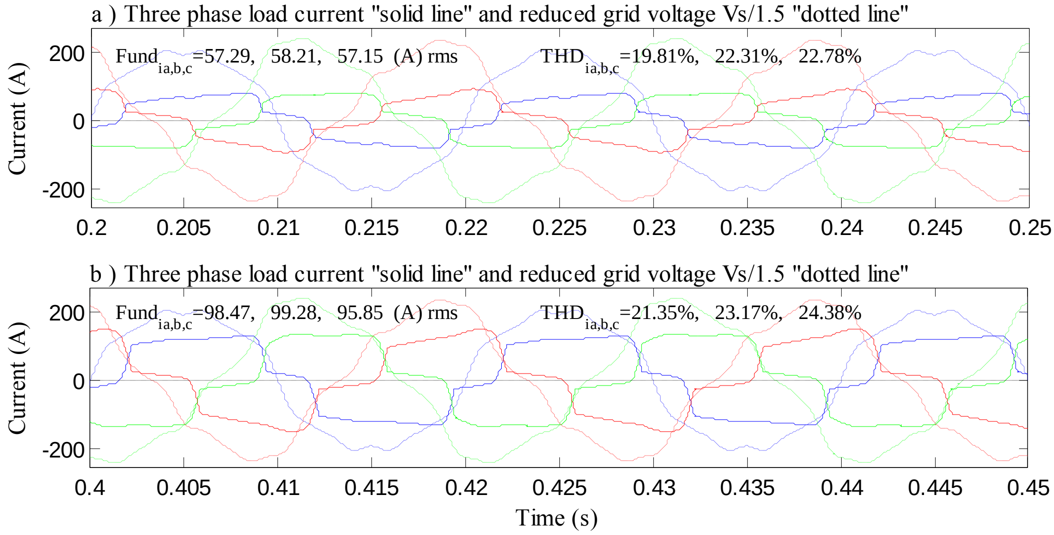

Figure 4.29: Three phase load current a) before and b) after load variation.

Figure 4.30 shows the grid currents and voltages after compensation using SAPF with active and reactive currents method. It has been noticed that this method cancels the phase shift between grid voltage and current ensuring unity power factor. The THD of grid current has been reduced to excellent levels under distorted voltage conditions. THD of 1.85% was achieved initially; this value has increased to 3.2% after load variation. At the moment of load variation, the DC capacitor voltage has passed by transient for less than 0.08 s before converging to its desired steady state.

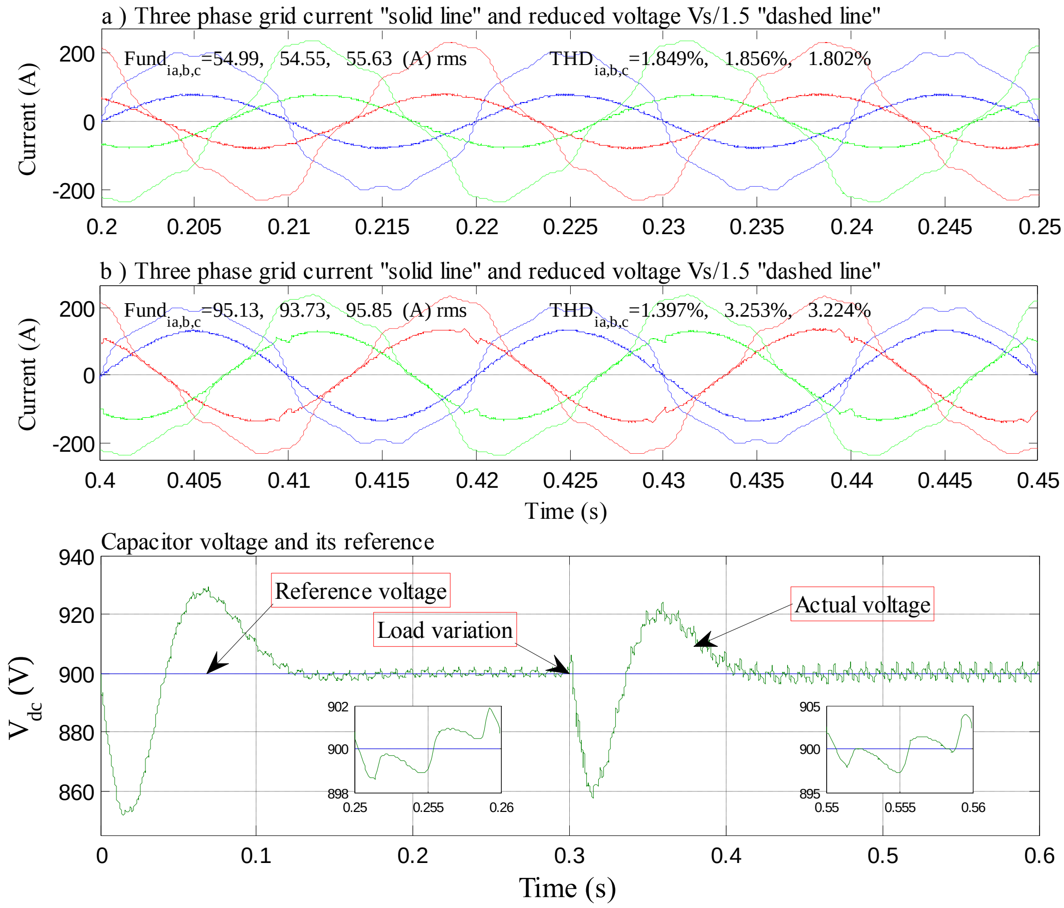

Figure 4.30: Three phase grid current a) before, b) after load variation, and DC voltage (Active and reactive currents method).

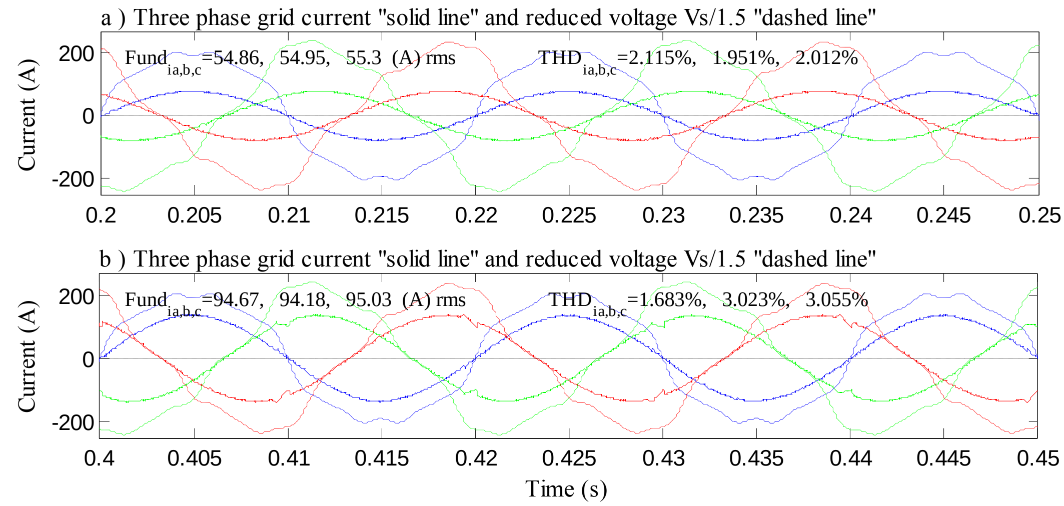

Figure 4.31: Grid current before and after load variation (d-q method, 3 PI controllers).

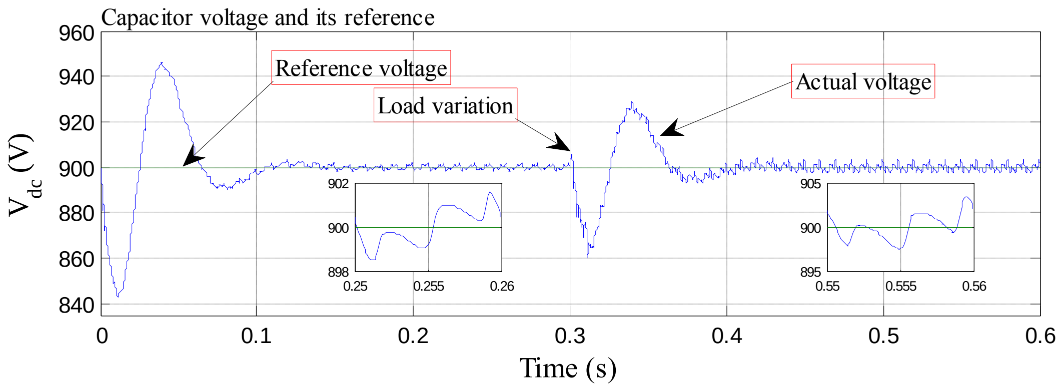

Figure 4.32: DC capacitor voltage (d-q method, 3 PI controllers).

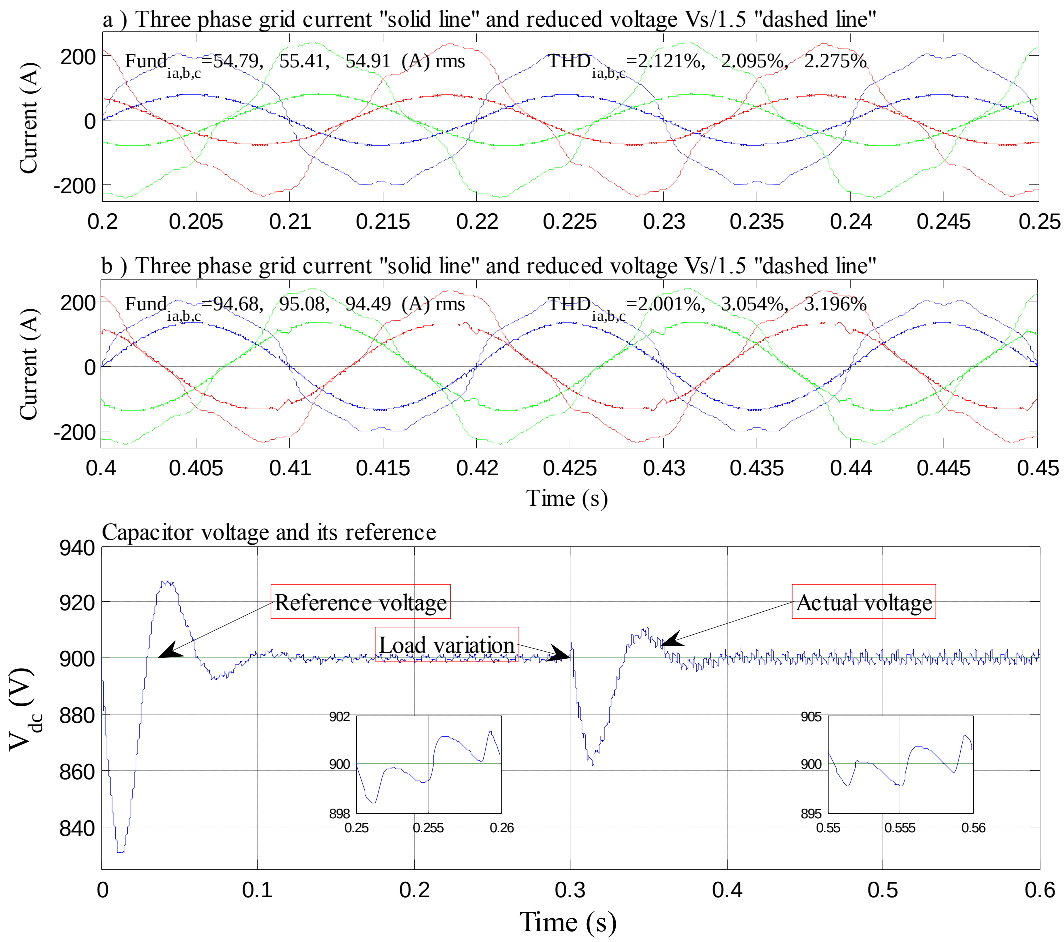

Figure 4.33: Grid current, voltage, and DC capacitor voltage (PI based reference generation).

Figures 4.30 and 4.32 present the voltage, current of the grid and the DC side voltage of APF that has been perfectly controlled to its desired reference. The THD of grid current has been decreased from more than 20% to less than 3.2% by using the d-q extraction method with three PI current regulators. In figure 4.33 describing the grid currents and voltages in addition to the DC voltage of APF using PI controller based reference generation, the THD values have been decreased to less than 3.2% while the DC voltage has been perfectly kept in its reference value.

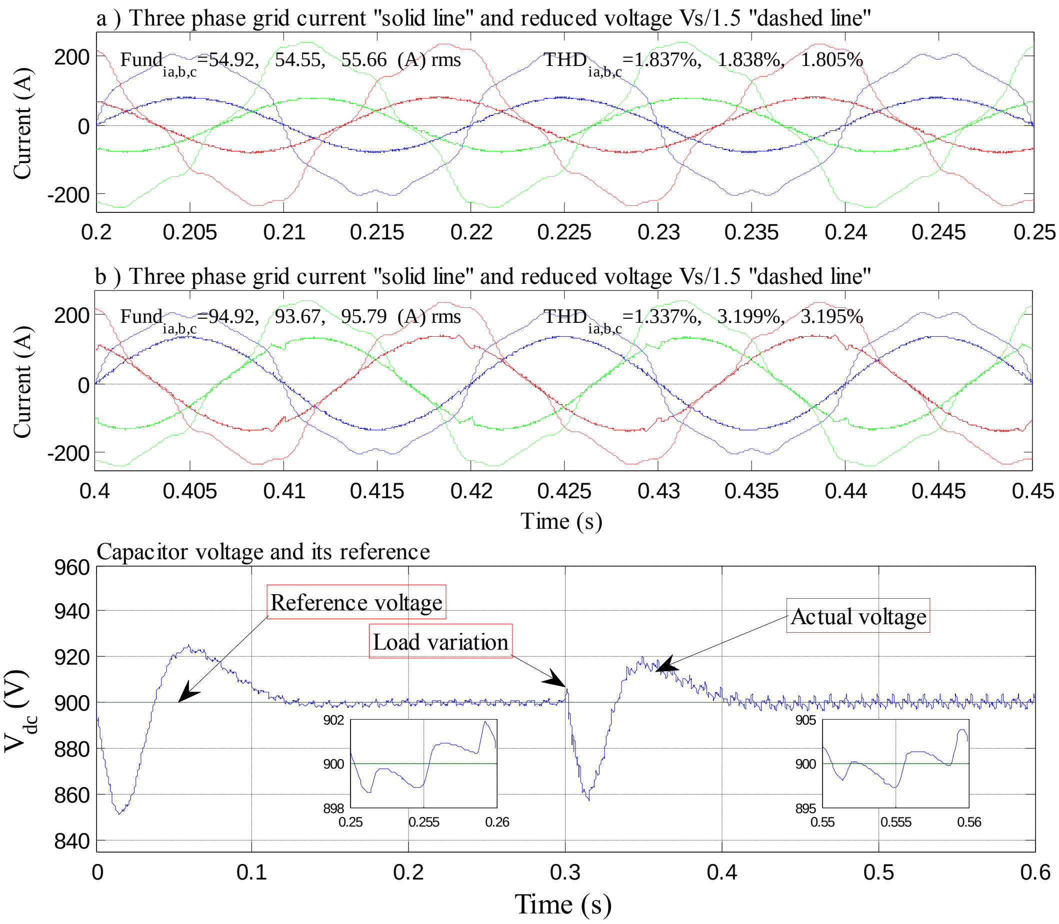

Figure 4.34: Grid current, voltage, and APF DC voltage (PQ, 3 PI controllers).

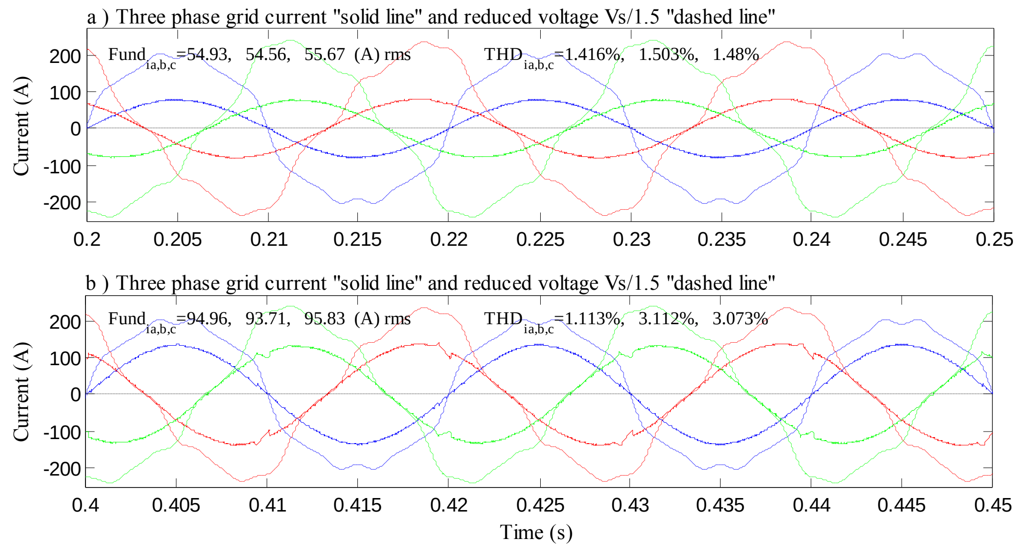

Figure 4.35: Grid current and voltage (PQ, 2 PI controllers).

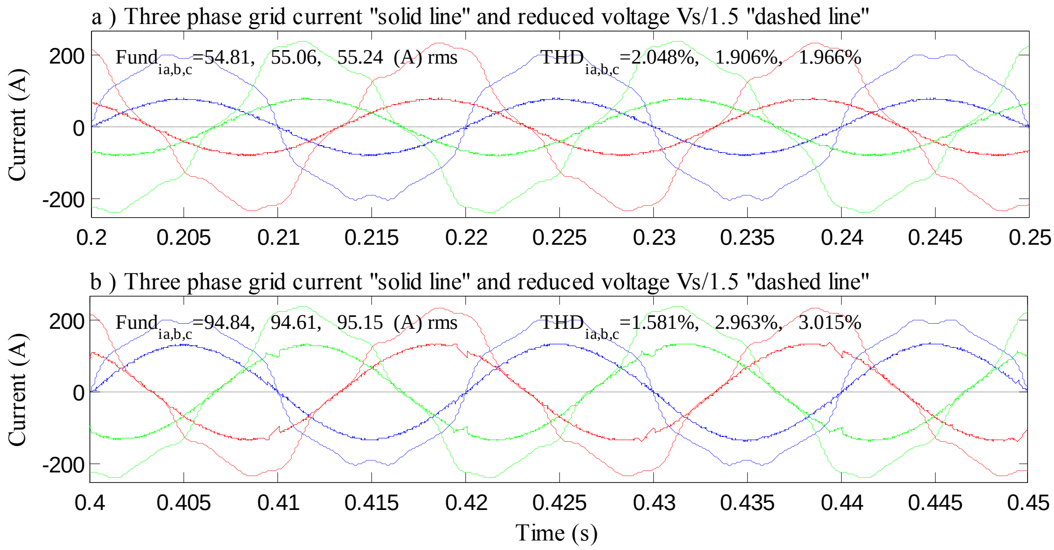

Figure 4.36: Grid current and voltage (RMS value algorithm).

Figures 4.34 and 4.35 present the simulation results of PQ theory with three, two current controllers respectively. Figure 4.36 shows the RMS value based algorithms' simulation results. From figures 4.34 and 4.35 it has been noticed that the grid current waveforms were perfectly sinusoidal and in phase with their voltages. The DC voltage converges perfectly to its reference. The THD was decreased to accepted limits in the case of three current controllers with values varying between 1.8% and 3.2% in its worst case, while the use of current controllers in the alpha-beta reference frame has ameliorated its performance with THD values between 0.9% and 1.9% in its worst case.

4.8 INDIRECT CONTROL OF SAPF

Indirect control strategy of SAPF with an appropriate hysteresis band was tested under distorted unbalanced voltage conditions. The simulation was performed under the same conditions of part 4.7. The hysteresis band was chosen such that the sampling frequency remains within accepted values (less than 20 kHz in our case). Simulation results are presented by figures 4.37- 4.40.

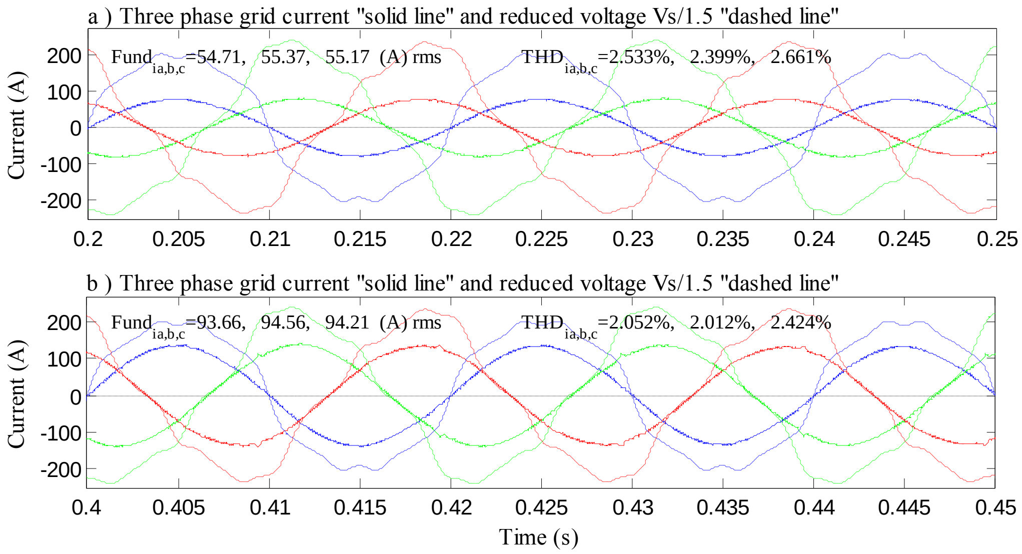

Figure 4.37: Grid current and voltage (Hysteresis control with sine multiplication).

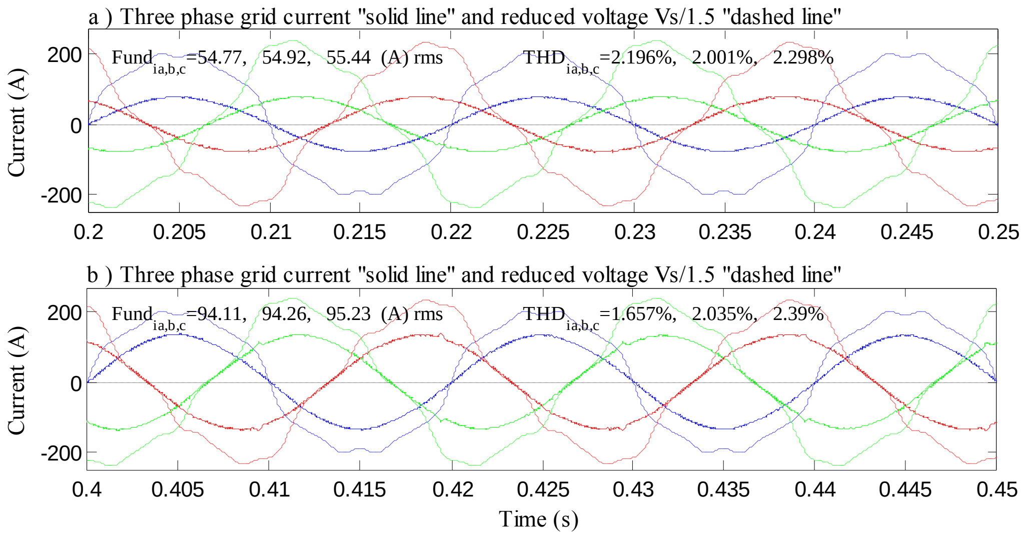

Figure 4.38: Grid current and voltage (d-q extraction method).

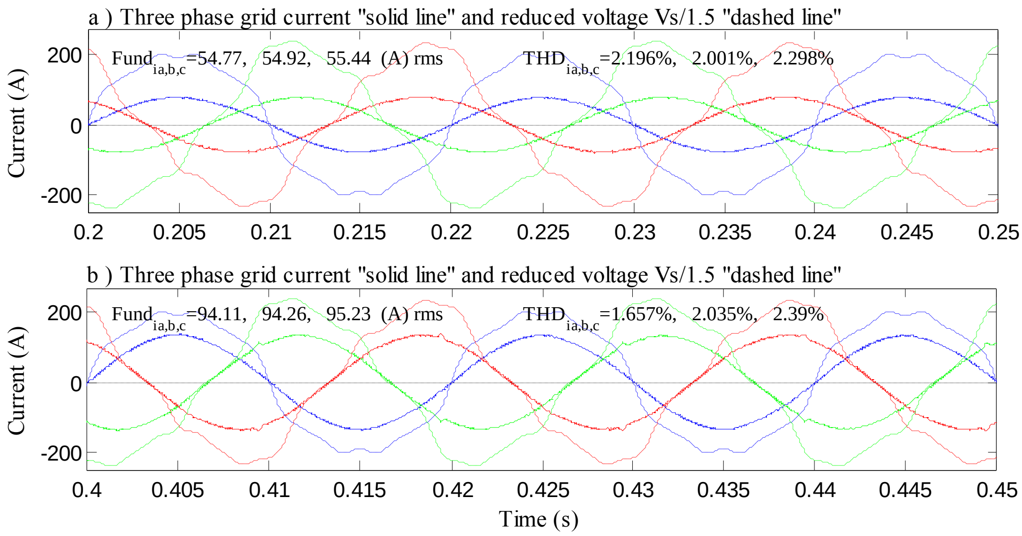

Figure 4.39: Grid current and voltage (PQ extraction method).

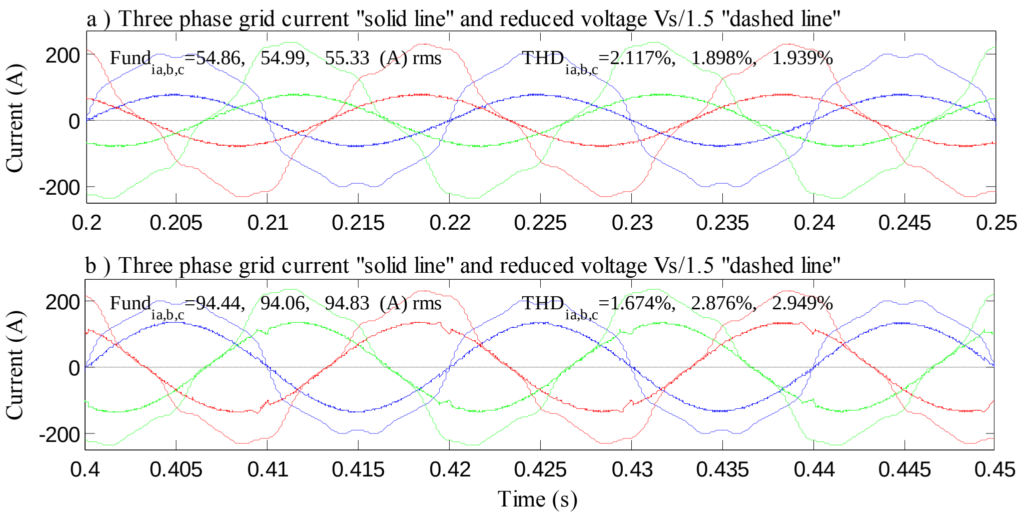

Figure 4.40: Grid current and voltage (sine multiplication with SVPWM indirect control).

CONCLUSIONS

In this thesis, a study of currents harmonics and thier consequences on the electrical systems has been discussed. In addition to the study of different proposed solutions for the problem of harmonics.

The literature studies claim that the parallel active power filters represent an efficient solution for the compensation of harmonics produced by the non linear loads. In this perspective, this thesis has been allocated for the study of different strategies used for the control of SAPF. The performance of active power filter depends not only on the choice of its power circuit, but also on the used control strategy. The harmonic extraction operation has been based principally on the active and reactive power theory, the synchronous reference currents, sine multiplication method, in addition to a method using the rms current value for harmonic extraction.

Different control methods of two level three phase voltage source inverter such as hysteresis control, PWM, and SVPWM control were studied and presented. The hysteresis control is stable and simple with high compensation performance, but its variable switching frequency which can't be supported by the power electronics elements constructing the VSI. The PWM presents a fix controllable switching frequency, this fix frequency make easier the problem of filtering the harmonics due to the switching function. The SVPWM improves the performance of APF while conserving a fix switching frequency.

The control of SAPF based on PI controllers in three-phase, two stationary phases, and synchronous reference system has been studied and discussed. Because of its simple structure, PI controllers have been used for the control of filter currents and its DC voltage, the simulation results shows that it offers a very good performance and stability.

Two control structures of APF have been proposed and discussed, the first called direct and allows the direct control of filter currents while the second called indirect and interests more in controlling filter currents by adjusting the flow of grid current. The indirect control strategy offered the advantage of simplicity and less need of sensors and measurement elements, while its performance was reduced compared to the direct control. Its stability was affected by the variation of grid and load parameters. The direct control is more stable and efficient which needs more sensors and complex calculations.

A comparison between the different control and extraction methods has been done under three cases of stable system, distorted voltage system without reactive power compensation, and distorted voltage system with reactive power compensation. The comparison proved the ability of active power filter for harmonic and reactive power compensation in the case of balanced voltage system. Under unbalanced voltage system, the performance of SAPF degrades from one control strategy to another. The dq method and the RMS value based method have proved better ability to overcome the voltage distortion problem. Although PQ theory has shown high performance in the case of balanced system, its performance has decreased noticeably in the case of unbalanced system.

For the amelioration of the performance of SAPF under non ideal voltage conditions a self tuning filter has been proposed and discussed. The use of STF cancelled most of the drawbacks of the classic methods in the case of distorted and unbalanced voltage system. It can be considered as an important tool for rejecting the effects of voltage distortion on the different extraction methods.

FUTURE WORKS

This work presented in this thesis has given a new perspective for future researches concerning power quality problems; this perspective includes:

- The investigation in the artificial intelligent techniques such as the artificial neural networks in the power quality problems.
- The use of modern extraction methods such as kalman filter.

REFERENCES

[1] *IEEE-519*, IEEE Recommended Practices and Requirements for Harmonic Control in Electric Power Systems, 1992.

[2] IEC 61000-3-4, Limitations of Emissions of Harmonic Currents Low-voltage Power Supply Systems for Equipment with Rated Current Greater than 16A, 1998.

[3] A. Sahbani, M. Labben-Ben Braiek, M. A.Dami et M. Jemli, ''*Commande d'un Filtre Actif Triphasé Shunt par la Logique Floue*'', *3rd International Conference, SETIT, Tunisia*, March 27-31, 2005.

[4] M. AlaaEddin Alali, ''*Contribution à l'Etude des Compensateurs Actifs des Réseaux Electriques Basse Tension*'', *Thèse Doctorat de l'Université Louis Pasteur, Strasbourg I,* 2002.

[5] Hanane Kouara, ''*Application d'un Filtre Série au Contrôle de la Tension d'un Réseau Basse Tension*'', *Mémoire de Magister, Univ. Batna,* Février 2006.

[6] M. Fatiha, ''*Etude et Commande d'un Filtre Actif Parallèle à Structure de Tension*'', *Mémoire de Magister, Univ. Oran,* Octobre 2001.

[7] N. Hanna Mandalek, ''*Qualité de L'onde Electrique et Moyens de Mitigation*'', *Thèse de Doctorat, Ecole de Technologie Supérieure Univ. Québec*, 2003.

[8] C. Sharmeela, M. R. Mohan, G. Uma, J. Baskaran et A.C. College, ''*Fuzzy Logic Controller Based Three-Phase Shunt Active Filter for Line Harmonics Reduction*'', *Univ Anna,* Vol. 3, No. 2, 2007, pp. 76-80.

[9] Leow Pei Ling, ''*SVM Based Hysteresis Current Controller for a Three Phase Active Power Filter*'', MSc Thesis, Universiti Teknologi Malaysia, 2004.

[10] M. Sc. Mariusz Cichowlas, ''*PWM Rectifier with Active Filtering*'', *Ph. D. Thesis, Warsaw University of Technology, Poland,* 2004.

[11] Smruti Ranjan Prusty, ''*FPGA Based Active Power Filter for Harmonics Mitigation*'', MSc. Thesis, National Institute of Technology Rourkela, India, 2011.

[12] Tan Perng Cheng, ''*A Single-Phase Hybrid Active Power Filter with Photovoltaic Application*'', Msc. Thesis, Universiti Teknologi Malaysia, 2007.

[13] Abdelmadjid Chaoui, Jean-Paul Gaubert, Fateh Krim, and Laurent Rambault, ''*IP Controlled Three-Phase Shunt Active Power Filter for Power Improvement Quality*'', IEEE, 1-4244-0136-4/06, pp 2384-2389, 2006.

[14] Ilhami Colak, Ramazan Bayindir, Orhan Kaplan, and Ferhat Tas, '' *DC Bus Voltage Regulation of an Active Power Filter Using a Fuzzy Logic Controller*'', IEEE Ninth International Conference on Machine Learning and Applications, pp 692-696, 2010.

[15] Rong Fei, Yu Jingrong, and Luo an, ''*Reference current computation method based on adaptive low-pass filter for active power filter*'', IEEE International Conference on Measuring Technology and Mechatronics Automation, pp 996-999, 2010.

[16] Wang Li-ping, Shi Zhen-yin, and Yang De-zhou, ''*A Three-phase Active Power Filter Based on the Space Vector Theory*'', IEEE 5th International Conference on Computer Science & Education Hefei, China, pp 1279-1282, 2010.

[17] Ziqiang Xi, Zhangiang Xin, Shiping Zhou, Wencong Huang, and Lei Qi, ''*A Novel Shunt Active Power Filter Under Condition of Unbalanced Voltage*'', 978-1-4244-4813-5/10, 2010.

[18] Mohamed El-Habrouk, ''*A new Configuration for Shunt Active Power Filters*'', PhD Thesis, Brunel University, 1998.

[19] B.Singh, K.AI-Haddad, and A.Chandra, ''*Active power filter with sliding mode control*'', IEE Proc.-Gener. Transm. Distrib., Vol. 144, No. 6, pp 564-568, 1997.

[20] Mohamed Muftah Abdusalam, ‘‘*Structures et Stratégies de Commande des Filtres Actifs Parallèle et Hybride avec Validations Expérimentales*’’, *PhD thesis, University H.Poincaré, Nancy-I,* Mai 2008.
[21] B. Mohamed Choukri, ‘‘*Contribution à l'Etude des Différentes Topologies et Commandes des Filtres Actifs Parallèles à Structure Tension : Modélisation, Simulation et Validation Expérimentale de la Commande*’’, Thèse de Doctorat, Univ. H. Poincaré, Nancy-I, Décembre 2004.
[22] Mohamed abdusalam, Philippe Poure, and Shahrokh Saadate, ‘‘*A New Control Scheme of Hybrid Active Filter Using Self Tuning Filter*’’, IEEE 1-4244-0895-4, powering 2007, pp35-40.
[23] Shahram Karimi, ‘‘*Continuité de Service des Convertisseurs Triphasés de Puissance et Prototypage 'FPGA in the Loop': Application au Filtre Actif Parallèle*’’, PhD thesis, *H.Poincaré, Nancy-I,* 2009.
[24] A. Jaya Laxmi, G.Tulasi Ram Das, K.Uma Rao, and K.Rayudu, ‘‘*Comparison of PI and ANN Control Strategies of Unified Shunt Series Compensator*’’, IEEE 0-7803-9525-5/06, 2006.
[25] Joy Mazumdar, and G. Harley, ‘‘*Recurrent Neural Networks Trained With Backpropagation Through Time Algorithm to Estimate Nonlinear Load Harmonic Currents*’’, IEEE Transactions on Industrial Electronics, Vol. 55, NO. 9, pp 3484-3491, 2008.
[26] Leong Hua Tey, Ping Lam So, and Yun Chung Chu, ‘‘*Adaptive neural network control of active filters*’’, ELSEVIER, Electric Power Systems Research 74, pp 37-56, 2004.
[27] Helder J.Azevedo, José M.Ferreira, António P.Martins and Adriano S. Carvalho ‘‘*Directe Current Control of an Active Power Filter For Harmonic Elimination, Power Factor Correction and Load Unbalancing Compensation*’’, *Proceedings of the 10th European Conference on Power Electronics and Applications*, EPE'03, Toulouse, 2003, pp. 1-10.
[28] D. Casadi, U. Reggiani and G. Grandi ‘‘*Active Power Filters Based on a Single Current Measurement System*’’, *System Proceedings Symposium on Power Electronics, Electrical Drives Advanced Machines Power Quality* (SPEEDAM'98), Italy, June 3-5, 1998.
[29] Antonio P. Martins, "*The Use of an Active Power Filter for Harmonic Elimination and Power Quality Improvement in a Nonlinear Loaded Electrical Installation*", Proceedings of the International Conference on Renewable Energies and Power Quality, ICREPQ'03, Vigo, 2003, pp. 1-6.
[30] K.H.Yiauw and M.S.Khanniche ‘‘*A Novel Three Phase Active Power Filter* ’’, *Rev. Energ. Ren. : Power Engineering,* 2001, pp 77-84.
[31] Ngac ky Nguyen, ‘‘*Approche Neuromimétique pour L'identification et la Commande des Systèmes Electrique : Application au Filtrage Actif et aux Actionneurs Synchrones*’’, PhD thesis, University Haute Alsace, MULHOUSE, 2010.
[32] Mohd Izhar Bin A Bakar, ‘‘*Active Power Filter with Automatic Control Circuit for Neutral Current Harmonic Minimization Technique*’’, PhD Thesis, Universiti Sains Malaysia, 2007.
[33] François Defay, ‘‘*Commande Prédictive Directe d'un Convertisseur Multicellulaire Triphasé Pour Une Application de Filtrage Actif*’’, PhD Thesis, Université de Toulouse, 2008.
[34] Keith H. Sueker, ‘‘*Power Electronics Design: A Practitioner's Guide*’’, Newnes, SciTech Publishing, 2005.

[35] MOHAMED Magraoul, ‘‘*Validation de Techniques de Commande d'un Filtre Actif Parallèle*’’, Mémoire de Maitrise en génie électrique, Université du Québec, 2007.
[36] AbdelHamid Hamadi, ‘‘*Amélioration des performance du filtre actif : Application du régulateur proportionnel Intégral et du régulateur flou*’’, Mémoire de Maitrise en génie électrique, Université du Québec, 2004.
[37] Schneider Electric Industries SAS, technical guide No 4, DBTP152GUI/FR, 2008, http://www.schneider-electric.com.
[38] Alireza Javadi, ‘‘*Modeling, Simulation and Real-Time Control of Active Filters*’’, mémoire de maitrise des sciences appliqués, École Polytechnique de Montréal, Université de Montréal, 2009.
[39] Qiongq Chen, Z. Chen, and Malcolm Mc. Cormick, ‘‘*The Application and Optimization of C-type Filter in a Combined Harmonic Power Filter*’’, 35th Annual IEEE Power Electronics Specialists Conference, PP 1041-1045, 2004.
[40] Nelms, Mark “*Power Electronics*”, The Electric Power Engineering Handbook,Ed.L.L. Grigsby, Boca Raton: CRC Press LLC, 2001.
[41] M. Kale, E. Ozdemir, “*An adaptive hysteresis band current controller for shunt active power filter*”, Electric Power Systems Research, vol. 73, no. 2, pp. 113-119, February 2005.
[42] Hanny H.Tumbelaka and Chem.V.Nayar ‘‘*Application Of An Active Power Filter to Compensate Multiple Non Linear Loads*’’, Australasian Universities Power Engineering Conference, 26-29 September 2004.
[43] Saheb Hussain MD, K.Satyanarayana, B.K.V.Prasad, ‘‘ *Power Quality Improvement by Using Active Power Filters*’’, International Journal of Engineering Science & Advanced Technology, Vol 1, No 1, PP 1-7, 2011.
[44] D. O. Abdeslam, P. Wira, J. Mercklé, Y. Chapuis et D. Flieller, ‘‘*Stratégie Neuromimétique d’Identification et de Commande d’un Filtre Actif Parallèle*’’, *Revue des Systèmes, Série Revue Internationale de Génie Electrique (RS-RIGE),* Vol. 9, No. 1, 2006, pp. 35-64.
[45] Amaia Lopez de Heredia Bermeo, ‘‘*Commandes Avancées des Systèmes Dédies à l’Amélioration de la Qualité de l’Energie : de la Basse Tension a la Montée en Tension*’’, PhD Thesis, Institut National Polytechnique de Grenoble, Novembre. 2006.
[46] S. Biricik, and O. C. Ozerdem, “*Investigation of Switched Capacitors Effect on Harmonic Distortion Levels and Performance Analysis with Active Power Filter*”, *Przeglad Elektrotechniczny, ISSN 0033-2097, R. 86 NR* Nov.2010, pp 13-17.
[47] Emílio F. Couto, Júlio S. Martins, and João L. Afonso, ‘‘*Simulation Results of a Shunt Active Power Filter with Control Based on p-q Theory*’’, International Conference on Renewable Energies and Power Quality, PP 1-6, 2003.
[48] G.Tsengenes, and G. Adamidis ‘‘*A New Simple Control Strategy for Shunt Active Power Filters under Non Ideal Mains Voltages*’’ International Symposium on Power Electronics, Electrical Drives, Automation and Motion, PP 1530-1536, 2010.
[49] Muhammad H. Rashid, ‘‘*Power Electronics Handbook*’’, Academic Press, 2001.
[50] B. Ouahid, ‘‘*Contribution à l’Analyse des Onduleurs Multiniveaux*’’, *MSc. Thesis, Univ. Batna, Algeria,* 2005.
[51] C. Lott, O. Lapierre, H. Pouliquen et S. Saadate, ‘‘*Filtrage Actif des harmoniques en Courant et en Tension des Réseaux Electriques : Modélisation, Simulation Numérique et Expérimentation*’’, *J. Phys. III France,* Vol. 7, No. 12, 1997, pp. 2433-2457.

[52] Tarek A. Kasmieh, and Hassan S. Omran, ‘‘*Active Power Filter dimensioning Using a Hysteresis Current Controller*’’, World Academy of Science, Engineering and Technology 52, PP 233-237, 2009.
[53] Mohamayee Mohapatra, B.Chitti Babu, ‘‘*Fixed and Sinusoidal-Band Hysteresis Current Controller for PWM Voltage Source Inverter with LC Filter*’’, IEEE Student’s Technology symposium 2010.
[54] G. S. Eskandar, ‘‘Apport de l’UPFC à l’Amélioration de la Stabilité Transitoire des Réseaux Electriques’’, *PhD Thesis, Univ. H. Poincaré, Nancy-I,* Octobre 2003.
[55] K. M. Rahman, M. R. Khan, M. A. Choudhury, "*Implementation of programmed modulated carrier HCC based on analytical solution for uniform switching of voltage source inverters*", IEEE Transactions on Power Electronics, vol. 18, no. 1, pp. 188-197, January 2003.
[56] M.A. Shamsi-Nejad, S. Pierfederici, J. P. Martin, F. Meibody-Tabar, "*Study of an hybrid current controller suitable for DC–DC or DC–AC applications*", IEEE Transactions on Power Electronics, vol. 22, no. 6, pp. 2176-2186, Nov. 2007.
[57] G. H. Bode, D. G. Holmes, "*Load independent hysteresis current control of three level single phase inverter with constant switching frequency*", IEEE Power Electronics Specialists Conference, pp. 14-19, 2001.
[58] Wei-Feng Zhang and Yue- Hui Yu, ‘‘*Comparison of Three SVPWM Strategies*’’, *Journal of Electronic Science and Technology of China,* Vol. 5, No. 3, 2007, pp. 283-287.
[59] José R. Espinoza, Géza Joós and Hua Jin, ‘‘*Modelling and Implementation of Space Vector PWM Techniques in Active Filter Applications*’’, *Elect. & Comp. Eng. Concordia Univ. Montréal, P. Q. Canada,* 1996.
[60] M. Sc. Mariusz Cichowlas, ‘‘PWM Rectifier with Active Filtering’’, *Ph. D. Thesis,Warsaw University of Technology, Poland,* 2004.
[61] H. Farid, ‘‘*Commande Robuste d’un Filtre Actif Shunt à Quatre Fils*’’, *MSc. Thesis, Univ. Batna, Algeria,* 2008.
[62] Thip Manmek, ‘‘*Real-Time Power System Disturbance Identification and its Mitigation Using an Enhanced Least Squares Algorithm*’’, *PhD Thesis, Univ. South Wales,* 2006.
[63] Thierry Gouraud, ‘‘Identification et Rejet de Perturbations Harmoniques dans des Réseaux de Distribution Electrique’’, *PhD Thesis, Ecole Centrale de Nantes,*1997.
[64] Hanny H.Tumbelaka, ‘‘*A Load Current Sensorless Shunt Active Power Filter*’’, *Jurnal Teknik Elektro,* Vol. 7, No. 1, March 2007, pp. 1-7.
[65] Domenico Casadi, Gabriele Grandi, Ugo Reggiani and Claudio Rossi ‘‘*Control Methods for Active Power Filters with Minimum Measurement Requirements*’’, *IEEE APEC,* Vol. 2, 1999, pp. 1153-1158.
[66] S.Biricik, O.C.Ozerdem, S.Redif and M.O.I.Kmail, " *Novel Hybrid Active Power Filter Structure to Compensate Harmonic Currents and Reactive Power*", *Accepted for MELECON 2012 - 2012 16th IEEE Mediterranean Electrotechnical Conference ,* 25-28 March 2012.

APENDIX A

Self Tuning Filter (STF)

The use of self tuning filter seems to be indispensable and very important for the construction of a harmonic extraction method; which must be insensible to the presence of voltage distortions and harmonics. The STF can be used either for instantaneous power calculation or to be used in conjunction with PLL circuits.

Principle of STF

Song Hong Scok has presented in his PhD works the transfer function of the equation defined by:

$$V_{xy}(t) = e^{j\omega t}\int e^{-j\omega t}U_{xy}(t)dt \tag{A.1}$$

He found the transfer function of this equation as:

$$H(S) = \frac{V_{xy}(S)}{U_{xy}(S)} = \frac{S + j\omega}{S^2 + \omega^2} \tag{A.2}$$

He has demonstrated using this transfer function that the output and the input are in phase with the effect of amplitude integration. Over more, Bode diagram shows that the effect of this transfer function is similar to band pass filter. If some constants will be added we will have the transfer function defined by:

$$H(S) = \frac{V_{xy}(S)}{U_{xy}(S)} = k_2\,\frac{(S + k_1) + j\omega}{(S + k_1)^2 + \omega^2} \tag{A.3}$$

It has been demonstrated in [21] and [22] that the choice of $k_1=k_2=k$ is very important to obtain a zero dB magnitude response with null phase angle between the input and the output. The transfer function will be then defined by:

$$H(S) = \frac{V_{xy}(S)}{U_{xy}(S)} = k\,\frac{(S + k) + j\omega}{(S + k)^2 + \omega^2} \tag{A.4}$$

The bloc diagram of the STF with equal constants is shown in fig A.1, where the inputs are the original signals in stationary reference and the outputs are the fundamentals at the given frequency.

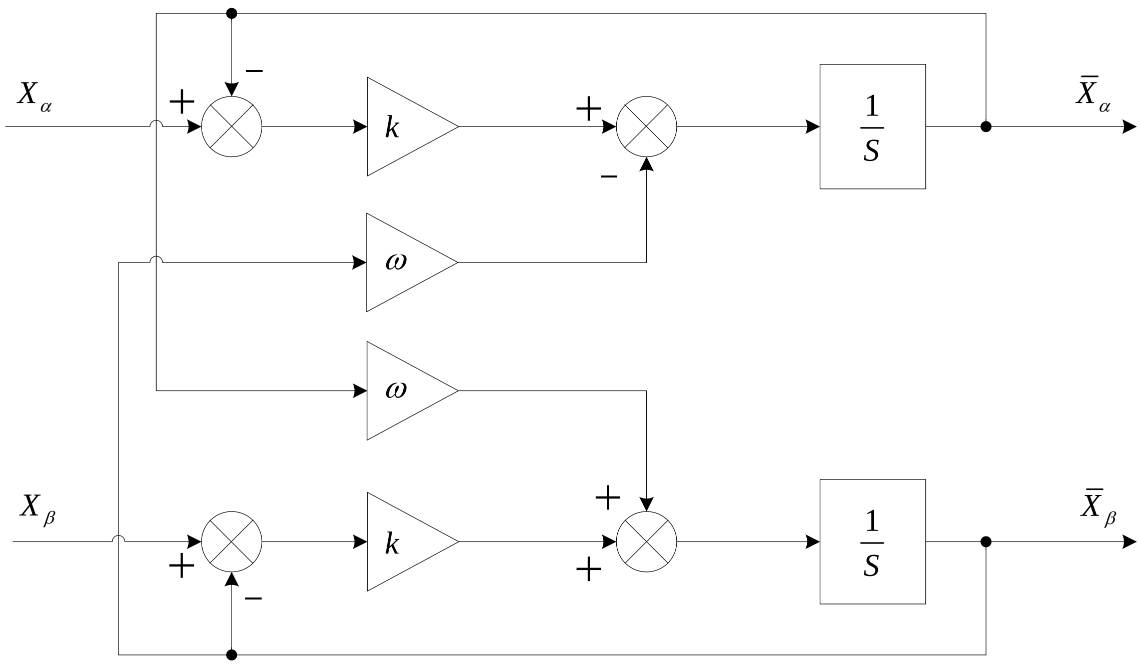

Figure A.1: Bloc diagram of Self Tuning Filter.

In the stationary reference, the expressions of the fundamentals of a given signal are given by:

$$\begin{aligned} \bar{X}_\alpha(S) &= \frac{k}{S}\left[X_\alpha(S) - \bar{X}_\alpha(S)\right] - \frac{\omega}{S}\bar{X}_\beta(S) \\ \bar{X}_\beta(S) &= \frac{k}{S}\left[X_\beta(S) - \bar{X}_\beta(S)\right] + \frac{\omega}{S}\bar{X}_\alpha(S) \end{aligned} \tag{A.5}$$

Where,

$x_{\alpha\beta}$: Input signals in stationary reference;

$\bar{x}_{\alpha\beta}$: Fundamental components of $x_{\alpha\beta}$;

$\omega = 2\pi f_s$: Fundamental angular frequency;

k : Constant to be adjusted.

Figure A.2 shows the bode diagram of the STF at the fundamental frequency of 50 Hz and different values of *k*. we can notice that for all values of k there is no phase at the fundamental angular frequency. We can notice also that the selectivity increases with decreasing *k* [20].

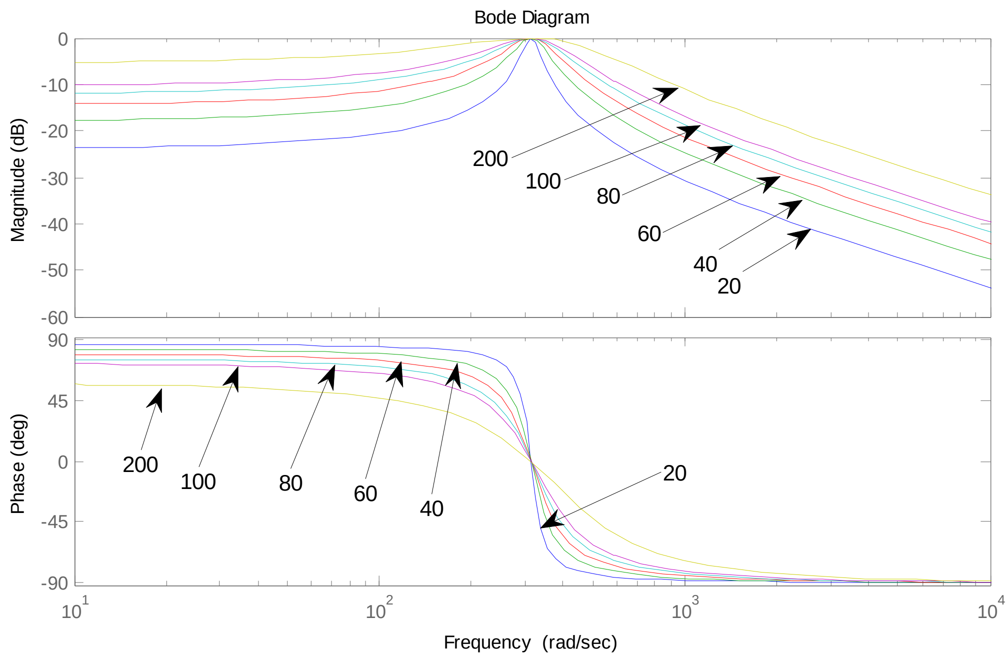

Figure A. 2: Bode diagram of the STF with different values of k.

In order to study the response of STF with a signal containing harmonics; the three phase system voltage is supposed to be balanced containing 5th , 7th , and 11th harmonics and defined by:

$$
\begin{aligned}
v_a &= \sqrt{2}\left[v_1 \sin(\omega t) - v_5 \sin(5\omega t) + v_7 \sin(7\omega t) + v_{11} \sin(11\omega t)\right] \\
v_b &= \sqrt{2}\left[v_2 \sin(\omega t - \varphi) - v_5 \sin(5\omega t - \varphi) + v_7 \sin(7\omega t - \varphi) + v_{11} \sin(11\omega t - \varphi)\right] \\
v_c &= \sqrt{2}\left[v_3 \sin(\omega t + \varphi) - v_5 \sin(5\omega t + \varphi) + v_7 \sin(7\omega t + \varphi) + v_{11} \sin(11\omega t + \varphi)\right]
\end{aligned}
\qquad (A.6)
$$

Where, $v_1 = v_2 = v_3 = 240, v_5 = 20, v_7 = 15 , v_{11} = 10, \varphi = \dfrac{2\pi}{3}$.

The simulation results were obtained with k=100 and presented in figure A.3. Figure A.3a presents three phase distorted signal while figure A.3b presents the same signal filtered using STF. It is well noticed that the filtered signal is sinusoidal with very low harmonic contents. The THD of the signal was reduced from 11.2% to 0.66% after filtering. The transient of the filter was of about 0.03 s which or the equivalent of 1.5 signal waves.

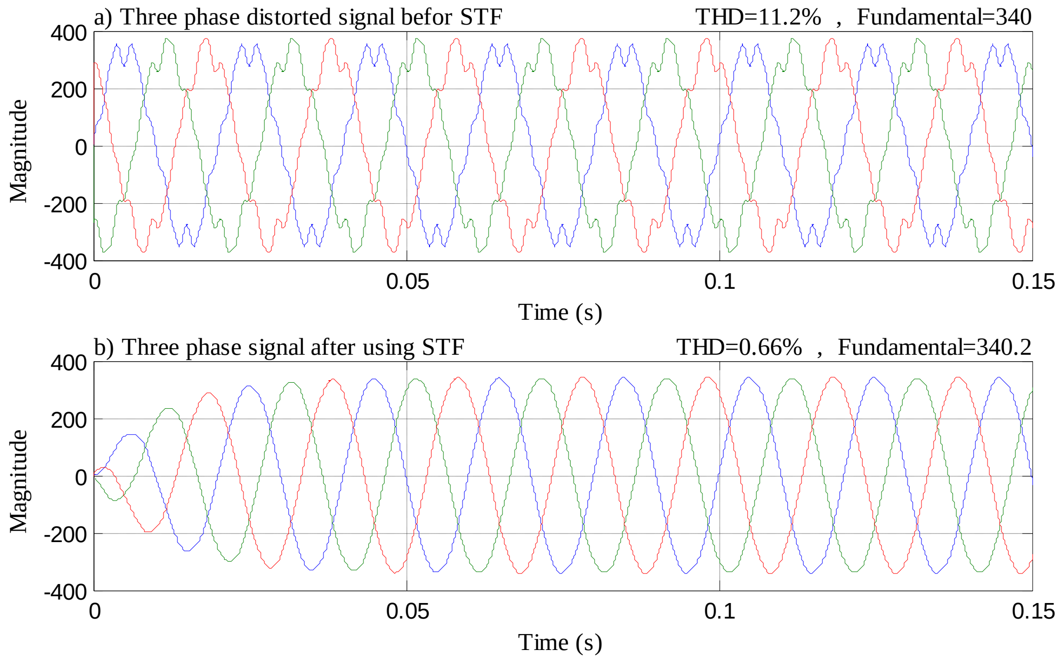

Figure A.3: a) Distorted signal. b) Extracted signal using STF.

The STF was also used for the extraction of fundamental in the case of distorted unbalanced three phase signal defined by:

$$\begin{aligned}
v_a &= \sqrt{2}\left[v_1 \sin(\omega t) - v_5 \sin(5\omega t) + v_7 \sin(7\omega t) + v_{11} \sin(11\omega t)\right] \\
v_b &= \sqrt{2}\left[v_2 \sin(\omega t - \varphi) - v_5 \sin(5\omega t - \varphi) + v_7 \sin(7\omega t - \varphi) + v_{11} \sin(11\omega t - \varphi)\right] \\
v_c &= \sqrt{2}\left[v_3 \sin(\omega t + \varphi) - v_5 \sin(5\omega t + \varphi) + v_7 \sin(7\omega t + \varphi) + v_{11} \sin(11\omega t + \varphi)\right]
\end{aligned} \tag{A.7}$$

Where, $v_1 = 226, v_2 = 212, v_3 = 240, v_5 = 20, v_7 = 15, v_{11} = 10, \varphi = \dfrac{2\pi}{3}$

Figure A.4 shows the simulation results of this case, it is clear from A.4b that the extracted signal is about balanced with low harmonic contents compared to the original signal.

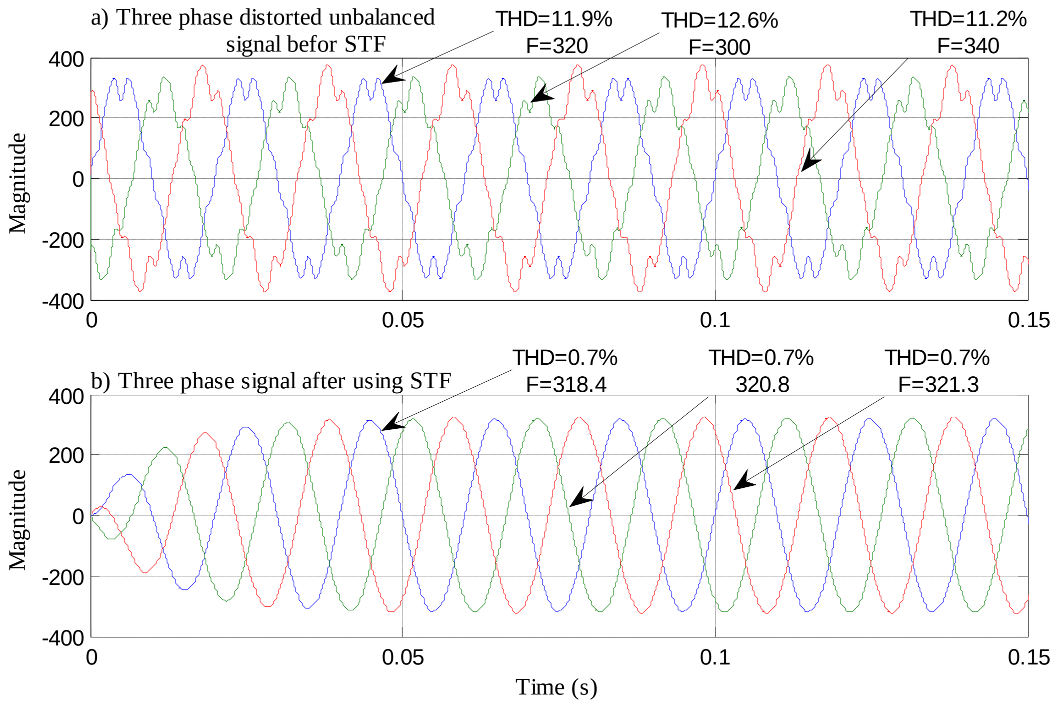

Figure A.4: a) Distorted unbalanced signal. b) Extracted signal using STF.